

# **Model development and study of human immune cell-hepatocyte interactions in response to HBV**

Dissertationsschrift zur Erlangung des akademischen Grades

Doktor der Naturwissenschaften (Dr. rer. nat.)

Im Fachbereich Biologie

Der Fakultät Mathematik, Informatik und Naturwissenschaften  
der Universität Hamburg

Vorgelegt von Yvonne Melanie Ladiges

Hamburg, September 2024



This doctoral dissertation was supervised by Prof. Dr. Maura Dandri and performed at the I. Department of Internal Medicine, University Medical Center Hamburg-Eppendorf, in Hamburg, Germany from May 2019 until September 2024.

Prüfungskommission:

Voritz:	Prof. Dr. Stefan Hoth
1. Gutachterin:	Prof. Dr. Maura Dandri
2. Gutachterin:	Prof. Dr. Julia Kehr
Weiteres Mitglied:	Prof. Dr. Baris Tursun

Disputation: 21.02.2025

## **Danksagung**

An dieser Stelle möchte ich allen danken, die mich während meiner Doktorarbeit unterstützt haben. Ohne ihre Hilfe und ihr Vertrauen wäre diese Arbeit nicht möglich gewesen.

Mein besonderer Dank gilt Prof. Dandri für ihre unermüdliche Unterstützung, wertvolle wissenschaftliche Anregungen und ihr stets offenes Ohr. Ihre fachliche Expertise, konstruktive Kritik und Menschlichkeit haben mir geholfen, mich weiterzuentwickeln und neue Perspektiven zu gewinnen.

Danke auch Prof. Kehr für die Begutachtung meiner Arbeit und Ihre Hilfe, wann immer sie nötig war. Ihre schnelle Reaktionszeit bei E-Mails war bemerkenswert.

Ein herzliches Dankeschön geht an meine Kolleginnen und Kollegen aus der AG Dandri für den inspirierenden Austausch und die angenehme Zusammenarbeit. Besonders möchte ich Dr. Annika Volmari hervorheben. Vielen Dank für deine unermüdliche Unterstützung, die neuen Methoden und dein wertvolles Feedback beim Korrekturlesen meiner Arbeit.

Auch Dr. Tassilo Volz, Dr. Andrea Piroso, Corinna Eggers und Manuela Mirow danke ich für ihre uneingeschränkte Hilfe und Unterstützung, sowie schallendes Gelächter und die schönste Büronachbarschaft. Die gemeinsamen Erlebnisse, insbesondere die Konfetti-Geburtstags-Schlachten, werde ich nie vergessen.

Abschließend danke ich meiner Familie: Jan, du hast immer an mich geglaubt und mich unterstützt – deine Einstellung ist eine wahre Inspiration. Phil und Ari, ich hoffe, euch ein gutes Beispiel zu sein und euch zu zeigen, dass Disziplin und Ehrgeiz jeden zum Ziel führen. Ich liebe euch!

Meinen Eltern, Manfred und Sabine, danke ich von Herzen für ihre unermüdliche Unterstützung, besonders seitdem ich Mutter wurde. Unser familiärer Zusammenhalt bedeutet mir sehr viel.

## Abstract

Chronic hepatitis B (HBV) infection is a major global health issue, affecting nearly 300 million people worldwide and closely linked to liver cirrhosis and hepatocellular carcinoma (HCC). Despite the availability of effective vaccines, curing chronic HBV infection remains elusive due to the persistence of cccDNA, integration of HBV DNA into the host genome, and impaired immune responses. While innate immunity may be inadequately activated, adaptive immune responses are pivotal for viral clearance. A better understanding of the mechanisms determining HBV sensing and responses is key for disease management and for the development of therapies achieving sustained control of treatment.

A major challenge in studying HBV infection and pathogenesis is the limited availability of infection models. This study uses liver chimeric USG mice lacking adaptive immunity to investigate the interaction of HLA molecules to HBV-infected hepatocytes. In chronic HBV infection, virus-directed cytotoxic T cells are often undetectable, leading to ineffective antiviral immune responses. The mechanisms underlying defective adaptive immunity remain elusive, driving research efforts to restore antiviral T cell immunity through adoptive transfer of engineered immune cells. However, the potential contribution of innate immune cells such as NK cells to viral clearance remains understudied.

This thesis aims to study interactions occurring between HBV-infected PHH and immune cells, and particular the role of HLA molecules expressed on human hepatocytes in HBV sensing. To perform this analysis, the study also aimed to expand the chimeric mouse model through the adoptive transfer of donor-matched non-parenchymal cells (NPCs). Insight into the sensing mechanisms may pave the way for novel antiviral strategies by targeting these checkpoints.

Using human liver chimeric mice, chronically infected liver samples were analysed for HBV-induced changes in mRNA expression of HLA molecules.

NPCs were transferred into HBV-infected humanized mice, which were transplanted with matched human hepatocytes for further analysis of gene expression, cytokine levels and viral load.

Analysis of HBV-induced changes in mRNA expression of HLA molecules in human liver

chimeric mouse samples indicates that HBV does not enhance HLA expression on hepatocytes but can be induced by interferons. In addition, successful recruitment of lymphocytes to the liver following NPC transfer into HBV-infected humanized mice is demonstrated, albeit with variable success rates. These findings highlight the evasive tactics of HBV and suggest potential markers for antiviral treatment and ways to improve lymphocyte recruitment in future studies, thus highlighting its stealthy nature. The induction of HLA molecules by IFNs suggests their potential as markers for antiviral treatment.

In summary, these data show that HBV is recognised by immune cells. Therefore, the HLA system is functional. However, in chronic HBV the T cells are absent (exhausted). Less is known about the role of other immune cells, such as NK cells or dendritic cells, in the immune response and as triggers of inflammation. Likewise, the role and function of interferons is not yet fully understood, although it continues to be used in combo therapies with promising results. Therefore, immunocompetent models for HBV are crucial to clarify the still open questions of the immune response to HBV infection.

## Zusammenfassung

Die chronische Hepatitis-B-Infektion (HBV) ist ein wichtiges globales Gesundheitsproblem, von dem weltweit fast 300 Millionen Menschen betroffen sind und das in engem Zusammenhang mit Leberzirrhose und hepatozellulärem Karzinom (HCC) steht. Obwohl wirksame Impfstoffe zur Verfügung stehen, ist eine Heilung der chronischen HBV-Infektion aufgrund der Persistenz der cccDNA, der Integration der HBV-DNA in das Wirtsgenom und der beeinträchtigten Immunreaktion nach wie vor schwer vorstellbar. Während die angeborene Immunität möglicherweise nur unzureichend aktiviert ist, sind die adaptiven Immunantworten für die Beseitigung des Virus von entscheidender Bedeutung. Ein besseres Verständnis der Mechanismen, welche die HBV-Erkennung und -Antwort bestimmen, ist der Schlüssel für das Krankheitsmanagement und für die Entwicklung von Therapien, die eine nachhaltige Kontrolle der Behandlung ermöglichen.

Eine große Herausforderung bei der Untersuchung der HBV-Infektion und -Pathogenese ist die begrenzte Verfügbarkeit von Infektionsmodellen. In dieser Studie werden chimäre USG-Mäuse ohne adaptive Immunität verwendet, um die Interaktion von HLA-Molekülen mit HBV-infizierten Hepatozyten zu untersuchen. Bei einer chronischen HBV-Infektion sind virusgesteuerte zytotoxische T-Zellen oft nicht nachweisbar, was zu einer unwirksamen antiviralen Immunantwort führt. Die Mechanismen, die der mangelhaften adaptiven Immunität zugrunde liegen, sind nach wie vor schwer zu ergründen, was die Forschung dazu veranlasst hat, die antivirale T-Zell-Immunität durch adoptiven Transfer von gentechnisch optimierten Immunzellen wiederherzustellen. Der potenzielle Beitrag angeborener Immunzellen, wie z. B. NK-Zellen, zur Virusabwehr ist jedoch noch nicht ausreichend erforscht.

In dieser Arbeit sollen die Wechselwirkungen zwischen HBV-infizierten PHH und Immunzellen untersucht werden, insbesondere die Rolle von HLA-Molekülen, die auf menschlichen Hepatozyten bei der Erkennung von HBV exprimiert werden. Um diese Analysen durchführen zu können, sollte das chimäre Mausmodell durch den adoptiven Transfer von angepassten nicht-parenchymalen Zellen (NPC) erweitert werden. Die Erkenntnisse über die Erkennungsmechanismen könnten den Weg für neue antivirale Strategien ebnen, die auf diese Kontrollpunkte abzielen.

Unter Verwendung von chimären Mäusen mit menschlicher Leber wurden chronisch infizierte Leberproben auf HBV-induzierte Veränderungen der mRNA-Expression von HLA-Molekülen untersucht. NPCs wurden in HBV-infizierte humanisierte Mäuse übertragen, denen zur weiteren Analyse der Genexpression, der Zytokin Spiegel und der Viruslast passende Hepatozyten transplantiert wurden.

Die Analyse der HBV-induzierten Veränderungen in der mRNA-Expression von HLA-Molekülen in chimären Mausproben aus menschlicher Leber zeigt, dass HBV die HLA-Expression auf Hepatozyten nicht verstärkt, aber durch Interferone induziert werden kann. Darüber hinaus konnte gezeigt werden, dass die Rekrutierung von Lymphozyten in die Leber nach NPC-Transfer in HBV-infizierte humanisierte Mäuse erfolgreich ist, wenn auch mit unterschiedlichen Erfolgsraten. Diese Ergebnisse verdeutlichen die Ausweichtaktik von HBV und geben Hinweise auf potenzielle Marker für eine antivirale Behandlung und Möglichkeiten zur Verbesserung der Lymphozytenrekrutierung in künftigen Studien, was die heimliche Natur des Virus unterstreicht. Die Induktion von HLA-Molekülen durch IFN lässt darauf schließen, dass sie als Marker für eine antivirale Behandlung in Frage kommen.

Zusammenfassend zeigen diese Daten, dass HBV von Immunzellen erkannt wird. Das HLA-System ist also funktionsfähig. Bei chronischer HBV sind die T-Zellen jedoch nicht vorhanden (erschöpft). Über die Rolle anderer Immunzellen, wie NK-Zellen oder dendritische Zellen, bei der Immunantwort und als Auslöser von Entzündungen ist weniger bekannt. Auch die Rolle und Funktion der Interferone ist noch nicht vollständig geklärt, obwohl sie weiterhin in Kombinationstherapien mit vielversprechenden Ergebnissen eingesetzt werden. Daher sind immunkompetente Modelle für HBV von entscheidender Bedeutung, um die noch offenen Fragen der Immunantwort auf eine HBV-Infektion zu klären.

# Table of Content

<b>1</b>	<b>Introduction .....</b>	<b>1</b>
1.1	Hepatitis viruses .....	1
1.2	Hepatitis B virus.....	2
1.2.1	Epidemiology and genotypes.....	2
1.2.2	Viral structure .....	4
1.2.3	Replication cycle .....	6
1.3	Immunity against HBV.....	8
1.4	The human leucocyte antigen (HLA) system.....	12
1.5	Current treatment approaches .....	14
1.6	HBV infection models.....	16
1.6.1	<i>In vitro</i> models .....	16
1.6.2	<i>In vivo</i> models.....	17
1.6.3	Human liver chimeric mice .....	18
1.6.4	The uPA/SCID mouse model .....	20
1.7	Non-parenchymal cells.....	23
1.8	Aim of the work .....	24
<b>2</b>	<b>Materials and Methods .....</b>	<b>26</b>
2.1	Materials .....	26
2.1.1	Consumables .....	26
2.1.2	Substances .....	26
2.1.3	Devices.....	28
2.1.4	Kits .....	29
2.1.5	Antibodies.....	29
2.1.6	Probes/primers .....	32
2.1.7	TaqMan Assays .....	32
2.1.8	Cells.....	33
2.1.9	Software .....	33

<b>2.2</b>	<b>Methods.....</b>	<b>34</b>
2.2.1	Isolation and separation of matched human hepatocytes and NPCs.....	34
2.2.2	Generation of human liver chimeric mice and viral infection .....	34
2.2.3	Isolation of peripheral blood mononuclear cells (PBMC) .....	35
2.2.4	mRNA preparation, electroporation, and adoptive transfer of activated T cells .....	36
2.2.5	Adoptive transfer of activated NPC .....	37
2.2.6	Interferon (IFN) treatment.....	38
2.2.7	Virological measurements and intrahepatic quantification .....	38
2.2.8	Immunofluorescence .....	40
2.2.9	Flow cytometry .....	40
2.2.10	CFSE proliferation assay.....	42
2.2.11	Imaging mass cytometry.....	43
<b>3</b>	<b>Results.....</b>	<b>45</b>
<b>3.1</b>	<b>Analysis of HLA class I and class II expression on hepatitis infected hepatocytes <i>in vivo</i> .....</b>	<b>45</b>
3.1.1	Different induction of HLA class I molecule expression on hepatocytes in the liver of chimeric mice upon HBV, HCV and HEV infections .....	45
3.1.2	HLA class II molecule expression is not induced by infection with different hepatitis viruses on hepatocytes of liver chimeric mice <i>in vivo</i> .....	47
3.1.3	IFN-gamma treatment of HBV-infected liver chimeric mice clearly induces HLA-class I and class II mRNA expression.....	48
3.1.4	IFN-beta treatment of HBV-infected liver chimeric mice clearly induces HLA-class I and class II mRNA expression .....	53
<b>3.2</b>	<b>Analysis of non-parenchymal cell fractions isolated from different donors .....</b>	<b>56</b>
3.2.1	Characterisation of non-parenchymal cells shows donor dependent differences in lymphocyte cell composition .....	56
3.2.2	Stimulation of NPC with IL-2 and IL-15 results in proliferation of intrahepatic lymphocytes.....	59
3.2.3	NK cells can efficiently be enriched within NPC fraction using an immunomagnetic selection tool.....	64
<b>3.3</b>	<b>Establishment of the adoptive transfer of NPC into liver humanized mice harbouring matched hepatocytes infected with HBV .....</b>	<b>66</b>
3.3.1	CD45 <sup>+</sup> lymphocytes are recruited into the liver of humanized mice after adoptive transfer of NPCs.....	68
3.3.2	Analysis of HLA class I and class II expression after NPC treatment of HBV infected liverchimeric mice.....	72

3.4	Mass cytometry technique opens new possibility for imaging virus infected cells in the presence of immune cells .....	73
4	Discussion .....	79
4.1	Human leucocyte antigen molecules are not induced upon HBV infection but can be differently upregulated upon IFN stimulation .....	79
4.2	Liver-derived non-parenchymal cells can be stimulated to proliferate in cell culture after cryopreservation .....	84
4.3	Lymphocytes can be recruited into the liver of HBV-infected humanized mice after adoptive transfer of non-parenchymal cells .....	86
4.4	Immune cell recruitment can be monitored in the presence of viral markers using imaging mass cytometry technique .....	91
4.5	Final conclusions.....	92
5	References .....	95
6	List of publications .....	109
7	Ehrenwörtliche Erklärung .....	110



## Table of figures

Figure 1. Geographical distribution of HBV infections by country. ....	4
Figure 2. Schematic diagram of HBV particles.....	5
Figure 3. HBV genome, viral RNAs and proteins. ....	<b>Fehler! Textmarke nicht definiert.</b>
Figure 4. The hepatitis B virus replication cycle. ....	7
Figure 5. Generation of liver humanized mice and infection with HBV. ....	<b>Fehler! Textmarke nicht definiert.</b>
Figure 6. Gating strategy for flow cytometry analysis.....	42
Figure 7. Expression levels of HLA class I molecules are not induced upon infection with HBV. ....	<b>Fehler! Textmarke nicht definiert.</b>
Figure 8. Relative expression of HLA complexes on hepatocytes infected with different hepatitis viruses. ....	<b>Fehler! Textmarke nicht definiert.</b>
Figure 9. Expression of different HLA class I and class II complexes on human HBV infected hepatocytes after treatment with IFN-gamma protein. <b>Fehler! Textmarke nicht definiert.</b>	
Figure 10. Expression of different HLA class II complexes on human HBV infected hepatocytes after treatment with IFN-gamma producing T cells. ....	<b>Fehler! Textmarke nicht definiert.</b>
Figure 11. Expression of different HLA complexes on human HBV infected hepatocytes after treatment with IFN-gamma producing T cells.....	<b>Fehler! Textmarke nicht definiert.</b>
Figure 12. Expression levels of different HLA class I and class II complexes on human HBV-infected hepatocytes after treatment with IFN alpha, beta or lambda. ....	<b>Fehler! Textmarke nicht definiert.</b>
Figure 13 Characterisation of human NPC thawed after cryopreservation. <b>Fehler! Textmarke nicht definiert.</b>	
Figure 14.Flow cytometric analysis of lymphocyte population derived from non-parenchymal cells under different stimulation in vitro indicate differences in cell proliferation upon stimulation. ....	<b>Fehler! Textmarke nicht definiert.</b>
Figure 15. Cell culture analysis of non-parenchymal cells demonstrates cell proliferation of hepatic lymphocytes. ....	<b>Fehler! Textmarke nicht definiert.</b>
Figure 16. Natural killer cells can be enriched from NPC fraction.....	65
Figure 17.Scheme of the adoptive cell transfer of NPC into liver humanized mice chronically infected with HBV.....	<b>Fehler! Textmarke nicht definiert.</b>
Figure 18. NPCs can be recruited into the liver of HBV-infected USG mice and reduce HBV viremia. ....	<b>Fehler! Textmarke nicht definiert.</b>
Figure 19. Upregulation of cytokines involved in lymphocyte signalling and HBV cell killing. <b>Fehler! Textmarke nicht definiert.</b>	
Figure 20. Identification of lymphocyte population that infiltrates the liver of humanized mice after NPC transfer.....	71

Figure 21. HLA class I and class II were clearly induced after treatment with NPC. ....	73
Figure 22. Imaging mass cytometry adapted for cryopreserved chimeric liver tissue. ....	75
Figure 23. IMC data analysis of HBV viral proteins within human hepatocytes. ....	76
Figure 24. IMC data analysis of HBV viral proteins within human hepatocytes. ....	77
Figure 25. IMC data analysis of human liver tissue. ....	77

## Table of tables

Table 1   List of consumables .....	26
Table 2   List of substances .....	28
Table 3   List of devices.....	29
Table 4   List of kits .....	29
Table 5   List of antibodies.....	32
Table 6   List of primers and probes .....	32
Table 7   List of TaqMan assays .....	33
Table 8   List of cells.....	33
Table 9   List of used software.....	34

## Abbreviations

Alb	Albumine
ALT	Alanine aminotransferase
AMP	Adenosine monophosphate
APC	Antigen presenting cell
APOBEC3	Apolipoprotein B mRNA editing enzyme, catalytic polypeptide 3
ATP	Adenosine triphosphate
BL	Baseline
BSA	Bovine serum albumin
CAM	Capsid assembly modulators
CAR-T	Chimeric antigen receptor T cell
CAS	Caspase
cccDNA	Covalently closed circular DNA
CD	Cluster of differentiation
cDNA	Complementary DNA
CFSE	Carboxyfluorescein diacetate succinimidyl ester of CFDA SE
cGAS	Cyclic GMP-AMP-synthase
CHB	Chronic hepatitis B
CK18	Cytokeratin-18
CTL	Cytotoxic lymphocyte
CXCL10	C-X-C motif chemokine ligand 10
CyTOF	Cytometry by time of flight
DC	Dendritic cell
DMSO	Dimethyl sulphoxide
DNA	Deoxyribonucleic acid
EDTA	Ethylenediaminetetraacetic acid
EGFR	Epidermal growth factor receptor
ELISA	Enzyme-linked immunosorbent assay
ES	End serum
FACS	Fluorescence associated cell sorting

FAH	Fumaryl acetoacetate hydrolase
FCS	Fetal calf serum
FFPE	Formalin-fixed paraffin-embedded
FSC	Forward scatter
Fw	Forward
GAPDH	Glyceraldehyde 3-phosphate dehydrogenase
GMP	Guanosine monophosphate
GWASs	Genome-wide association studies
GZMB	Granzyme B
HBc	Hepatitis B core protein
HBcAg	Hepatitis B core antigen
HBeAg	Hepatitis B envelope antigen
HBsAg	Hepatitis B surface antigen
HBV	Hepatitis B virus
HBxAg	Hepatitis B x antigen
HCC	Hepatocellular carcinoma
HCV	Hepatitis C virus
HDV	Hepatitis D virus
HEV	Hepatitis E virus
HIV	Human immunodeficiency virus
HLA	Human leucocyte antigen
HSA	Human serum albumin
HSC	Hepatic stellate cell
HSPG	Heparan sulphate proteoglycan
i.p.	Intraperitoneal
IFI16	Interferon-gamma inducible protein 16
IFN	Interferone
IKK	I $\kappa$ B kinase
Il2rg	Il-2 receptor gamma
Il2rg	Interleukin
IMC	Imaging mass cytometry
ImmTAV	Immune mobilising monoclonal T cell receptors against virus

IRF3	Interferon regulatory factor 3
ISG	Interferon-stimulated gene
IU	International units
JAK	Janus kinase
KC	Kupffer cell
LLoD	Low limit of detection
LSEC	Liver sinusoidal endothelial cell
MACS	Magnetic associated cell sorting
MAIT	Mucosal-associated invariant T cell
MAVS	Mitochondrial antiviral signalling protein
MDA5	Melanoma differentiation-associated gene 5
MHC	Major histocompatibility complex
mRNA	Messenger RNA
MxA	Myxovirus resistance protein 1
MYd88	Myeloid differentiation primary response gene 88
NA	Nucleos(t)ide analogues
NK cell	Natural killer cell
NKT cell	Natural killer T cell
NPC	Non-parenchymal cell
NTCP	Sodium taurocholate cotransporting peptide
ORF	Open reading frame
PAMP	Pathogen-associated molecular pattern
PBMC	Peripheral blood mononuclear cell
PBS	Phosphate buffer saline
PCR	Polymerase chain reaction
PEG	Polyethylene glycol
pen/strep	Penicillin/streptomycin
PFA	Paraformaldehyde
pgDNA	Pregenome DNA
PHH	Primary human hepatocyte
pol	Polymerase
PRR	Pattern recognition receptor

qRT-PCR	Quantitative real-time PCR
rcDNA	Relaxed circular DNA
RIG-I	Retinoic acid-inducible gene I
RLR	RIG-I-like receptor
RNA	Ribonucleic acid
ROI	Region of interest
RPL30	Ribosomal protein L30
RT	Reverse transcriptase
SCID	Severe Combined Immune Deficiency
siRNA	Small interfering RNA
SNP	Single nucleotide polymorphism
SSC	Side scatter
STAT1	Signal transduction and activator of transcription 1
STING	Stimulator of interferon gene
TAK1	Transforming growth factor- $\beta$ activated kinase 1
TCR	T cell receptor
TLR	Toll-like receptor
TRIF	TIR-domain containing adapter-inducing interferon-beta
TSA	Tyramide Signal Amplification
tSNE	T-distributed stochastic neighbor embedding
uPA	Urokinase plasminogen activator

# 1 Introduction

## 1.1 Hepatitis viruses

Viral hepatitis is a global public health problem affecting hundreds of millions of people and causing thousands of deaths from acute and chronic infections, cirrhosis and liver cancer. To date, five viruses (hepatitis A, B, C, D and E) have been identified that selectively infect the liver [1].

Hepatitis A virus (HAV) is a single-stranded RNA virus that is not or quasi-enveloped. It primarily uses the faecal-oral route of transmission and causes an acute self-limited infection. A major challenge is to increase HAV vaccination coverage worldwide to reduce new infections and achieve eradication of the virus.

Similar to HAV, hepatitis E virus (HEV) is also a single-stranded RNA virus that is not or quasi enveloped. HEV is mainly transmitted by faecal-oral and food-borne routes. In most of the cases HEV is self-limiting but in immunosuppressed patients the infection can become chronic [2]. Only one vaccine against HEV has been licensed in China, and data are limited, limiting its use [1].

Hepatitis C virus (HCV) is an enveloped single-stranded RNA virus. HCV is mainly transmitted by exposure to infected blood and causes both acute and chronic infection, with a high chronic infection rate of 80% [1]. There are numerous HCV vaccine approaches, including some candidates that have completed phase I trials, but a prophylactic HCV vaccine that can contribute to the goal of eradication remains an open question. However, the use of direct antiviral agents (DAAs) has revolutionised HCV therapy, allowing interferon-free therapies with high cure rates (>98%) and is the first curable hepatitis virus that causes chronic infection [3].

The hepatitis B virus (HBV) is the only hepatitis virus harbouring a DNA genome, a partially double-stranded DNA virus. This enveloped virus causes both acute and chronic infection. However, the course of infection is strongly age-related, with a high chronicity in children below the age of 5 (>90%), compared to adults (<5%). HBV is predominantly transmitted

by vertical and parenteral routes. Protection from HBV infection is possible through vaccination. Chronic HBV infection (CHB) can be treated with various drugs. However, there is currently no cure [1, 2].

The smallest member of the hepatitis family is the hepatitis D virus (HDV). This virus is a single-stranded and enveloped RNA virus. Similar to HBV, it causes both acute and chronic infection via the parenteral route of transmission [1]. HDV is also known as a satellite virus, since it uses the envelope proteins expressed by HBV to become enveloped and release HDV infectious particles [4]. Therefore, HDV is usually associated with HBV superinfection but HBV/HDV co-infections also occur [5]. The only way to protect against HDV infection is by HBV vaccination. Chronic HDV infections are treated with Peg-IFN-alpha [1].

## **1.2 Hepatitis B virus**

### **1.2.1 Epidemiology and genotypes**

Chronic hepatitis B is a serious infectious liver disease that often progresses to liver cirrhosis and hepatocellular carcinoma in humans [6]. Hepatitis B virus (HBV) is a noncytopathic virus of the Hepadnaviridae family that exclusively infects hepatocytes [7]. Infection with this small enveloped DNA virus, first discovered by Baruch Blumberg in 1967 [8], can lead to either an acute or chronic course [9]. However, clinical outcomes following viral exposure vary widely between patients [6]. The severe outcome of chronic HBV infection with a strong liver injury is mainly due to the host immune response leading to persistence of viral replication [7]. In untreated patients with CHB the progression to liver cirrhosis or liver cancer occurs in 15-40% of cases [10, 11]. Despite the availability of an effective vaccine, the World Health Organization estimates that there are at least 296 million chronically HBV-infected patients worldwide in 2019 and 1.5 million new infections each year. Moreover, deaths from HBV-related liver disease are estimated to exceed 1.1 million per year for 2022 [12]. These figures highlight the need to develop effective treatments that focus on curing HBV infection.

The main modes of HBV transmission are diverse but require contact of infectious blood or body fluids with blood of healthy individuals. In countries defined as high prevalence areas, perinatal transmission from mother to child during birth is the predominant mode

[13, 14], followed by horizontal transmission (exposure to infected blood in the absence of sexual contact or perinatal modes of spread), especially between infected children and uninfected children before the age of 5 years [15]. In areas with low prevalence, hepatitis B cases are predominantly attributed to unprotected sexual contact or needlestick injuries [16]. The likelihood of developing chronic HBV infection is strongly related to age. Acute infections acquired in adults resolve spontaneously in 95% of cases, whereas 95% of infected children below the age of 5 develop CHB [17].

Acute HBV infection appears asymptomatic in up to 70% of cases [11], but symptoms may include yellowing of the skin and eyes, dark urine, fatigue, weight loss, fever and/or abdominal pain [7]. The diagnosis of HBV infection and the differentiation between acute and chronic HBV infection is based on the detection of different serum markers. During the acute phase of infection HBV S antigen (HBsAg) and anti-HBV core antigen (HBcAg) IgM are measurable. There is additional protein secreted, the HBV e antigen (HBeAg) [18]. Failure to lose HBsAg after 6 months indicates that HBV infection has become chronic [19]. Measurement of serum viral DNA is an additional marker for HBV diagnosis and phase of classification [20].

Seroprevalence studies for HBsAg in the world population estimated the global prevalence of chronic HBV in all ages to be 4.1% in 2019, with the highest prevalence in the Western Pacific region (7.1%), followed by the African region (6.5%). The European region had the lowest HBV prevalence, at 1.1% [21]. The variation in HBV prevalence by country in 2019 is shown in **Figure 1**.

Today, 10 different major viral variants are known (A-J). Analysis of genotyping data suggests that most HBV infections worldwide (~96%) are caused by 5 of these genotypes (A-E) [22]. These data also show the geographical distribution of HBV around the world. Genotype A is most prevalent in East Africa and Northwestern Europe with an estimated 17% share of global HBV infections. In Southeast Asia and Oceania, genotypes B (14% of global HBV infections) and C (26% of global HBV infections) are prevalent. Genotype D is largely distributed over Southern Europe, Middle Eastern and Central Asia showing a share of 22% of global HBV infections. West Africa is mostly affected by genotype E (18% of global HBV infections). While genotype F is mainly restricted to South America, genotype G affects only the United States of America and Mexico. In Mexico, however, HBV infection is predominantly associated with genotype H. Genotype I is found only in Laos and Vietnam.

Genotypes F to I together are responsible for only ~1% of all HBV infections worldwide. The most recently recovered genotype J has been identified in Japan [23]. These data are represented in **Figure 1**.

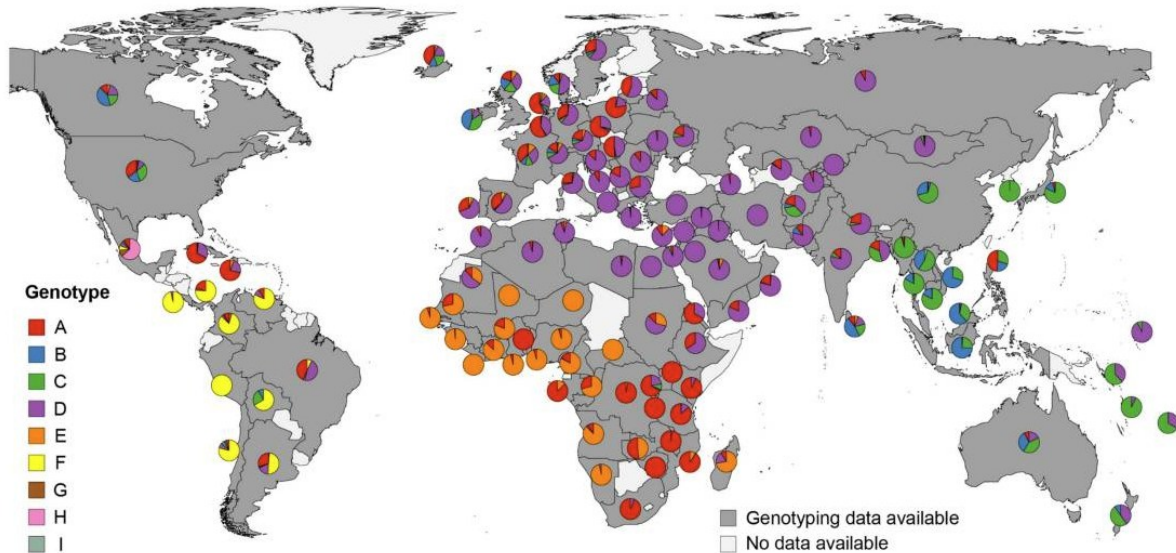


**Figure 1. Geographical distribution of HBV infections by country.** The proportional HBV genotype distributions are indicated as pie charts. Only countries with successful genotyping are presented. Recombinant viruses and co-infections with different genotypes are excluded [22].

### 1.2.2 Viral structure

The hepatitis B virus is a non-cytopathic DNA virus with high liver tropism and species specificity [24, 25]. Dane and colleagues first visualized three types of HBV particles via electron microscopy in the serum of infected humans (**Figure 2**) [26]. These particles include spheres with a diameter of 22 nm, and filamentary structures with the same diameter of 22 nm but have a variable length of 80-400 nm [27]. These particles do not contain the viral genome and are not infectious. The third particle is the infectious virion (Dane particle). It has a double-shelled spherical structure with a diameter of 42 nm. The outer lipid membrane contains the three HBV surface proteins and forms the viral envelope, which confers resistance to the environment. The inner layer is the nucleocapsid, which is assembled by the hepatitis B core protein (HBcAg) and contains the viral DNA genome polymerase (Pol)[27-30].

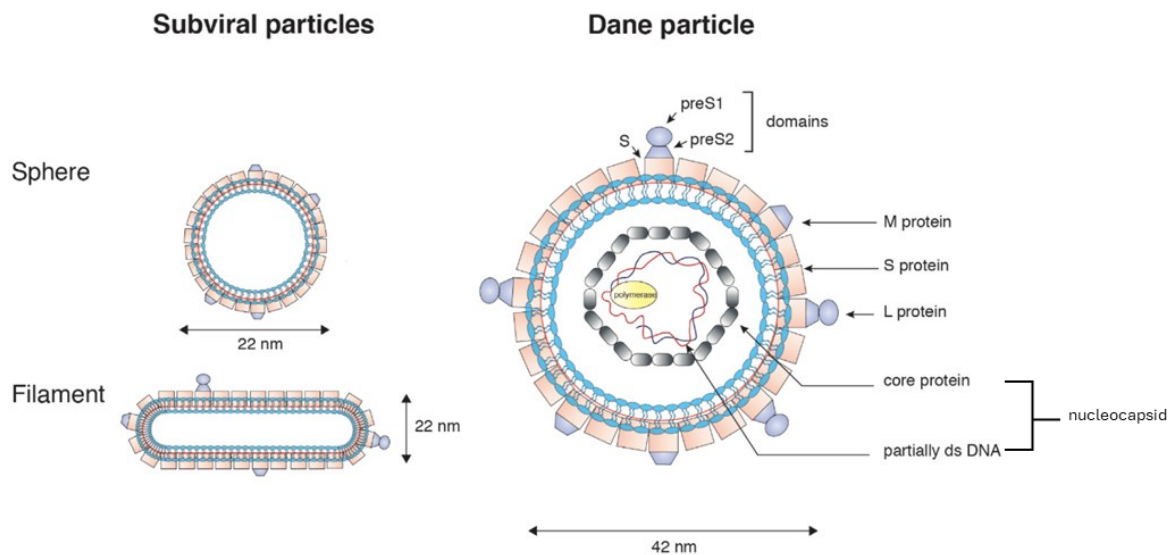


**Figure 2. Schematic diagram of HBV particles.**

Three viral particles are described for hepatitis B virus. The outer lipid membrane contains the three HBV surface proteins (S, M, L) and forms the envelope. Spheres and filaments do not contain the viral genome and are consequently not infectious. The infectious Dane particle additionally includes nucleocapsid, which is formed by HBV core protein and consists the viral partially double-stranded DNA and DNA polymerase. Adapted from Herrscher et al. [30].

The HBV genome is a relaxed circular, partially double-stranded DNA (rcDNA) of approximately 3.2 kb pairs. The coding minus (-) strand is complete and its 5' end is covalently bound to the viral polymerase [31, 32]. In contrast, the non-coding plus (+) strand contains a fixed 5' end and an incomplete variable size 3' end [33]. This very compact genome contains four distinct overlapping open reading frames (ORFs) encoding the four genes C, P, S and X, which produce 7 functional proteins [29, 34] (**Figure 3**). The C gene encodes for two proteins. The core protein (HBcAg) has a structural role in the formation of the nucleocapsid. Hepatitis e antigen (HBeAg) is derived from both the pre-core (pre-C) and core (C) domains and is reported to be involved in immune evasion. While the P gene encodes for the viral polymerase, the regulatory X protein (HBxAg) is derived from the X region [35]. The three surface proteins small (S), medium (M) and large (L) are produced from the S region which is divided into three domains: pre-S1, pre-S2 and S [36].

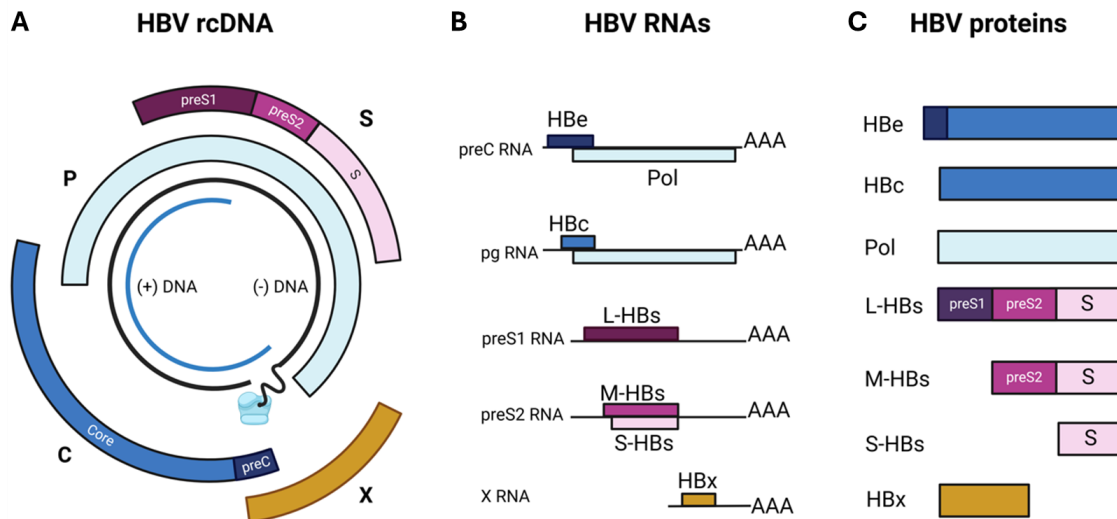


**Figure 3. HBV genome, viral RNAs and proteins.**

HBV genome (black line) is linked with the polymerase (turquoise) (A). The four ORFs are shown as coloured ribbon and consist of the *preS1*, *preS2* and *S* genes (pink), the polymerase gene (turquoise), the *preC/Core* genes (blue) as well as the *X* gene (orange). Five different mRNAs are transcribed during viral replication, the two genomic *preC* and *pg* RNA as well as the three subgenomic *preS1*, *preS2* and *X* RNAs (B). All RNAs share a common poly-A tail. Seven viral proteins are translated from five viral mRNAs (C).

### 1.2.3 Replication cycle

The proliferation of HBV within its host hepatocytes follows a unique strategy, using both viral proteins and host derived factors to form new virions and exhibiting a sophisticated mechanism to evade the host immune system.

Multiple steps are required to internalize the HBV virion into the hepatocyte. This process is still not completely decrypted. However, the identification of the sodium taurocholate cotransporting peptide (NTCP) as an entry receptor for HBV internalization in 2012 was a major step towards unravelling the complete process [37]. NTCP is exclusively located in the cell membrane of the hepatocyte and is a symporter for bile acids into hepatocytes [38]. Once in the liver, the earliest step of the HBV entry is mediated by the binding to factors including heparan sulphate proteoglycans (HSPGs) on the hepatocyte surface in a non-specific and low affinity manner [39, 40]. Subsequently, the pre-S1 region of HBV binds with high affinity to NTCP [41]. This virus-receptor interaction is considered to provoke virus internalization via endocytosis [42, 43]. In addition, epidermal growth factor receptor (EGFR) has been reported to act as a cofactor for HBV entry [44, 45].

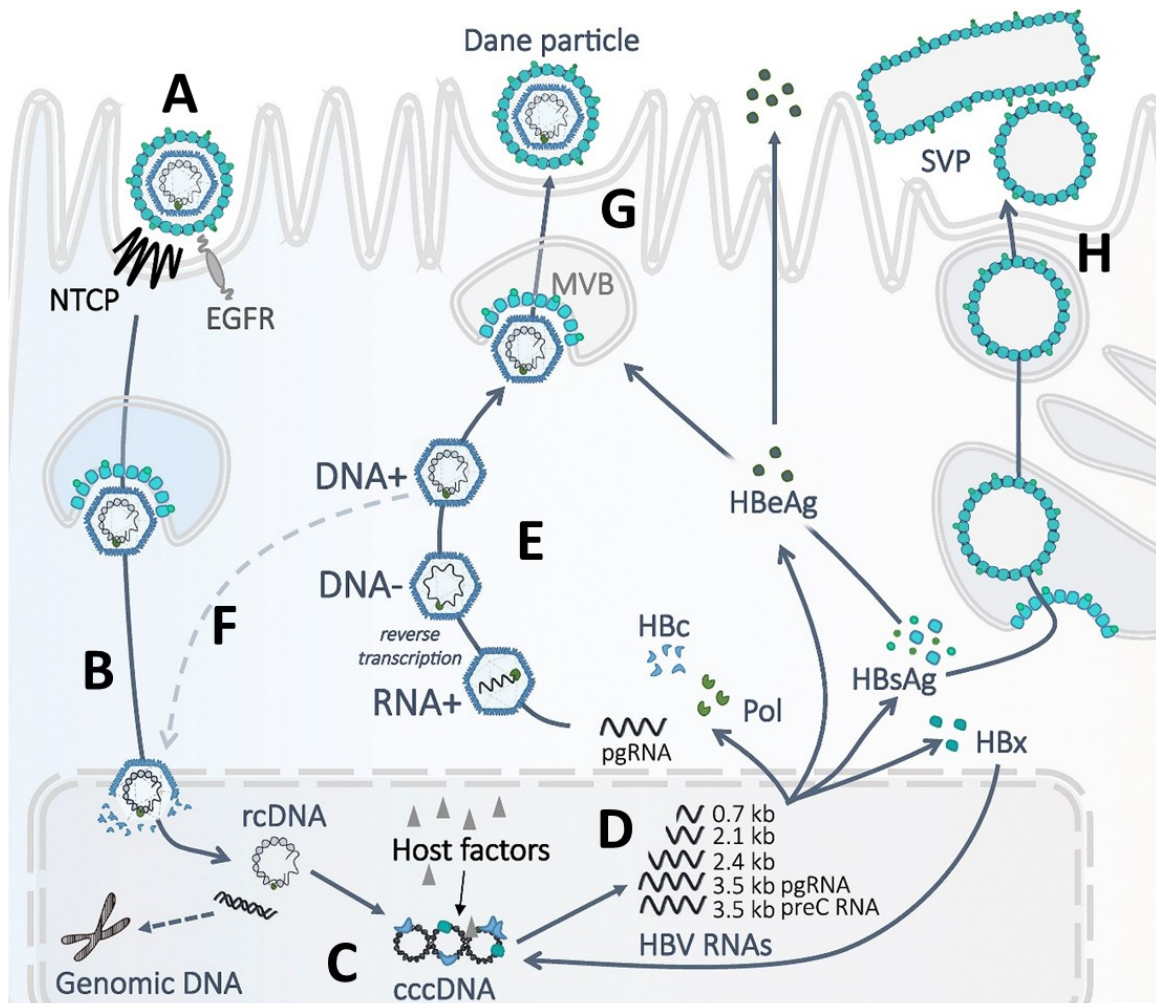


**Figure 4. The hepatitis B virus replication cycle.**

Binding of HBV to NTCP receptor (A). Internalization of HBV, supported by EGFR, and release of the nucleocapsid. rcDNA, HBcAg and polymerase containing nucleocapsid is transported to the nucleus through nuclear pore complex (B). Formation of cccDNA minichromosome (C). cccDNA is transcribed by host polymerase to viral RNAs (D). HBcAg, viral polymerase and pgRNA form the nucleocapsid and reverse transcription synthesizes viral rcDNA (E). Genome containing nucleocapsid can either re-enter the nucleus (F) or be released from host cell via MVB(G). SVPs are released via general secretory pathways (H). Adapted from [29].

As a result of the viral entry, the rcDNA containing nucleocapsid is released into the cytoplasm and transported microtubule-mediated to the nucleus, where it enters through the nuclear pore complex [46, 47]. Next, host cellular factors release the viral polymerase from the (-) strand of the rcDNA, while the (+) strand is completed and remaining gaps are filled by DNA polymerases, ligases and topoisomerases [48-50]. This ultimately leads to the formation of the covalently closed circular DNA (cccDNA) [51]. This molecule, also

known as the minichromosome, serves as a viral transcription template for all viral mRNAs, remains stable within the infected hepatocyte, and thus appears to be responsible for HBV persistence [52, 53].

Several types of genomic and subgenomic RNAs are transcribed and transported to the cytoplasm. All transcripts are unspliced, polyadenylated and have a 5' cap structure. There are two types of genomic RNA, pregenome (pg) RNA and precore mRNA, which differ in their 5' ends. While precore mRNA is used as a template for the translation of the HBeAg, pgRNA is translated into HBcAg by the viral polymerase and serves as a template for the viral transcription. Three subgenomic mRNAs are transcribed, which serve as templates to produce the viral envelope proteins and the regulatory HBx protein [29, 54, 55]. The viral polymerase and pgRNA interact to form a ribonucleoprotein complex that is incorporated into a capsid that is self-assembled by HBcAg [56, 57]. Once RNA incorporation is complete, reverse transcription of the pgRNA by the viral polymerase is initiated. The polymerase uses its RNase H domain to degrade the template while synthesizing the (-) strand at the same time. Thereafter, the (+) strand is transcribed from the (-) strand of the rcDNA [29]. Genome-containing nucleocapsids are enveloped by HBs proteins and secreted outside the hepatocyte through multivesicular bodies (MVBs) with the help of the endosomal sorting complex required for transport (ESCRT) machinery [58]. Otherwise, nucleocapsids are transported back to the nucleus where they amplify the cccDNA pool [59]. Subviral particles (SVPs), which do not contain viral DNA, are also assembled from HBsAg and released from the endoplasmic reticulum via general secretory pathways [60] (

Figure 4).

### **1.3 Immunity against HBV**

Activation of innate immune responses is the first line of defence against infiltrating microbial pathogens, such as viruses. In principle, the innate immune system follows an activation protocol to respond to viral infections. First step is the recognition and binding of pathogen-associated molecular patterns (PAMPs), which are small molecular motifs

highly conserved across pathogens. There, PAMPs are sensed by pattern recognition receptors (PRRs) localized either on the cell surface or within several intracellular compartments [61]. These PRRs encompass the group of transmembrane Toll-like receptors (TLRs) as well as cytosolic DNA sensors, e.g. cyclic GMP-AMP-synthase (cGAS), and cytosolic RNA sensors, e.g. retinoic acid-inducible gene I (RIG-I)-like receptors (RLRs). The RNA sensors RIG-I and melanoma differentiation-associated gene 5 (MDA5) specifically identify viral proteins and nucleic acids [62]. Upon activation, these receptors recruit various adaptor proteins, e.g. myeloid differentiation primary response gene 88 (Myd88), mitochondrial antiviral signalling protein (MAVS), stimulator of interferon genes (STING), interferon-gamma inducible protein 16 (IFI16) and TIR-domain containing adapter-inducing interferon-beta (TRIF), which initiate downstream signalling to rapidly induce the production of type I/III interferons and other inflammatory cytokines in the infected cell [63, 64]. As a result, secreted interferons (IFNs) induce the expression of many interferon-stimulated genes (ISGs), the products of which then inhibit viral replication [65]. Inflammatory factors and ISG products can mediate the degradation of viral DNA, RNA, and proteins [66, 67] and recruit innate immune cells. In addition, innate immune cells respond to viral infection.

Natural killer (NK) cells can directly recognize virus-infected cells. Dendritic cells (DCs) in addition to macrophages can engulf viral components [68-70]. Located exclusively in the liver, liver sinusoidal endothelial cells (LSECs) and hepatic stellate cells (HSCs) also contribute to the innate immune cell group [64, 71]. These responses to viral attacks usually control the infection until it is cleared by the adaptive immune system [72].

The crosstalk between HBV-infected hepatocytes and immune cells involves complex interactions that significantly influence the immune response and the course of the infection. Key interactions involve the viral antigen presentation of hepatocytes by human leucocyte antigen (HLA) class I molecules. This presentation is crucial for activation of CD8<sup>+</sup> cytotoxic T cells, which recognize and destroy HBV-infected T cells. CD4<sup>+</sup> helper T cells can also be activated and assist in orchestrating a broader immune response [73]. As a next important step, the activated T cells release cytokines (IFN-gamma; tumour-necrosis factor (TNF)-alpha) that enhance the antiviral state within hepatocytes and recruit additional immune cells to the site of infection. NK cells play a significant role in the early stages of HBV infection by directly killing infected hepatocytes. They also secrete cytokines like IFN-

gamma, which modulate the activity of T cells and macrophages. However, in chronic HBV infection, NK cells can suppress CD8<sup>+</sup> T cells through the expression of TRAIL (TNF-related apoptosis-inducing ligand), contributing to immune dysfunction [74]. HBV has developed mechanisms to evade the immune response. For example, HBV-infected hepatocytes can produce large amounts of viral proteins that may interfere with the function of T cells [75]. Additionally, HBV can modulate the immune environment to create a tolerogenic state, reducing the effectiveness of T cell-mediated clearance. In chronic HBV infection, the immune system often fails to completely clear the virus. This is partly due to the continuous presence of viral antigens, which can lead to T cell exhaustion or anergy [73]. The persistent antigenic stimulation can cause T cells to become less effective over time. Regulatory T cells can also be involved in HBV infection. They help maintain immune tolerance and prevent excessive inflammation, but in the context of chronic HBV infection, they might contribute to the suppression of effective antiviral responses [73-75]. In summary, the interaction between HBV-infected hepatocytes and immune cells is a dynamic process involving antigen presentation, immune cell activation, cytokine release, and immune evasion. The balance of these interactions can determine the outcome of HBV infection, ranging from clearance to chronic disease.

Resolution of acute HBV infection, which occurs in 95% of immunocompetent adults and results in long-lasting immunity, requires an effective viral recognition strategy and well-orchestrated induction of innate and adaptive immune responses [61, 76]. During acute self-limited HBV infection, CD4<sup>+</sup> and CD8<sup>+</sup> T cell responses react strong and polyclonal, whereas in CHB patients' immune responses are weak and undirected, resulting in the persistence of high antigen loads and thus suppression of virus-specific T cell immunity [76-78]. However, the mechanisms involved in innate immune activation during HBV infection appear to be incompletely understood but are urgently needed [66]. Due to the early asymptomatic phase of HBV infection, it appears to be very difficult to collect patient material for further investigation [76, 79]. Therefore, appropriate infection models that mimic natural HBV infection are needed to study innate immune mechanisms.

Primary human hepatocytes (PHHs) are capable of sensing various pathogens, such as hepatitis C virus, due to their broad expression of PRRs [80-82]. Nevertheless, HBV remains poorly detectable by the innate sensing machinery [72] and therefore it has been termed a "stealth virus" due to its ability to evade the activation of the innate immune

system [83]. However, the mechanism by which HBV protects itself from innate immune recognition is still partially unknown [72], but the ability of the HBV genome to persist as a minichromosome within the hepatocyte nuclei appears to be a key replication strategy to evade host immune recognition [61]. Moreover, HBV RNAs are 5' capped and 3' polyadenylated (polyA-tailed) by cellular enzymes, so that they are similar to host mRNAs. An unusual hairpin loop, identified as a packaging signal on HBV pgRNA, induced cytosolic RIG-I under specific experimental conditions [56, 84]. The encapsulation of replicating RNA/DNA genomes within cytoplasmic nucleocapsid particles is also involved in immune escape mechanism [85].

The detection of HBV by innate immune components and the subsequent initiation of antiviral responses is controversially discussed and many aspects remain to be elucidated [86]. However, studies in chimpanzees and patients with acute HBV infection have failed to demonstrate the induction of type I/III IFNs or a clear enhancement of ISGs [87, 88]. Similar results were shown for the early phase of infection in a woodchuck model [89], and minimal or no significant IFN/ISG response was detected in HBV-infected human liver chimeric mice [84, 90, 91]. And *in vitro* studies demonstrate the inability of HBV-infected hepatocytes to induce cell-intrinsic immune responses [92].

HBV has been reported to abort cell intrinsic immunity by actively suppressing TLR pathways *in vitro* [93, 94]. Moreover, the abortion prevents the induction of IFN- $\alpha$  signaling by inhibiting the nuclear translocation of signal transduction and activator of transcription 1 (STAT1) demonstrated using a chimeric mouse model [95]. The viral proteins HBxAg, HBeAg, HBsAg, HBcAg and HBV polymerase have been shown to inhibit the activation of TLR [96-99], the JAK/STAT pathway, RIG-I and IRF3 [100, 101] and TAK1/IKK [102-104] and thus hinder the upregulation and production of pro-inflammatory cytokines and interferons [72]. The IFN-induced MxA protein is a key antiviral protein kinase that can be inhibited by HBcAg [72, 105]. While pro-inflammatory cytokines are weakly induced, the production of suppressing molecules (IL-10, arginase) is actively forced, which is discussed to be the reason for an asymptomatic course during the acute phase of infection [72, 86, 88, 106]. However, the use of different experimental approaches, representing different phases of HBV infection, and overexpression of viral proteins, in addition to the use of recombinant viral proteins, may partly explain the controversial data [61, 86]. In addition, different HBV genotypes can induce different innate immune responses.

## 1.4 The human leucocyte antigen (HLA) system

The HLA system is involved in the regulation of immune responses [107]. It can be divided into class I and class II molecules. HLA class I molecules include HLA-A, HLA-B and HLA-C, which are known as the classical HLA molecules. Their genes encode for the heavy chain of class I molecules [108]. In addition, HLA-E, HLA-F and HLA-G are members of the HLA class I family, but belong to the non-classical group of HLA class I (Ib) group [109], which has a limited polymorphism restricted expression pattern [110].

HLA class II molecules include the DR gene family, spanning from a single DRA gene up to nine DRB genes (DRB1-DRB9), the DP family and the DQ family, both of which have an expressed gene for the alpha chain and beta chain (DQA1 and DQB1; DRA1 and DRB1) [108].

Whereas class I molecules show surface expression on almost all nucleated cells, class II expression is restricted to B lymphocytes and antigen-presenting cells. The presentation of processed virus-derived foreign antigens on the surface of an infected cell and the recognition of these HLA-peptide complexes by CD8<sup>+</sup> cytotoxic T cells and/or CD4<sup>+</sup> T helper cells is one of the key factors in the modulation of immune responses against viruses [111, 112]. The interaction of HLA-restricted T lymphocytes, antibody-secreting B lymphocytes, NK cells and cytokines is required to develop a functional immune response to viral infections [113]. Both, HLA class I and class II genes are highly polymorphic and can affect the outcome of infections by manipulating the ability of HLA proteins to elicit immune responses [114, 115]. The HLA system is a host factor that correlates with the outcome of HBV infection [115]. HBV-derived peptides presented by HLA class I to cytotoxic lymphocytes (CTLs) are essential for clearance of HBV infection. They raise the ability of CTLs to induce the identification and killing of HBV-infected cells [115-117]. Previous studies have demonstrated associations of certain HLA class I genes with disease progression [115, 118]. However, this relationship does not seem to be universal as the analysed groups are different [118].

Polymorphism studies determining the effects of different HLA class I genes show that there are protective polymorphisms and those associated with a more severe outcome of

HBV infection [118-120]. However, less is known about the underlying molecular mechanisms that contribute to either protective or severe outcomes of HBV infection. Tan et al. demonstrated that even minimal differences in HLA class I molecules can significantly alter CD8 T cell responses during acute HBV infection [121]. The kinetics and efficiency of HLA class I presentation during acute and chronic infections remain to be thoroughly investigated. Understanding these changes could reveal new therapeutic targets by clarifying the role of HLA class I in activating T cell immune responses. Interestingly, unlike HBV, HLA class I expression is significantly increased in HCV-infected hepatocytes. Functional impairment of T cell responses has been described as a hallmark of the development of chronic HCV infection [122]. Certain HLA class I alleles provide protection by facilitating rapid antigen processing and preventing viral escape mutations [123, 124]. Lunemann et al. highlighted that HLA-F is induced during HCV infection, leading to the activation of NK cells via KIR3DS1, which helps control the infection. While protective HLA class I alleles have also been found for HBV infection, a similar mechanism has not yet been clarified [125].

The proteogenomic-based identification of an increasing number of HLA-restricted viral peptides is leading to a rapidly expanding repertoire of targets for immunotherapeutics against HBV-infected tissues. These include bispecific antibodies, engineered T cell receptors (TCRs) or chimeric antigen receptor T cells (CAR-Ts). Indeed, the genetic variability between different HBV strains as well as differences in the HLA allele repertoire of patients pose difficulties for the development of therapeutics against these targets [112]. Therefore, it is crucial to analyse specific allele variants associated with disease progression and viral clearance in CHB in different ethnic groups.

Genome-wide association studies have recently shown a significant correlation of HBV disease progression with single nucleotide polymorphisms (SNPs) near the locus of the HLA class II molecules HLA-DP, HLA-DQ and HLA-DR [115, 126-128]. In particular, SNPs within the HLA-DP  $\beta$  chain have been identified as major genetic risk factor for chronic HBV infection within different ethnicities (rs3077 and rs9277535 for Asian populations; rs9277534 for European and African-American populations) [6, 129]. Clearance of acute HBV infection is mediated by CD8<sup>+</sup> and CD4<sup>+</sup> T cells, which secrete high levels of IFN-gamma and TNF-alpha [87, 130, 131]. However, solely T cell-based models alone cannot explain the association between low HLA-DP expression and protection against chronic

HBV because of the weak T cell immunogenicity of these low-expressed HLA-DP molecules associated with rs9277534 [132, 133]. A subset of low-expressed HLA-DPB1 was newly identified as new ligands for the activating NK cell receptor NKp44 [134]. NK cells contribute to the cytotoxic innate effector cells involved in the elimination of virus-infected cells [107, 135]. An increased number of peripheral NK cells after HBV infection suggests a potential role in the early clearance of the infection [65, 88]. Moreover, during the chronic stage of HBV infection NK cells have been suggested to contribute to liver damage [136-138]. However, the molecular mechanisms underlying NK cell recognition of HBV-infected hepatocytes, and their support of viral clearance are insufficiently understood.

In summary, the HLA system with its highly polymorphic HLA genes is an essential component in the activation of the host immune system. HLA gene variations appear associated with some susceptibility or resistance to HBV, as well as spontaneous clearance, disease progression, response to vaccination and efficacy of viral treatments [115]. Further studies are needed to establish the role of HLA molecules in the context of HBV sensing.

## **1.5 Current treatment approaches**

The hepatotropic and non-cytopathic hepatitis B virus can establish a persistent infection leading to varying degrees of hepatic inflammation with a high risk of developing liver cirrhosis and hepatocellular carcinoma (HCC) [139]. The enormous number of CHB patients (nearly 300 million individuals worldwide ) [16] and the high number of HBV-related deaths each year highlight the need for potent antiviral treatment that can completely eradicate the infection. Unfortunately, this is still a future goal [140]. The inability of the immune system to recognize and eliminate HBV-infected cells is the greatest challenge to finding a cure [141].

Current treatments for CHB involve the administration of nucleos(t)ide analogues (NAs) and PEGylated interferon-alpha (PEG-IFN-alpha), but do not achieve a functional cure [142]. In contrast to an absolute cure of the infection, in which the virus is eradicated from the host serum and from every infected cell, a functional cure is achieved by the loss of HBsAg and undetectable HBV DNA for a sustained period of time following finite treatment with or without seroconversion [143], alanine aminotransferase levels are normal

and hepatitis B surface antibodies (anti-HBsAg) are developed [139]. PEG-IFN-alpha is a potent drug for enhancing the host anti-viral immune response [141] and can epigenetically suppress the transcriptional activity of the cccDNA [144]. However, IFN-alpha therapy is only responsive in 30% of HBsAg-positive and 40% of HBeAg-negative cases [145-147]. In addition, IFN-alpha therapy is associated with serious side effects spanning from psychiatric effects over bone marrow suppression and exacerbation of autoimmune diseases [146, 148]. NAs are a group of well-tolerated therapeutics that are able to inhibit the HBV DNA polymerase and suppress viral replication in host cells in the vast majority of patients [141]. Although this reduces viral load, HBsAg seroconversion, the hallmark of effective immune response to HBV, is only rarely achieved [142, 149]. Moreover, these drugs likely need to be administered lifelong to maintain suppression of viral replication. Next to cost burden, there is still some risk to develop drug-associated toxicity and to develop resistant strains, in particular with suboptimal adherence [141].

For these reasons, new therapeutic approaches are highly needed. Several strategies are under investigation. Bulevirtide (formerly known as Myrcludex B) is a potent entry inhibitor for HBV and HDV, because the peptide competitively binds to the entry receptor NTCP, thereby blocking *de novo* viral infection [150]. The use of Bulevirtide was recently authorised by the European Medicines Agency (EMA) for the treatment of chronic HDV infection [151]. Capsid assembly modulators (CAMs) bind to HBV core proteins and thus disrupt the formation of viral nucleocapsids [152-154]. The degradation of HBV transcripts using siRNA results in gene silencing in order to lower the production not only of viral particles but also of circulating subviral particles and antigens, which may contribute to hinder immune responses in CHB [155]. Therapeutic strategies targeting the innate and adaptive immunity are currently developed to restore potent immune responses. In this regard, Toll-like receptor (TLR) or RIG-I agonists have been proposed to increase the activation of innate cytokines, dendritic cells, and NK and mucosal-associated invariant T (MAIT) cells [156, 157]. The use of engineered HBV-specific T cells (i.e. as adoptive T cell transfer) is explored to promote recognition of HBV-infected cells and efficiently reduce HBV DNA infection loads [158, 159]. Therapeutic vaccination is used to increase the number and antiviral efficacy of T cells in CHB patients [139, 160].

## 1.6 HBV infection models

The poor availability of human material, in particular liver biopsies to investigate the site of infection, from people infected with HBV makes the search for a cure very difficult. Comprehensive and effective research is needed. It is therefore essential to switch to suitable infection models to study the pathogenesis of HBV infection and possible therapies. They are necessary to study the natural life cycle, host-virus interactions and the potential of antiviral drugs or molecules.

A main problem in studying the natural HBV infection is its high liver tropism and high species specificity. The only animals that are fully susceptible to HBV infection are chimpanzees and tree shrews [161, 162]. Woodchucks, ducks and squirrels can be infected with HBV-related viruses, which provides the opportunity to study the pathogenesis of chronic hepadnaviral infection, the development of HCC and antiviral therapeutic approaches in animals, although it is not a suitable model for HBV infection [163-166].

### 1.6.1 *In vitro* models

Primary human hepatocytes (PHH) are the natural target of HBV infection. Therefore, PHHs have been the gold standard for the *in vitro* study of HBV infection and replication cycle. Although the entire life cycle of HBV infection can be studied using the PHH cell culture system, their behaviour in cell culture is challenging. PHHs rapidly dedifferentiate and lose their biological characterization as a hepatocyte and consequently the susceptibility to HBV, requiring complicated cell culture protocols [167]. In addition, due to the very low frequency of biopsies and the small sample size, mostly cryopreserved PHHs are the main source for experimental approaches. To guarantee the availability of PHHs, it is necessary to use isolated and cryopreserved PHHs from liver explants. The use of cryopreserved cells in general has severe limitations. Cell death due to thawing processes is a major problem for the use in *in vitro* systems. This can also lead to reduced proliferation rates. The HBV infection rates *in vitro* are not as reliable as in *in vivo* models.

To overcome some of these limitations, cell line-based models have been developed. HepG2 cells (hepatoblastoma) and Huh7 cells (hepatocellular carcinoma) are two cell lines used to study HBV. Their main disadvantage is the lack of the HBV entry receptor NTCP. Neither cell line can be infected with HBV. However, viral expression can be achieved by

transfection of a cloned HBV DNA construct, which serves as a transcriptional template and mimics the function of the cccDNA. The cells can therefore be used as a model system for the analysis of gene expression and DNA replication of HBV in human cells [168, 169]. Both cell lines have also been described to be transfected with the NTCP receptor, which allows HBV infection in HepG2 or Huh7 cell lines [37, 41]. HepaRG cells (HCV-related HCC-derived bipotent cell line), maintained in cell culture under special conditions, are susceptible to HBV infection. They produce viral molecules and show a stable HBV replication for at least 3 months [170]. This cell line has been used in studies to develop and evaluate antiviral drugs. However, HBV infection rates are low and the transcriptomic and metabolic processes of these tumour cell lines differ from that of primary hepatocytes, limiting key studies on virus-host interactions and long-term efficacy [171].

### **1.6.2 *In vivo* models**

The use of chimpanzees as an HBV infection model has led to crucial insights into the pathogenesis of HBV disease and the development of HBV vaccine and antiviral therapies [162]. In particular, the possibility to obtain sequential liver biopsy samples from the same animal opened the door to intensive analysis of viral parameters and host immune responses towards both acute and chronic HBV infection. However, there are strong concerns regarding the use of chimpanzees as an infection model. These include a milder clinical outcome of disease, high animal husbandry costs and above all, strong ethical concerns. For these reasons, the number of subjects is greatly reduced, which highlights another major drawback. The reduced number of experimental animals has been overcome by the development of another non-human primate model. Rhesus macaques have been transduced with the human NTCP receptor, which renders them susceptible to HBV [172]. The naturally HBV-susceptible tree shrews develop a mild and transient hepatitis, but infection efficiency is low and neonatal infection is required to induce CHB [161, 173].

Most of these limitations can be circumvented by using the mouse as an *in vivo* model. Mice are well-characterized small laboratory animals. Their dominant advantages are ease of breeding resulting in high numbers of descendants, lower costs and large number of inbred strains. Due to the natural insensitivity of mice to HBV, transgenic mice have been designed to produce either selected HBV proteins, HBsAg [174], HBeAg [175], or HBxAg [176], or infectious virions [177]. Unfortunately, the use of transgenic mice to study

HBV infection, spreading processes and the formation of cccDNA does not allow scientists to gain a better understanding of HBV replication and chronicity [178]. For still unknown reasons, the formation of cccDNA is not observed in murine hepatocytes. Therefore, HBV transgenic mice cannot be used for studying the destabilization of the cccDNA. This system allows the analysis of immune responses during acute HBV infection [178, 179]. Viral vector-mediated transfection mouse models are based on genetic engineered HBV genome containing viral vectors, derived from Adenoviruses (Ad) or Adeno-associated viruses (AAV) [180]. The mice are transfected with HBV containing viral vectors which then initiate viral replication including the expression of replication intermediates, and secretion of infectious HBV virions. Both vector-based systems establish a persistent HBV infection. Transduction of Ad-based and AAV-based HBV genomes results in the transient production of HBV proteins before HBV-specific immune responses are able to eradicate the virus. This model allows studying the underlying mechanisms of immune-mediated viral clearance of acute self-limiting HBV infection [178, 181]. However, AAV-HBV vectors are a more suitable tool for the establishment of a chronic HBV infection, due to minimal AAV genomes that do not encode for AAV proteins. This results in a clear background that does not induce any non-HBV-related immune responses. These systems are limited due to mostly low pathological changes in liver. Additionally, these models do not represent a natural infection [180].

### **1.6.3 Human liver chimeric mice**

The liver has the unique ability to regenerate to a high degree after severe liver damage or invasive surgery without loss of hepatocyte function or liver structure. Taking advantages of these properties of hepatocytes, researchers have concentrated efforts by developing models based on the transplantation of human hepatocytes into mice to overcome the limitations of using the transgenic mouse model [178]. Four different approaches to transplanting primary human hepatocytes into mice have been reported: via the dorsal fat pads [182], the peritoneal cavity [183], under the renal capsule [184] or via the spleen [185]. The transplanted hepatocytes then migrate to the liver where they must engraft, expand and survive. Therefore, it is necessary to induce injury to endogenous

hepatocytes to provide physical space and the regenerative stimulus for liver reconstitution. In addition, the absence of an immune response is required to prevent the xenogeneic hepatocytes from being targeted and killed by mouse immune cells [178].

Over the past decades several chimeric mouse models have been developed.

The uPA mouse model was the first reported model that based on strong repopulation of transplanted hepatocytes and is described below in more detail. An additional chimeric mouse model was developed by inducing a fumaryl acetoacetate hydrolase (FAH) knock-out in mice. The absence of FAH in the tyrosine breakdown pathway leads to the accumulation of toxic tyrosine catabolites that cause liver damage [186, 187]. Liver injury can be induced and controlled by withdrawing the protective pathway inhibitor 2-(2-nitro-4-trifluoro-methylbenzoyl)-1,3-cyclohexanedione (NTBC), which prevents the catabolite accumulation [53]. To increase repopulation rates, the FAH-deficient chimeric mice were crossed with double knockout mice (Rag2 and gamma chain of Il-2) to create the newly named FRG mouse model [188].

A newly established chimeric mouse model uses the expression of a herpes simplex virus type 1 thymidine kinase (HSVtk) transgene, controlled by a liver-specific albumin promoter. Backcrossing with immunodeficient NOG (Nod/Scid/Il2rg<sup>-/-</sup>) mice generated the immunodeficient, liver damaged mouse strain named TK-NOG. In contrast to the FRG mouse model, the administration of ganciclovir actively induces liver failure by destroying tyrosine kinase harbouring hepatocytes. It should be noted that male TK-NOG mice are sterile which is a major drawback of this mouse model [53].

First steps have been taken to generate double chimeric mouse systems harbouring human hepatocytes and human immune cells. AFC8 is a model based on BALB/c background model carrying combined Rag2<sup>-/-</sup>/Il2rg<sup>-/-</sup> immunodeficiency genes. Liver failure is caused by an inducible transgene based on caspase 8 induction [189]. Another approach uses NSG mice carrying a human HLA-A2 transgene to drive the development of MHC-restricted T cells. Administration of CD95 activating antibody is responsible for liver damage [190]. However, by using human fetal liver and immune progenitor cells, both systems show decreased immune cell function and reduced levels of hepatocyte repopulation and HBV replication [53]. Other approaches include transplantation of adult human hepatocytes for liver repopulation and human cord blood-derived hematopoietic stem cells (HSCs) for dual reconstitution in uPA/NSG mice [191] or FRGN mice [192]. BALB/c Rag2<sup>-/-</sup>

Il2rg<sup>-/-</sup> NOD.sirpa uPA<sup>tg/wt</sup> mice have been used to generate dual reconstituted mice by co-transplantation of human hepatocytes and human HSCs. This system shows good liver repopulation and stable accumulation of human immune cell lineages [193].

Although the generation of dual reconstituted chimeric systems is still challenging for the study of HBV infection and pathogenesis remains a challenge, the existing systems represent initial successes in the development of immunocompetent humanized mouse models. This will be very useful to study the underlying mechanisms involved in the immune regulation of HBV infection.

To investigate the immune responses in the presence of an HBV infection, liver chimeric mice can be used for an adoptive transfer of human immune cells. Several approaches have been described recently. Humanized uPA/SCID mice have been reconstituted with either HLA-matched complete human peripheral blood mononuclear cells (PBMCs) [194] or HLA-matched T cells expressing HBV-specific T cell receptors (TCRs) [158, 159]. To date, no experimental approaches have been described in which liver-derived immune cells from the non-parenchymal cell fraction of the liver are transplanted into competent liver chimeric mice. This may be due to the extensive planning involved, as the most appropriate cells would be matched hepatocytes and non-parenchymal cells (from the same donor). Isolation of these cell fractions from liver explants is often limited by scarcity and logistic. In addition, there are only a few companies offering matched cells, and these are both very cost expensive and often contain one of the cell populations at a reduced quality.

#### **1.6.4 The uPA/SCID mouse model**

The uPA mouse model was the first reported model that based on strong repopulation of transplanted hepatocytes [195] and exploited the fact that overexpression of the hepatotoxic transgene urokinase plasminogen activator (uPA) under the control of the murine albumin (Alb) promoter induces liver damage in murine hepatocytes [196]. The uPA mouse strain was backcrossed with several immunodeficient mouse strains to tolerate human hepatocyte engraftment [178]. The immunodeficient mouse strains used were Rag2<sup>-/-</sup> (recombination activating gene 2 knock out) [197], Scid (Severe Combined Immune Deficiency) lacking functional B and T cells [198], or Scid/beige mice that lack additionally

NK cell functions [199]. The Scid/beige model has been further improved by including a knockout of the Il-2 receptor gamma chain ( $Il2rg^{-/-}$ ), which results in better repopulation due to impaired receptor formation of interleukins, also called USG. After birth, the mice develop a sublethal liver damage requiring intrasplenic transplantation of isolated human hepatocytes 3-4 weeks after birth. After migrating through the portal vein and integrating into the liver parenchyma the migrating human hepatocytes begin to proliferate, replacing dying mouse hepatocytes. Although only a minority of human hepatocytes reach the murine liver, the proliferation results in the reconstitution of mouse liver with human hepatocytes that maintain normal metabolic functions and exhibit infrequent cell death [178, 200, 201]. During the regenerative phase of approximately 8 weeks human chimerism is constantly increasing, which can be estimated by detecting human serum albumin levels in mouse blood [53].

When reviewing the existing human liver chimeric mouse models for studying HBV infection and replication, the uPA model is still the most reliable and convenient model. Its main advantages are high repopulation rates of up to 50%, resulting in high infection rates and the establishment of a chronic HBV infection after approximately 12 weeks of infection (**Figure 5**). This model is essential for studying the efficacy of potent antiviral drugs and their potential side effects. In addition, every aspect of the HBV life cycle can be analysed. However, the lack of an immune system does not allow studies of adaptive and innate mechanisms based on immune cells. Only intrinsic innate immune responses of hepatocytes can be analysed. However, the adoptive cell transfer of immune cells is one way of overcoming this disadvantage [158].

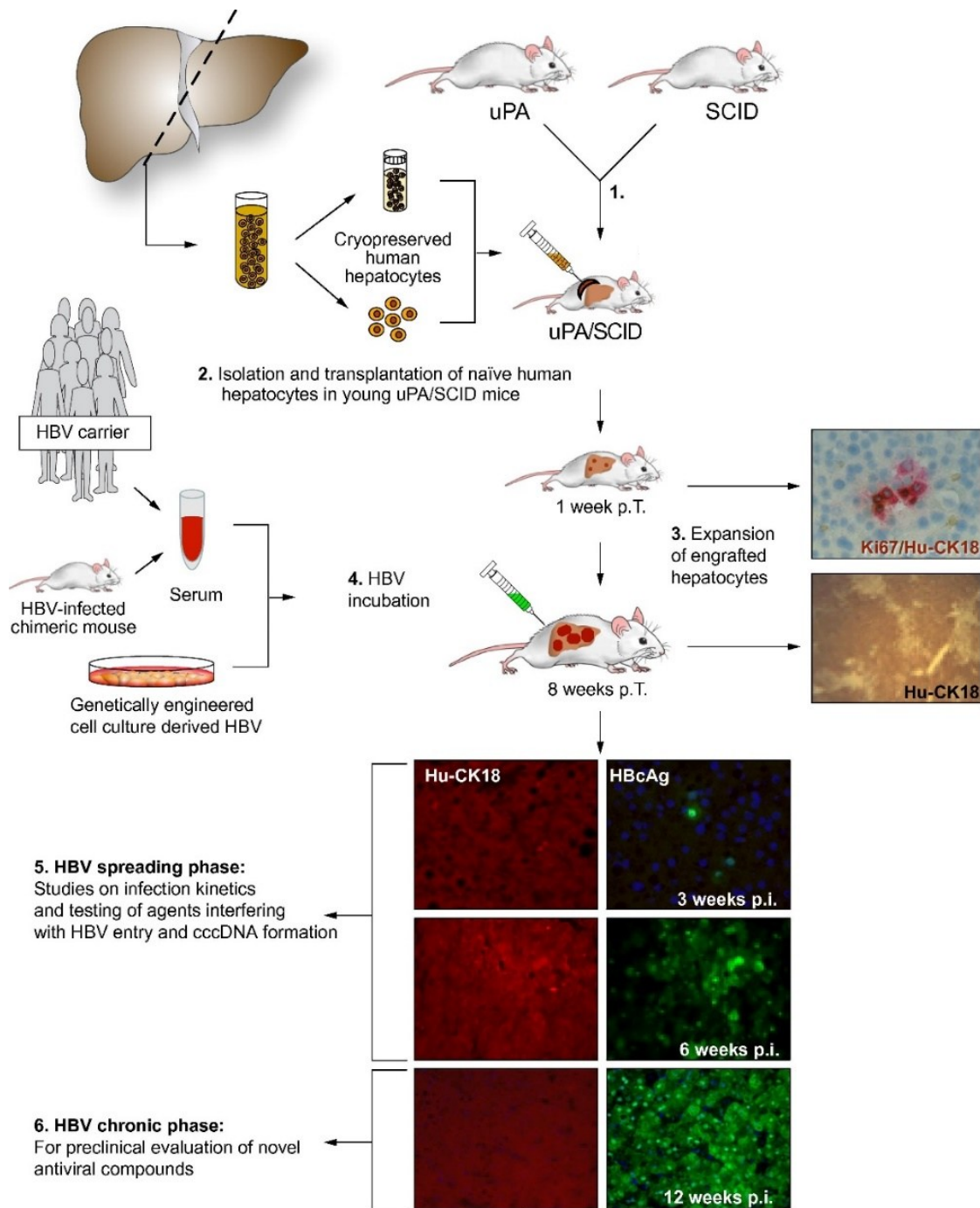


**Figure 5. Generation of liver humanized mice and infection with HBV.**

Isolated and cryopreserved human hepatocytes were thawed and injected into the spleen of uPA/Scid (or USG) mice to create livers harbouring both murine and human hepatocytes. One week post transplantation first clusters of human hepatocytes can be visualized by human cytokeratin-18 and Ki-67 (proliferation marker) double staining. After 8-10 weeks mouse liver repopulation is stable displaying huge human clusters. After inoculation with HBV a stable chronic infection is reached within 12 weeks. Staining with HBcAg is visualizing productive HBV infection. Modified from [199].

All experiments and analysis presented in this doctoral thesis were performed using the improved human liver chimeric uPA/Scid/Il2rg<sup>-/-</sup> (USG) model.

## 1.7 Non-parenchymal cells

The liver is generally composed of hepatocytes, which make up about two-thirds of the total cell population (60%-70%), and non-parenchymal cells (30%-40%). NPCs in the liver play crucial roles in maintaining liver function, immune response, and tissue architecture [202, 203].

The non-parenchymal cell population includes liver sinusoidal endothelial cells (LSECs) (approximately 50%), lymphocytes (approximately 25%), Kupffer cells (approximately 20%), biliary cells (approximately 5%) and hepatic stellate cells (HSCs) (approximately 1%). Liver sinusoidal endothelial cells (LSECs) are a unique group of endothelial cells in the liver, crucial for maintaining liver homeostasis. They are also pivotal in liver disease, as disruptions in their quiescent state can drive pathological processes such as inflammation, microvascular thrombosis, fibrosis, and portal hypertension [204]. The population of liver sinusoidal endothelial cells exhibit a distinct morphological feature known as fenestrated endothelium. Typically, LSECs have a flat shape with a regular nucleus and organelles. Their distal cytoplasm forms a lamina with numerous fenestrations, and there is no basement membrane beneath the endothelium [205]. These fenestrations, which are less than 100 nm in diameter, allow the diffusion of nano molecules, giving LSECs a sieve-like function [206]. As a result, LSECs are critical for removing various macromolecules from the blood, such as proteins, polysaccharides, lipids, and nucleic acids [207].

Kupffer cells (KCs), the liver-resident macrophages, are located in the liver sinusoids near the portal vein. Studies have shown heterogeneity among KCs. Adult KCs are derived from both embryonic precursors and adult bone marrow. In a healthy liver, embryonic-derived KCs make up the majority and are maintained by self-renewal. When the proliferation of embryonic-derived KCs is impaired, they are replenished by bone marrow monocytes [208]. KCs express specific surface markers that distinguish from other liver macrophages. The microenvironment shapes the unique immunosuppressive properties and functions of Kupffer cells. By removing gut-derived foreign products and apoptotic cells without triggering excessive inflammation, KCs maintain liver and body homeostasis and are key regulators of liver immunity. They also play a central role in the pathogenesis of acute and chronic liver injury, contributing to each stage of liver disease. By initiating inflammation

and regulating fibrosis, cirrhosis and tumour cell proliferation, KCs contribute to the resolution of liver injury and the restoration of tissue architecture [208]. Upon activation, Kupffer cells produce pro-inflammatory cytokines such as interleukin (IL)-1-beta, TNF-alpha and transforming growth factor (TGF)-beta [203, 209].

Liver lymphocytes are distributed throughout the liver parenchyma and portal tract. The liver is particularly rich in innate immune cells, including natural killer (NK), natural killer T (NKT) and  $\gamma\delta$  T cells, which make up almost half of liver lymphocytes. NK and NKT cells make up approximately 30-40% of total liver lymphocytes, while  $\gamma\delta$  T cells make up 3-5% in both mice and humans [202, 203]. Lymphocyte infiltration in the liver occurs in response to various insults, including autoimmune and toxic injury, and the pattern of infiltration varies depending on the inflammatory stimulus [210].

Hepatic stellate cells (HSCs) are located in the space between hepatocytes and sinusoids. In healthy livers, HSCs are generally quiescent and store vitamin A (retinol). However, during liver injury they undergo morphological changes and become activated. These activated HSCs differentiate into myofibroblastic cells, which are characterised by a loss of vitamin A and increased collagen production [211-213].

## **1.8 Aim of the work**

Chronic HBV infection remains a major public health burden worldwide, with more than 290 million people chronically infected. To date, there is no functional cure. The life-threatening complications, such as liver cirrhosis and hepatocellular carcinoma, currently have a very poor therapeutic prognosis, with HBV-related deaths estimated at 800,000/year. Lifelong treatment with antiviral drugs is generally required to control chronic HBV infection. Although intensive research has led to a vast knowledge of HBV infection, life cycle and therapeutic approaches, many mechanisms remain to be elucidated. Much remains to be learned about HBV-related immune responses and how these can be induced in chronic carriers. The innate immune system plays a key role in defence against viruses in general. Less is known about the mechanisms that lead to reduced and dysfunctional immune responses in chronic HBV infection. Enhancing the HBV-directed

innate immune response may provide new insights into novel therapeutic options. Therefore, it is necessary to understand HBV-hepatocyte interactions, especially how infected cells sense the virus and how sensing is communicated to immune cells. The knowledge about this crosstalk shall contribute to the development of future therapeutic approaches aiming to achieve a functional cure.

This work aims at gaining new insights into how HBV is sensed by hepatocytes. Different viruses induce different innate immune responses in host cells. And the response of different viruses to immune components varies within virus families. Due to the lack of sufficient amounts of human liver biopsies and proper animal models of infection, the processes involved in HBV sensing and the crosstalk of immune cells with HBV-infected hepatocytes are not fully understood. Among current unmet needs, is the lack of understanding of interactions occurring between infected hepatocytes and non-parenchymal cells, as well as a better understanding of the role of distinct HLAs and HLA complexes as part of the HBV sensing machinery. Investigating this may provide a better understanding of how HBV is recognised by hepatocytes and is therefore one objective of this work.

Adoptive transfer of immune cells into humanized mice with HLA-matched hepatocytes chronically infected with HBV has been shown to significantly reduce the number of HBV-infected hepatocytes. Nevertheless, the adoptive transfer of NPCs into mice harbouring human hepatocytes infected with HBV may provide unique information on the role of various immune cells in HBV recognition.

A major aim of this study is to develop a model enabling successful transplantation of matched human hepatocytes and NPCs, intensive analysis of available human material has to be undertaken. Cells obtained from different sources shall be compared in terms of cell type composition, quality and behaviour in cell culture. Finally, adoptive transfer of NPCs into humanized mice harbouring matched human hepatocytes shall be established for the first time being the second objective of this work.

## 2 Materials and Methods

### 2.1 Materials

#### 2.1.1 Consumables

Consumable	Manufacturer
Aqua Braun	B. Braun
Cell culture plates 6- well, 96-well	Sarstedt
Combitips advanced 0.2 mL, 1 mL, 5 mL, 10 mL	Eppendorf
C-Chip Neubauer Counting chamber	Carl Roth
Falcon tubes 5 mL, 15 mL, 50 mL	Sarstedt
Microscope cover object High precisio	Superior Marienfeld
Microscope slides Superfrost Plus	Thermo Fisher Scientific
Multiply - $\mu$ Strip Pro 8-strip 0.1 mL, 0.2 mL	Sarstedt
Pipet tips	Sarstedt
Polystyrene tube 12x75 mm for flow cytometry	Sarstedt
Qubit tubes	Invitrogen
Safeseal tubes 1,5 mL, 2 mL	Sarstedt
Serological pipets	Greiner bio-one
Sterile Petri dishes	Sarstedt

**Table 1:** List of consumables

#### 2.1.2 Substances

Substance	Manufacturer
2-Methylbutane	Carl Roth
Acetone	CHEMSOLUTE

ARCHITECT HBeAg Assay	Abbott Laboratories
ARCHITECT HBsAg Assay	Abbott Laboratories
ARCHITECT Multi-Assay Manual Diluent	Abbott Laboratories
BSA stock solution 10%	Miltenyi Biotec
CellGenix GMP SCGM	CellGenix
Cell-ID Intercalator-IR	Fluidigm
Ethanol absolute	CHEMSOLUTE
FACS Clean Solution	BD Biosciences
FACS Flow Sheath Fluid	BD Biosciences
FACS Rinse Solution	BD Biosciences
Fetal Calf Serum (FCS)	PAA Laboratories GmbH
Fluorescent Mounting Medium	Dako
Hepatocyte Wash Medium	Invitrogen
Isofluorane	Baxter International
Isopropyl alcohol	Baxter International
Maxpar PBS	Fluidigm
Maxpar water	Fluidigm
MeOH free Formaldehyde 16%	Thermo Fisher Scientific
Natrium chloride	Carl Roth
Natrium chloride solution 0,9%	B. Braun Melsungen AG
OneComp eBeads	Invitrogen
Paraformaldehyde	Carl Roth
Paraformaldehyde	Thermo Scientific
Percoll	Cytiva
PBS 1x	Thermo Fisher Scientific
Penicillin/Streptomycin 10,000 U/mL	Gibco Life Technologies
Plasmid-Safe ATP-Dependent DNase	Lucigen
Proteinase K	Lucigen
QIAGEN Protease	Qiagen
RNase A	Lucigen
RNase free water	Qiagen

RPMI 1640 Medium	Thermo Fisher
T-Per Tissue Protein Extraction Reagent	Pierce
TaqMan Fast Advanced Master Mi	Applied Biosystems
TaqMan Fast Virus 1-Step Master Mix	Applied Biosystems
Triton X-100	Thermo Scientific

**Table 2: List of substances**

### 2.1.3 Devices

Device	Manufacturer
Absorbance Microplate Reader ELx808	BioTek
Centrifuge 5427R	Eppendorf
Centrifuge 5810	Eppendorf
Centrifuge Galaxy Mini	VWR
Chemiluminescent Microparticle Immunoassay ARCHITECT	Abbott Laboratories
CO <sub>2</sub> Incubator	Sanyo
Cryostat Cryostar NX50	Thermo Fisher Scientific
Dispenser Multipipette Stream	Eppendorf AG
DRI-CHEM NX500	FUJIFILM
Flow cytometer LSRII	BD Biosciences
Light microscope	Leica
Microscope BZ-X710	Keyence
Nanodrop-1000 spectrophotometer	NanoDrop Technologies
Neubauer counting chamber	Optik Labor Frischknecht
Nucleofector II	Amaxa Biosystems
Pipets	Eppendorf AG
Qubit Fluorometer 4.0	Invitrogen
Safety workbench Lamin Air	Thermo Fisher Scientific
Veriti 96-well fast thermal cycler	Applied Biosystems

ViiA™ 7 Real Time PCR System	Life Technologies GmbH
Vortexer MS2 Minishaker	IKA
Vortexer Reax Top	Heidolph

**Table 3: List of devices**

#### 2.1.4 Kits

<b>Kit</b>	<b>Manufacturer</b>
Amaya Cell Line Nucleofactor Kit V	Lonza
Architect HBeAg assay	Abbott Ireland Diagnostics
Architect HBsAg assay	Abbott Ireland Diagnostics
CFSE Cell Division Tracker Kit	BioLegend
Human Albumin ELISA Kit	ICL
MasterPure DNA Purification Ki	Epicentre
MinElute PCR Purification Kit	Qiagen
mMESSAGE mMACHINE T7 Ultra Kit	Qiagen
NucleoSpin Plasmid EasyPure Kit	Machery Nagel
PureLink PCR Purification Kit	Thermo Fisher Scientific
QiAamp MinElute Virus Spin Kit	Qiagen
QuBit dsDNA broad range kit	Invitrogen
QuBit RNA broad range kit	Invitrogen
RNeasy RNA Mini Kit	Qiagen
TaqMan Gene Expression Assays	Applied Biosystems
Transcriptor First Strand cDNA Synthesis Kit	Roche
TSA Fluorescein System	Perkin Elmer
Zombie Aqua™ Fixable Viability Kit	BioLegend

**Table 4: List of kits**

#### 2.1.5 Antibodies

<b>Histology</b>			
<b>Primary anti-body</b>	<b>Source</b>	<b>Dilution</b>	<b>Manufacturer</b>
Calnexin	Rabbit	1:50	Cell Signalling
CD3	Rat	1:400	Bio-Rad
CD4	Rabbit	1:200	CellSignalling
CD8	Rat	1:200	LSBio
CD45	Mouse	-	Dako
Core HBcAg (B0586)	Rabbit	1:2000	Dako
Cytokeratin 18 (sc-6259)	Mouse	1:400	Santa Cruz
HCV core Ag	Mouse	1:500	Abcam
HEV	Rabbit	1:1600	Bioss
<b>Secondary antibody</b>	<b>Color</b>	<b>Dilution</b>	<b>Manufacturer</b>
Goat-anti-mouse anti-body	Alexa Fluor 488	1:400	Invitrogen
Goat-anti-rat antibody	Alexa Fluor 488	1:400	BioLegend
Goat-anti-rabbit antibody	Alexa Fluor 488	1:400	Invitrogen
Goat-anti-mouse anti-body	Alexa Fluor 555 Plus	1:1200	Invitrogen,
Goat-anti-rabbit antibody	Alexa Fluor 555 Plus	1:1200	Invitrogen
Goat-anti-mouse anti-body	Alexa Fluor 633	1:400	Invitrogen

Goat-anti-rabbit antibody	Alexa Fluor 633	1:400	Invitrogen	
Hoechst 33258	DAPI	1:20,000	Invitrogen,	
<b>Flow cytometry</b>				
<b>Antibody</b>	<b>Color</b>	<b>Clone</b>	<b>Dilution</b>	<b>Manufacturer</b>
CD3	Alexa Fluor 700	UCHT1	1:100	BioLegend
CD4	Pacific Blue	SK3	1:50	BioLegend
CD4	FITC	A161A1	1:100	BioLegend
CD8	PE/Cyanine7	SK1	1:50	BioLegend
CD45	APC	HI30	1:50	BioLegend
CD56	PE	5.1H11	1:100	BioLegend
CD56	FITC	5.1H11	1:100	BioLegend
<b>Imaging mass cytometry</b>				
<b>Antibody</b>	<b>Metal conjugate</b>	<b>Dilution</b>	<b>Manufacturer</b>	
Caspase-3	172Yb	1:100,1:400,1:800,1:1600	Fluidigm	
CD3	170Er	1:100,1:400,1:800,1:1600	Fluidigm	
CD4	156Gd	1:100,1:400,1:800,1:1600	Fluidigm	
CD8A	162Dy	1:100,1:400,1:800,1:1600	Fluidigm	
CD31	151Eu	1:100,1:400,1:800,1:1600	Fluidigm	
CD45	152Sm	1:100,1:400,1:800,1:1600	Fluidigm	
CD274/PD-L1	150Nd	1:100,1:400,1:800,1:1600	Fluidigm	
CD279/PD-1	165Ho	1:100,1:400,1:800,1:1600	Fluidigm	
Collagen I	169Tm	1:100,1:400,1:800,1:1600	Fluidigm	
HBcAg	146Nd	1:100,1:400,1:800,1:1600	Abcam (label by Fluidigm)	
HBsAg	141Pr	1:100,1:400,1:800,1:1600	Biolegend (label by Fluidigm)	
HLA-ABC	144Nd	1:100,1:400,1:800,1:1600	Fluidigm	
Keratin 8/18	174Yb	1:100,1:400,1:800,1:1600	Fluidigm	
Ki-67	168Er	1:100,1:400,1:800,1:1600	Fluidigm	

Pan-Keratin	148Nd	1:100,1:400,1:800,1:1600	Fluidigm
Perforin	176Yb	1:100,1:400,1:800,1:1600	Fluidigm

**Table 5: List of antibodies**

### 2.1.6 Probes/primers

Primer/Probe	Sequence (5' ->3')
cccDNA fw	CCG TGT GCA CTT CGC TTC
cccDNA rv	GCA CAG CTT GGA GGC TTG A
cccDNA probe	CAT GGA GAC CAC CGT GAA CGC CC
pgRNA fw	GGT CCC CTA GAA GAA GAA CTC CC
pgRNA rv	CAT TGA GAT TCC CGA GAT TGA GAT
pgRNA probe	TCT CAA TCG CCG CGT CGC AGA

**Table 6: List of primers and probes**

### 2.1.7 TaqMan Assays

Assay Name	Assay ID
CAS1	Hs00354836_m1
CAS3	Hs00991558_g1
CAS8	Hs01018151_m1
CXCL10	Hs00171042_m1
HBV X	Pa03453406_s1
HLA-DPB1	Hs03045105_m1
HLA-DQA1	Hs03007426_mH
HLA-DQB1	Hs03054971_m1
HLA-DRA	Hs00219575_m1
FASR	Hs00236330_m1
GAPDH	Hs99999905_m1

$\beta$ -Globin	Hs00758889_s
GZMB	Hs01554355_m1
IFN-gamma	Hs00989291_m1
NKG2A	Hs00970273_g1
NKp46	Hs00183118_m1
NKp80	Hs01044622_m1
Perforin	Hs00169473_m1
RPL30	Hs00265497_m1
TAP1	Hs00388675_m1
TNF $\alpha$	Hs99999043_m1

**Table 7: List of TaqMan assays**

### 2.1.8 Cells

Cell type	Lot	Manufacturer/isolated by
NPC	182001	Lonza
NPC	CHF2101	Cytes Biotechnologies
NPC	TM48	University Medical Center Hamburg-Eppendorf
NPC	H1	Hannover Medical School

**Table 8: List of cells**

### 2.1.9 Software

Software / tool	Producer
BD FACS Diva 8	BD Biosciences

BZ-X Viewer	Keyence
FlowJo V10	Flowjo
GraphPad Prism 9.01	GraphPad Software Inc.
Magellan	Tecan Trading AG
Microsoft 365 (Office)	Microsoft Corporation
ViiA™ 7 Software	Applied Biosystems

**Table 9: List of used software**

## 2.2 Methods

### 2.2.1 Isolation and separation of matched human hepatocytes and NPCs

Primary human hepatocytes and non-parenchymal cells were isolated from rejected explant livers using protocols approved by the Ethical Committee of the city and state of Hamburg (OB-042/06) and accorded to the principles of the Declaration of Helsinki. Separation of hepatocytes and NPCs was performed by alternating centrifugation steps where hepatocytes were pelleted by a 50 g centrifugation step, and supernatants were centrifuged with 500 g to pellet NPCs. These steps were repeated five times to achieve a high level of purity. Both cell types were stored in liquid nitrogen until use.

For cell culture experiments matched human hepatocytes and NPCs were acquired from Lonza (**Table 8**).

All mice used for adoptive transfer of NPCs in this study were transplanted with hepatocytes from a single donor and matched NPCs.

### 2.2.2 Generation of human liver chimeric mice and viral infection

Human liver chimeric uPA/SCID/IL2rg<sup>-/-</sup> (USG) mice were generated by crossing uPA transgenic mice (Jackson Laboratories) with Scid/beige mice (Taconic Farms) and subsequently with IL2rg<sup>-/-</sup> mice. Homozygous USG mice were used for intrasplenic injection of 0.5 million thawed viable cryopreserved human hepatocytes at the age of 4 weeks under isoflurane anaesthesia [158]. Human hepatocyte repopulation levels were determined by

measuring human serum albumin (HSA) in mouse serum using the human Albumin ELISA Quantification Kit (ICL). Only mice with HSA serum levels higher than 2 mg/mL were used for this study.

To establish HBV infection, mice received a single intraperitoneal injection of HBV-infectious serum ( $1 \times 10^7$  HBV DNA genome equivalents of genotype D) 10 weeks after hepatocyte transplantation. Therefore, HBV-positive patient serum was passaged in humanized mice. All animal experiments started when a stable HBV titre was detected in serum, usually after 12 weeks of infection. This was confirmed by isolation and quantification of viral DNA from serum samples, purified using the QiAmp MinElute Virus Spin Kit (Qiagen) and detected by qPCR.

To establish HCV infection, animals received a single intraperitoneal injection of patient-derived HCV inoculum containing  $1 \times 10^7$  HCV RNA copies/mL (genotype 1a). Viral loads were monitored 2-4 weeks post infection.

To establish HEV infection, humanized mice received an intravenous injection of 100 or 200  $\mu$ L patient-derived HEV-positive purified faecal suspension ( $1 \times 10^5$  IU/mouse, genotype 3). Blood and faeces samples were collected from HEV-infected mice for at least 8 weeks. RNA was isolated from serum and stool. Viral loads were determined by qPCR.

All mice were maintained under specific pathogen free conditions in accordance with institutional guidelines under approved animal research protocols. Animal experiments were conducted in accordance with the European Communities Council Directive (86/EEC).

### **2.2.3 Isolation of peripheral blood mononuclear cells (PBMC)**

For the generation of T cells directed against HBV antigens human PBMC from HLA-A2 positive donors were isolated by Percoll density centrifugation. For this purpose, 15 mL of whole blood was filled into a 50 mL Falcon with up to 35 mL PBS and gently mixed by inversion. Separately, a 50 mL Falcon was filled with 15 mL Percoll (Cytiva). Blood/PBS solution was then carefully layered on top of the Percoll. The falcon was then placed in a centrifuge and ran with 600 g for 20 minutes at room temperature with the brakes released to avoid disrupting the density gradient. After centrifugation, several layers were

obtained: plasma layer, PBMC layer at the interphase ring, Percoll layer and erythrocyte/granulocyte layer. The PBMC-containing interphase ring was carefully collected with a serological pipette and placed in an empty 50 mL falcon. The falcon was filled to 50 mL with PBS and centrifuged at 500 g for 5 minutes at room temperature. The supernatant was discarded to remove residual Percoll and plasma. This washing step was repeated once. The cell pellet was resuspended in an appropriate volume of PBS for cell counting using a Neubauer chamber. Isolated PBMCs were either used immediately for activation or centrifuged and resuspended in FCS + 10% DMSO and frozen for later use.

#### **2.2.4 mRNA preparation, electroporation, and adoptive transfer of activated T cells**

The generation of activated T cells transiently expressing the HBsAg183-191-specific TCR or the HBcAg18-27-specific TCR has been reported previously [158]. Transformed E. Coli bacteria were used to produce an HBV-directed TCR sequence containing plasmid (kindly provided by Prof. Antonio Bertoletti, Duke-NUS Medical School, Singapore). A small amount of E. Coli was scratched from a bacterial pellet stored at -80°C and cultured in 10 mL of LB medium for 17 hours at 37°C at 200-210 bpm. The bacteria were then vortexed and centrifuged at 4700 g for 10 minutes at 4°C. The supernatant was discarded. The bacteria-containing pellet was used for miniprep of plasmid DNA (NucleoSpin Plasmid Easy-Pure Kit, Machery Nagel) and manufacturer instructions were followed. DNA concentration was determined using Qbit and following manufacturer's instructions. The purified plasmid DNA was then linearised. Three reaction tubes were prepared with 3 µg plasmid DNA, 4 µL 10x buffer (Thermo Scientific 10x fast digest buffer) and 3 µL XbaI digestion enzyme and filled up to 40 µL. After 30 min. incubation at 37°C, the reaction tubes were pooled, and DNA was purified using the PureLink PCR Purification Kit (Qiagen) according to manufacturer's instructions. DNA concentration was determined using Qbit. To prevent recombination to circular DNA, the linearised DNA was transcribed within a few hours. The capped transcription of mRNA followed by PolyA tailing and recovery by LiCl<sub>2</sub> precipitation was performed using the mMESSAGE mMACHINE T7 Ultra kit (Thermo Fisher). The mRNA was stored at -80°C until use.

PBMC from HLA-A2 positive donors were stimulated in vitro with IL-2 (600 IU/mL) and

anti-CD3/anti-CD28 with Dynabeads (50  $\mu$ L/well; 6-well plate) for 8 days in AIMV + 2% AB at 37°C / 5% CO<sub>2</sub> in an incubator. After 4 to 5 days, the cells were split and cultured with fresh medium and stimulating interleukins. On the evening of day 8, the concentration of IL-2 was increased to 1000 IU/mL. The next morning activated T cells were electroporated using the Amaxa Cell Line Nucleofector Kit V according to the manufacturer's instructions.  $10 \times 10^6$  cells were transferred to a 25 mL white Falcon and filled with HBSS medium to a final volume of 20 mL. After centrifugation at 350 g for 5 minutes at room temperature, the supernatant was removed, the falcon closed and inverted to prevent backflow of medium to the cells. Cells were resuspended in 100  $\mu$ L reaction solution (82  $\mu$ L Nucleofector + 18  $\mu$ L Supplement) and 20  $\mu$ g mRNA was added. The cells were then carefully transferred to the Nucleovette, taking care to avoid air bubbles. The Nucleovette was placed in the electroporation chamber and the electroporation process was started. Afterwards, 500  $\mu$ L of AIMV + 10% AB was added dropwise and transferred to a cell culture plate where the cells were cultured for further 24 hours at 37°C / 5% CO<sub>2</sub> with 100 IU/mL IL-2 stimulation. Non-electroporated control cells were cultured under the same conditions. The cells were then harvested, counted and 0.5 million cells/mouse were resuspended in 100  $\mu$ L 37°C PBS. The T cell suspension was injected i.p. into HBV-infected and uninfected mice. This treatment was repeated after four and eight days. All mice, infected (n=7) and uninfected (n=5), were sacrificed four days after the last injection of T cells.

In a different approach, a group of HBV-infected humanized mice received retrovirally transduced T cells stably expressing HBV-specific TCRs, HLA-A2-restricted HBV core- or envelope-specific TCRs, which have been previously characterised [159]. Two million retrovirally transduced T cells (1:1 core and envelope specific, kindly provided by Prof. Ulrike Protzer of the Technical University of Munich) were injected once into HBV-infected mice. All mice analysed in this study (n=4) were sacrificed 6 or 9 days after T cell transfer.

### **2.2.5 Adoptive transfer of activated NPC**

For administration of NPC to HBV-infected humanized mice repopulated with matched hepatocytes, isolated and cryopreserved NPC were thawed by gentle agitation in a 37°C water bath until semi-frozen. The cells were then gently transferred to 37°C culture me-

dium (RPMI+10% FCS+1% pen/strep) and rapidly centrifuged (5 minutes, 500 g, room temperature) to remove cryopreservation medium (70% HTK+20% FCS+10% DMSO). The cell pellet was then washed twice with warm culture medium (centrifugation steps: 5 minutes, 500 g, room temperature). NPCs were resuspended in 37°C RPMI+10% FCS+1% pen/strep and stimulated with 100 ng/mL IL-15 overnight. The next day, cells were harvested, counted and centrifuged (5 minutes, 500 g, room temperature). NPCs were then resuspended in 37°C PBS at a concentration of 0.4 million cells/100 µL and kept warm until transferred into mice. Blood samples were taken before NPC transfer (baseline, BL) and 3 days after transfer (intermediate serum, IS) to compare serum data. Immediately prior to intraperitoneal injection, the NPC suspension was gently pipetted up and down to ensure homogeneity. Then 100 µL cell suspension/mouse was carefully filled into a syringe and injected. Six days after NPC transfer, the mice were sacrificed, and the livers were placed in 2-methylbutane before being cryopreserved at -80°C for subsequent intrahepatic and histological analysis. In addition, blood was collected and centrifuged (10 minutes, 10,000 g, room temperature) and the serum was stored at -80°C for subsequent analysis.

### **2.2.6 Interferon (IFN) treatment**

Human chimeric USG mice stably infected with HBV were treated with either PEG-IFN alpha (6 weeks), PEG-IFN beta (4 or 6 weeks) or PEG-IFN lambda (2 weeks). IFN-alpha and IFN-beta were injected twice a week at a concentration of 25 ng/g body weight per mouse. After IFN-alpha treatment some mice (n=2) were monitored for 3 more weeks without IFN treatment (rebound of HBV infection). IFN-lambda was injected 3 times per week at a concentration of 500 ng/mouse.

Mice receiving 500 ng/mouse human IFN-gamma (Cell GS) were treated with either a single dose (n=3) or 5 injections (n=3) every 12 h. Mice were sacrificed 8 h after the last injection.

### **2.2.7 Virological measurements and intrahepatic quantification**

Viral DNA was extracted from 5 µL of mouse serum samples using the QiAamp MinE-lute Virus Spin Kit (Qiagen). All qPCR measurements for this study were performed on the ViiA

7 Real-Time PCR System. TaqMan Fast advanced Master Mix and TaqMan Gene expression Assay System (Thermo Fisher) were used for detection of viral DNA. HBV-specific primers and probes were used to quantify serum titres (**Table 6**). The amplification of known references of HBV DNA plasmid was used to construct a standard curve for the quantification of absolute HBV serum DNA.

For quantification of HBsAg and HBeAg, mouse serum was diluted 1:200 in the diluent serum (ARCHITECT Multi-Assay Manual Diluent serum, Abbott Laboratories) and measured on the ARCHITECT (Abbott Laboratories) using the HBsAg quantitative kit and the HBeAg kit (Abbott Laboratories) according to the manufacturer's recommendations.

DNA and RNA were extracted from humanized mouse liver samples using the Master Pure DNA Purification Kit (Epicentre) and the RNeasy Mini Kit (Qiagen), respectively. The specific primer and probe set used for serum DNA was used to amplify intrahepatic HBV DNA by qPCR. The detection of human haemoglobin beta (single copy gene) was used to estimate and normalise the number of human hepatocytes within the analysed liver sample. The number of copies of haemoglobin beta was calculated from a prepared standard curve with a known number of copies. Intrahepatic viral RNA was quantified using TaqMan Virus 1-Step Master Mix (Applied Biosystems) and human-specific primers and probes (**Table 6**). Human single copy housekeeper genes, GAPDH and RPL30, were used to normalise viral RNA expression.

For the detection of the cccDNA copies by PCR, enzymatic digestion of relaxed circular DNA (rcDNA) was first performed using plasmid-safe ATP-dependent DNase (Lucigen) according to the manufacturer's instructions. However, the qPCR conditions were modified: forward primer concentration 100 nmol/L; reverse primer 800 nmol/L; cycling conditions: 1 initial denaturation step for 10 minutes at 95°C, 40 cycles for 1 second at 95°C and 1 minute at 65°C. The result was compared to a standard curve with a known copy number of HBV plasmid and normalised to the amount of human cells.

To determine gene expression levels in humanized mouse livers, 1 µg of total purified RNA from the liver sample was reverse transcribed using the Transcriptor First Strand cDNA Synthesis Kit (Roche) according to the manufacturer's instructions. Oligo-dT primers were used to selectively identify mRNA by annealing to its poly(A) sequence. The constructed complementary DNA (cDNA) was then diluted 1:1 with sterile water. Subsequent qPCR

was performed using TaqMan Fast Advanced Master Mix (Thermo Fisher) and specific TaqMan assays (**Table 7**) to detect gene expression. TaqMan assays were chosen to avoid cross-reactivity with murine liver structures or murine transcripts, which was tested prior to use. For comparison of different liver species, the mean of GAPDH and RPL30, two human housekeeping genes, was used to normalise gene transcription.

For gene expression analysis of HLA genes, 1  $\mu$ L of total RNA was used for qRT-PCR using TaqMan Fast Virus 1-Step Master Mix according to the manufacturer's recommendations (Thermo Fisher).

### **2.2.8 Immunofluorescence**

All immunofluorescence staining was performed on 12  $\mu$ m thick frozen sections of human chimeric mouse livers cut on a Cryostat Cryostar NX50 (Thermo Fisher Scientific). Sections were either fixed with acetone or paraformaldehyde, washed with PBS or TN buffer (used for CK18/HBcAg co-staining) and incubated overnight at 4°C with primary antibodies (**Table 5**). Specific signals were visualised with secondary antibodies conjugated to Alexa 488, Alexa 555 plus or Alexa 633 (**Table 5**) and incubated for 45 minutes at room temperature in the dark. For CK18/HBcAg staining, signal enhancement was required using the TSA fluorescein system (Perkin Elmer). Nuclear staining was achieved by diluting Hoechst 3258 (1:20,000) and incubating sections for 1-2 minutes. Stained sections were mounted with fluorescent mounting medium (Dako) and stored at 4°C for at least 20 minutes. Signals were then visualised using a BZ-x710 fluorescence microscope (Keyence).

### **2.2.9 Flow cytometry**

Flow cytometry can simultaneously detect physical and chemical characteristics of cells such as size, granularity, and fluorescence. This allows the detection and cellular concentration of fluorescence-labelled molecules. The cell suspension is in a flow and focused so that only one cell at a time is hit by a laser beam. Forward and side scatter allow cells to be distinguished by size and granularity. If cells are fluorescently labelled or have autofluorescence, different lasers can be used to excite their fluorochromes. Mirrors and detectors direct and record the different characteristic wavelengths that are emitted to form

electrical signals that can be analysed and converted into a graphical representation. This method allows the analysis of proteins on the surface and within cells at a single cell level [214, 215].

The first step was to block human Fc receptors to prevent false signals when stained with antibodies. Human TruStain FcX receptor blocking solution (Biolegend) was used according to the manufacturer's instructions.  $1 \times 10^6$  cells were transferred to a 5 mL polystyrene tube and washed twice with PBS to remove any protein from the cell culture medium. Subsequently, 5  $\mu$ L of Human TruStain FcX Receptor Blocking Solution was added to the cells in 100  $\mu$ L staining volume. The cells were mixed and incubated for 15 minutes at room temperature. Dead cells had to be excluded. For this purpose, the Zombie Aqua™ Fixable Viability Kit (Biolegend) was used as recommended by the manufacturer. Dead or apoptotic cells were labelled because the dye enters the cytoplasm and reacts with amine groups on proteins, increasing the amount of total protein labelling, as opposed to live cells with intact cell membranes where only surface proteins could be labelled. Cells were centrifuged (500 g, 5 minutes, 4°C) and resuspended in 100  $\mu$ L of 1:100 diluted Zombie Aqua solution. The cells were incubated for 15 minutes at room temperature in the dark. Without washing, the surface staining antibody cocktail was added. (**Table 5**). Cells were incubated for 20-30 minutes on ice in the dark. Then 2 mL FACS staining buffer (PBS+2.5% FCS) was added and cells were centrifuged to pellet (500 g, 5 minutes, 4°C). The supernatant was discarded and the cells were washed again with FACS staining buffer before being resuspended in 200  $\mu$ L of FACS staining buffer and kept on ice until measured on the flow cytometer. Compensation was required due to overlapping emission spectra. This was done by detecting the emission of OneComp Beads previously stained with each fluorophore used in the experiment. 1  $\mu$ L of antibody was added to 1 drop of vortexed beads. For live/dead staining compensation,  $1.5 \times 10^5$  cells were killed by incubation at 50°C for 15 minutes and stained with Zombie Aqua. An unstained control of  $1.5 \times 10^5$  cells was also used for compensation. Compensation was performed on the cytometer according to the instructions of the FACS Diva software.

The following gating strategy was always used to analyse a specific cell population (**Figure 6**). The lymphocyte gate was set based on characteristic size and granularity. Doublets were then excluded by plotting FSC-A against FSC-H. Dead lymphocytes were then excluded by analysing the dead cell marker zombie aqua and discriminating positive cells. Within the CD45<sup>+</sup> cell population, CD4 T cells were identified as CD3<sup>+</sup>/CD4<sup>+</sup> cells, CD8 T cells as CD3<sup>+</sup>/CD8<sup>+</sup> cells, NKT cells as CD3<sup>+</sup>/CD56<sup>+</sup> cells and NK cells as CD3<sup>-</sup>/CD56<sup>+</sup> cells.

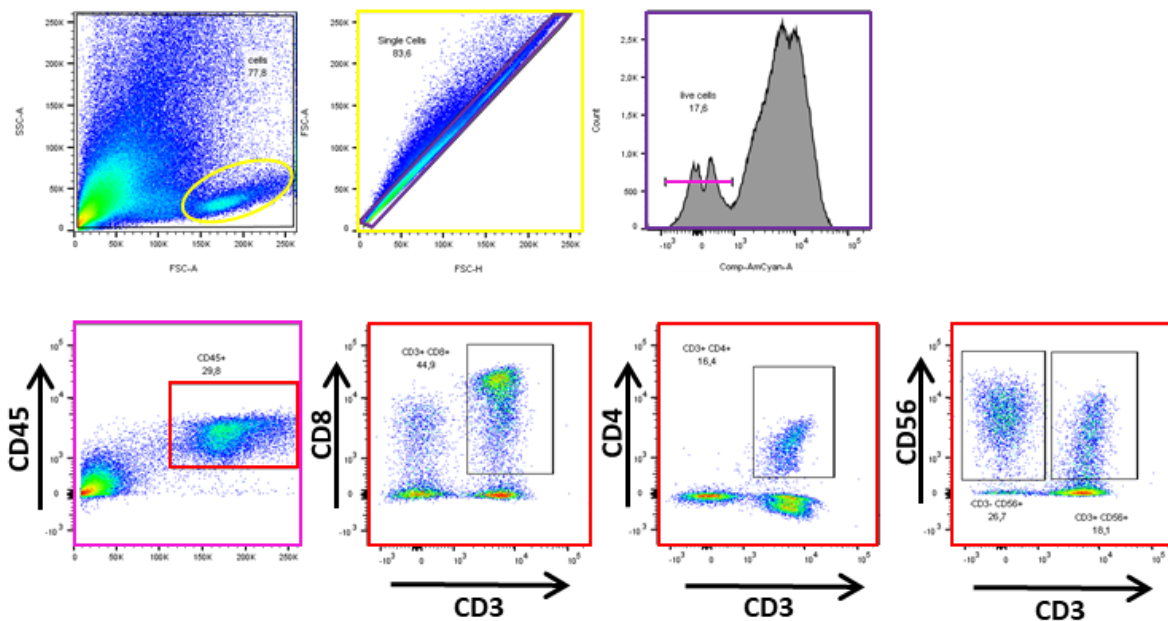


**Figure 6. Gating strategy for flow cytometry analysis**

## 2.2.10 CFSE proliferation assay

The CFSE proliferation assay, formally known as 5-(and 6)-carboxyfluorescein diacetate succinimidyl ester of CFDA SE, is an effective and popular method for visualising lymphocyte cell division in cell culture. The fluorescent dye stably labels long-lived intracellular molecules. During cell division, the number of labelled molecules in the daughter cells is progressively reduced. This reduction can be monitored as a dilution of the fluorescence with a flow cytometer.

The CFSE Cell Division Tracker Kit (Biolegend) was reconstituted and used as recommended by the manufacturer.  $1.5 \times 10^5$  NPCs were pelleted and resuspended in 1 mL of 5  $\mu$ M CFSE working solution. The cells were incubated for 20 minutes at room temperature in the dark. The addition of 5 mL cell culture medium (RPMI+10% FCS+1% pen/strep)

quenched the staining. The cells were then pelleted and resuspended in pre-warmed (37°C) cell culture medium and maintained in cell culture at 37°C and 5% CO<sub>2</sub> for 6 days. Cells were then prepared for flow cytometry with cell surface staining antibodies and measured as described above.

### **2.2.11 Imaging mass cytometry**

In patients with chronic HBV, both virus-specific and generalised adaptive immune responses are weakened by multiple regulatory pathways. Due to the lack of liver biopsies and limited technologies, most studies of human HBV have focused on the analysis of PBMC. In addition, approaches using hepatic immune cells derived from liver perfusates or processed liver tissue can provide important insights but cannot directly visualise the liver parenchyma and characterise infiltrating immune cells. The development of imaging mass cytometry (IMC) may help to fill this gap within the HBV-infected liver [216]. Since its original description 10 years ago, this technique has rapidly developed into a commercial tool with unprecedented power to analyse histological tissue sections [217]. IMC combines laser ablation with 1 µm<sup>2</sup> resolution and time-of-flight cytometry to detect target cells labelled with metal-conjugated antibodies. The use of up to 40 markers in parallel on a single tissue section allows analysis at the single cell level while providing additional information on tissue architecture and cell morphology [218].

In this study, IMC was only performed on frozen tissue sections. The metal-conjugated antibodies used for this approach had to be tested for binding to frozen tissue sections and then titrated to find the optimal dilution for analysis of frozen liver tissue.

First, a slide holder was stored overnight at -20°C. Slides containing 8 µm tissue sections were then transferred from -80°C to the slide holder and allowed to equilibrate at -20°C for 1 hour. A 4% PFA solution was freshly diluted in a plastic jar and stored in the refrigerator at 4°C. The slide holder (containing the tissue sections) was placed in the refrigerator at 4°C for 10 minutes. The slides were then placed in the plastic jar and fixed with PFA for 30 minutes at 4°C. The slides were rinsed 3 times with PBS for 5 minutes at room temperature. The samples were circled using an ImmEdge PAP pen. Tissue was blocked with freshly diluted 3% BSA solution. Antibody cocktail was prepared in 3% BSA in Maxpar PBS using antibody dilutions of 1:100, 1:400, 1:800, 1:1600 and 1:3200. Slides were placed in

a hydration chamber and the antibody cocktail (100  $\mu$ L/slide) was dropped onto the sections. Staining was performed overnight at 4°C in the refrigerator within the hydration chamber. The next day, the slides were washed with 0.2% Triton X-100 in Maxpar PBS for 8 minutes at slow agitation in Coplin jars. Washing was repeated once. Tissue sections were stained with Intercator-Ir in Maxpar PBS at a 1:800 dilution for 30 minutes at room temperature in a hydration chamber. The slides were then washed 3 times with PBS Maxpar for 5 minutes each time. The slides were then immersed in water 3 times. Finally, the slides were air dried at room temperature for at least 20 minutes. When the staining protocol was complete, the slides were packaged and sent to the Core Facility Berlin for measurement.

## 3 Results

### 3.1 Analysis of HLA class I and class II expression on hepatitis infected hepatocytes *in vivo*

#### 3.1.1 Different induction of HLA class I molecule expression on hepatocytes in the liver of chimeric mice upon HBV, HCV and HEV infections

Cellular immune responses directed by human leucocyte antigen (HLA) molecules are associated with the outcome of any acute or chronic viral infection [113]. This is regulated by highly polymorphic HLA class I and II genes which influence the ability of HLA proteins to elicit immune responses [115]. Virus-specific CD8<sup>+</sup> cytotoxic lymphocytes (CTLs) can recognize short viral antigenic peptides (epitopes) presented by HLA class I-expressing hepatocytes [116]. Therefore, peptide presentation is elementary for the clearance of viral infections by boosting the capability of CTLs to identify and kill virus-infected cells [115]. However, it is not yet completely understood how human cells recognise HBV infection, because of the lack of human biopsies and infection models. It is possible that innate immune responses assist in this process. To investigate the influence of different hepatitis virus infections on the expression of HLA class I molecules, human liver chimeric mice were infected with HBV, HCV or HEV.

Immunofluorescence staining of cryopreserved liver sections demonstrated the effectiveness of viral hepatitis infections (**Figure 7 E-G**). HBV core protein staining was identified on almost every human hepatocyte (**Figure 7 E**). HCV infection was also visualised by staining the core protein and microscopy data revealed that about half of the human hepatocytes were HCV positive (**Figure 7 F**). For the detection of HEV infection the HEV ORF3 protein was used. This protein is essential for viral particle egress and the biogenesis of lipid membrane-enveloped HEV particles. Fluorescence staining of ORF3 showed HEV infection of nearly all human hepatocytes (**Figure 7 G**). Livers were analysed for the mRNA expression of HLA-A, HLA-B, HLA-C, HLA-E and HLA-F and expression levels were compared with uninfected controls.

Expression analysis revealed no changes in the mRNA expression levels for HLA-A, -B, -E and -F in HBV-infected hepatocytes compared to uninfected controls (**Figure 7 A-D**). For HLA-C the expression levels of uninfected controls and HBV-infected livers were mainly below the detection limit. For this reason, HLA-C expression data are not shown in this study. Interestingly, HCV infection significantly induced gene expression of HLA-A (~ 0.5

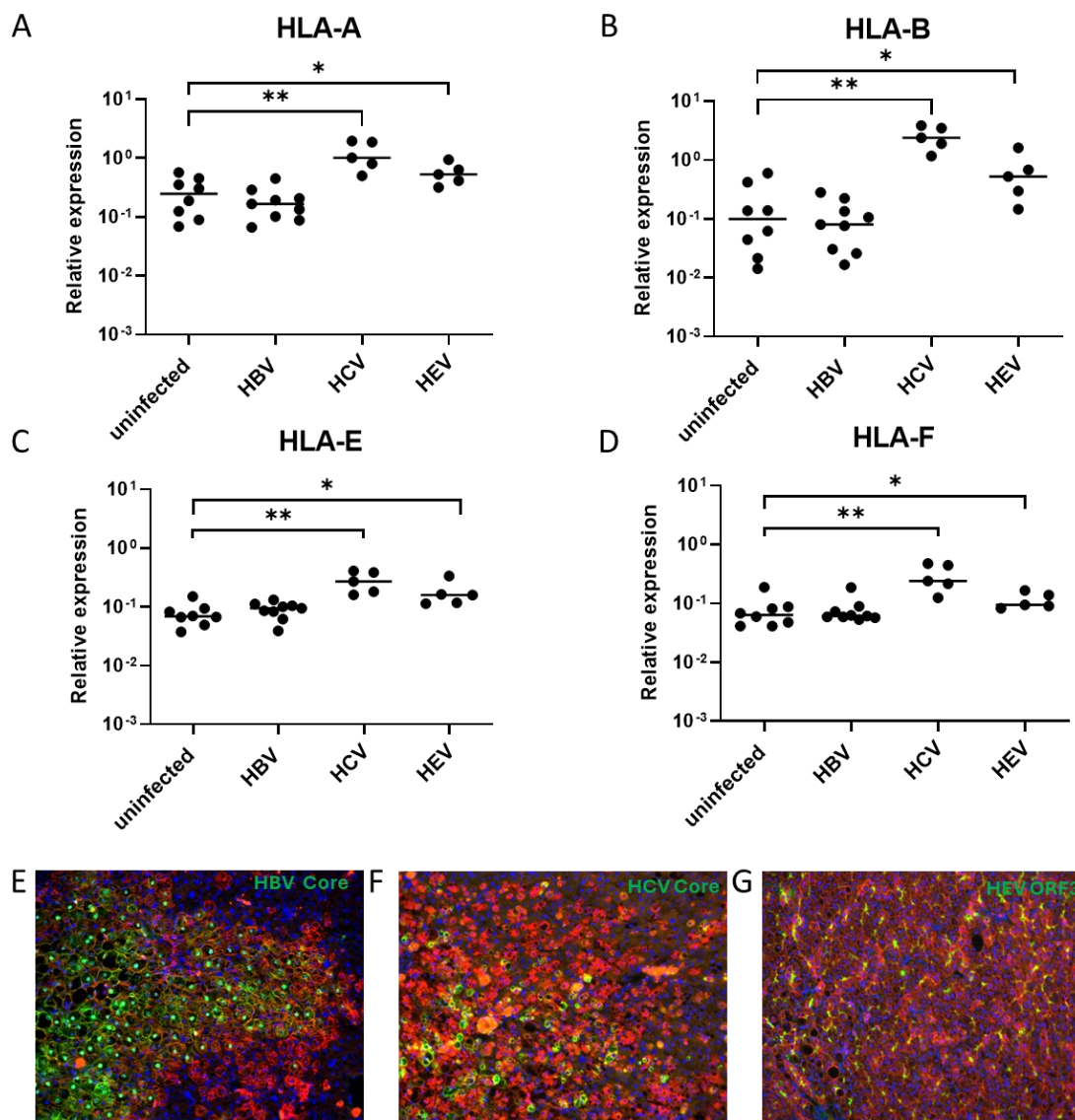


**Figure 7. Expression levels of HLA class I molecules are not induced upon infection with HBV.**

mRNA expression levels of HLA-A(A), HLA-B(B), HLA-E(C) and HLA-F(D) were determined by qPCR in mice infected with HBV(n=9), HCV(n=5) and HEV(n=5) and compared with uninfected control mice (n=8). Expression levels were normalised to the mean of GAPDH and RPL30. P values were calculated via Mann-Whitney U test \* p<0.05; \*\* p< 0.005. Immune fluorescence-staining visualise hepatitis infection of liver humanized mice. Cryopreserved liver sections were stained with HBV core protein (green) and CK18 hepatocyte marker (red)(E), HCV core protein (green) and hepatocyte marker calnexin (red)(F) and HEV ORF3 protein (green) and CK18 (red)(G).

log), HLA-B (> 1 log), HLA-E (~ 0.5 log) and HLA-F (~ 0.5 log) molecules compared to uninfected controls (\*\*p < 0.005; **Figure 7 A-D**). In addition, also mRNA expression levels of HLA-A, HLA-B, HLA-E and HLA-F were increased upon HEV infection (\*p < 0.05; **Figure 7 A-D**). These data demonstrate an increase in antigen presentation for hepatocytes of liver humanized mice infected with HCV and HEV. For HBV infected humanized livers there was no indication of an induction of HLA antigen presentation.

### **3.1.2 HLA class II molecule expression is not induced by infection with different hepatitis viruses on hepatocytes of liver chimeric mice *in vivo***

Parenchymal cells normally do not express major histocompatibility complex (MHC) class II, but in viral and autoimmune hepatitis these molecules can be aberrantly detected [219]. Clearance of acute HBV infection is orchestrated by CD8<sup>+</sup> and CD4<sup>+</sup> T cells, which secrete high levels of IFN-gamma and TNF-alpha [87, 130, 131]. HLA class II gene variations have various effects on HBV persistence, spontaneous clearance, seroconversion, disease progression and the development of liver cirrhosis and HCC [115]. Detailed knowledge of the expression of HLA class II proteins in the context of hepatitis infection may give new insights into sensing and immune modulations of CTLs.

To investigate the influence of not only HBV but also HCV and HEV infection on the expression of HLA class II molecules, human liver chimeric mice were infected with these human hepatitis viruses and stable infection was established. The livers were then analysed for the expression of HLA-DP, HLA-DQA1, HLA-DQB1 and HLA-DRA and compared with uninfected controls. Infection of liver humanized mice with HBV and HEV did not affect the mRNA expression levels of HLA-DPB1. Only HCV infection slightly, but significantly, induced HLA-DPB1 expression by < 0.5 log (**Figure 8 A**). Almost all expression levels of HLA-DQA1 were below the (LLoD) (**Figure 8 B**). Similar expression was observed for HLA-DQB1, with most samples were below the detection limit (**Figure 8 C**). None of the virus tested affected the expression levels of HLA-DRA in the livers of humanized mice (**Figure 8 D**).

In conclusion, there were almost no changes in mRNA expression levels for HLA class II complexes detectable when comparing hepatitis-infected liver chimeric mice with uninfected control mice. Only HCV significantly increased the expression of HLA-DPB1 compared to uninfected controls.

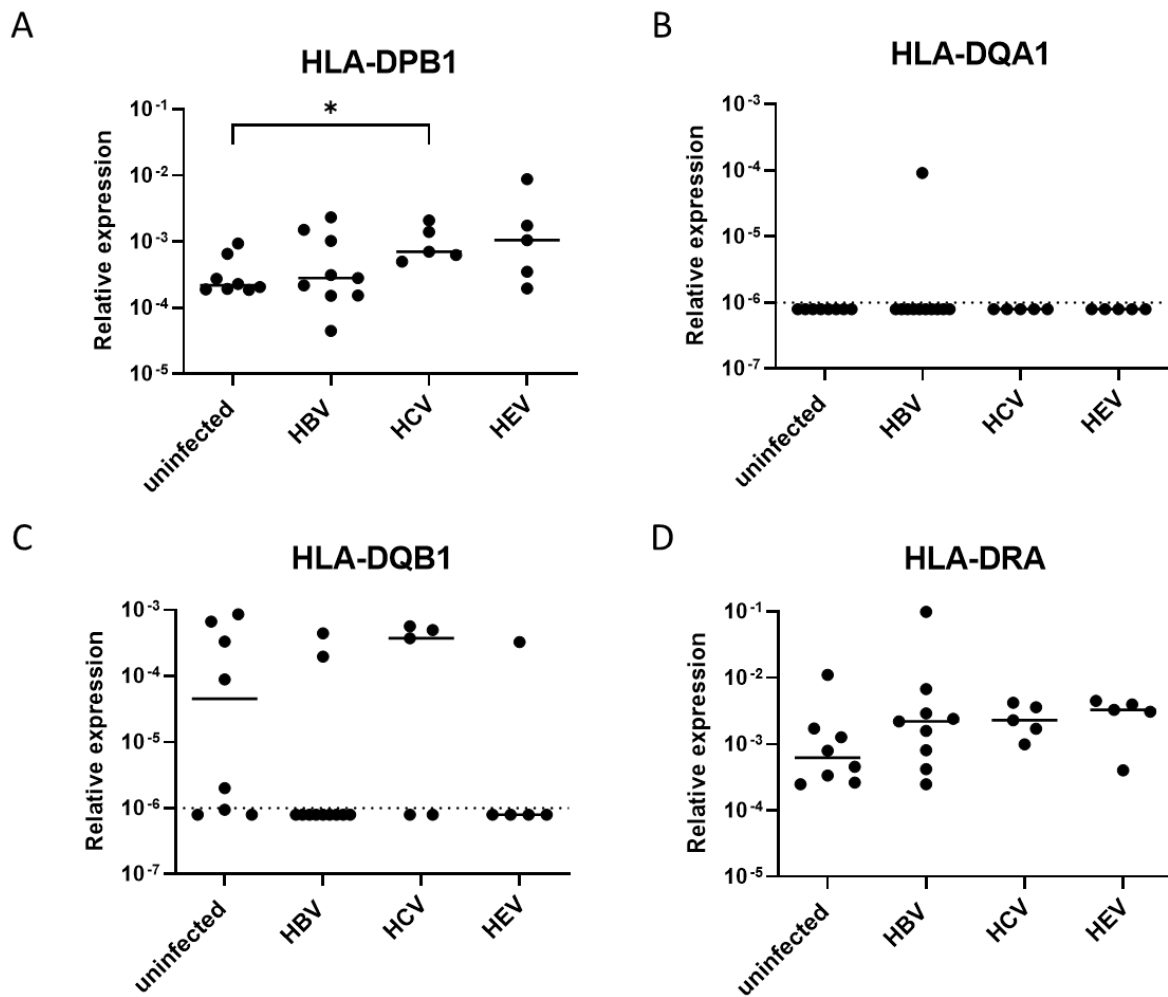


**Figure 8. Relative expression of HLA complexes on hepatocytes infected with different hepatitis viruses.**

mRNA expression levels of HLA-DPB1(A), HLA-DQA1(B), HLA-DQB1(C) and HLA-DRA(D) were determined by qPCR in mice infected with HBV(n=9), HCV(n=5) and HEV(n=5) and compared with uninfected control mice (n=8). Expression levels were normalised to the mean of GAPDH and RPL30. P values were calculated via Mann-Whitney U test. \* $p < 0.05$ ; \*\* $p < 0.01$ .

### 3.1.3 IFN-gamma treatment of HBV-infected liver chimeric mice clearly induces HLA-class I and class II mRNA expression

Interferons are cytokines that promote antiviral, immunomodulatory and antitumour properties. Their potent antiviral activity plays an important role in innate and adaptive immune responses [220]. Different signalling pathways initiated by interferons exert inhibitory effects on HBV at different stages of the infection, such as prevention of cccDNA formation, transcription, and translation of viral proteins [220]. IFN-gamma is one of the

key players in orchestrating immunological processes due to infectious diseases. It is known to be able to induce HLA class II upregulation [11]. To investigate the potential of IFN-gamma to induce HLA expression of HBV-infected hepatocytes in liver chimeric USG mice, animals were treated with IFN-gamma protein once or five times. The livers of mice were collected 8 hours after the last IFN-gamma injection and analysed for HLA expression. IFN-gamma treatment significantly increased the mRNA expression of all eight HLA class I and class II proteins analysed in a dose-dependent manner (**Figure 9 A-H**). HLA-A (~0.5 log), HLA-B (~1.5 log), HLA-E (1 log) and HLA-F (~1 log). mRNA expression levels were significantly induced after five repeated doses of IFN-gamma (**Figure 9 A-D**). A single dose of IFN-gamma already resulted in an upregulation of all HLA class II genes showing the strongest result for HLA-DQB1 with an induction of nearly 2 log compared to the two detectable HBV controls (**Figure 9 G**). Of note, the induction of HLA-DPB1 (~1 log) and HLA-DRA (~1.5 log) is already clearly detectable after one single dose of IFN-gamma. After five repeated doses of IFN-gamma the upregulation of HLA-DPB1 and HLA-DRA became significant (**Figure 9 E+H**). The striking trend of HLA-DQA1 and HLA-DQB1 expression was sustained after five doses of IFN-gamma (**Figure 9 F+G**). In conclusion, the treatment of HBV-infected liver chimeric USG mice with either a single or repeated doses of IFN-gamma resulted in a clear induction of HLA-A, HLA-B, HLA-E and HLA-F, as well as HLA-DPB1, HLA-DQA1, HLA-DQB1 and HLA-DRA.

Intrahepatic HBV-specific T cells have been described as mediators of control of HBV infection and produce IFN-gamma in response to antigen-specific stimulation [130, 158, 219]. MHC class II molecules expressed on antigen-presenting cells normally activate CD4 T cells in response to an infection.

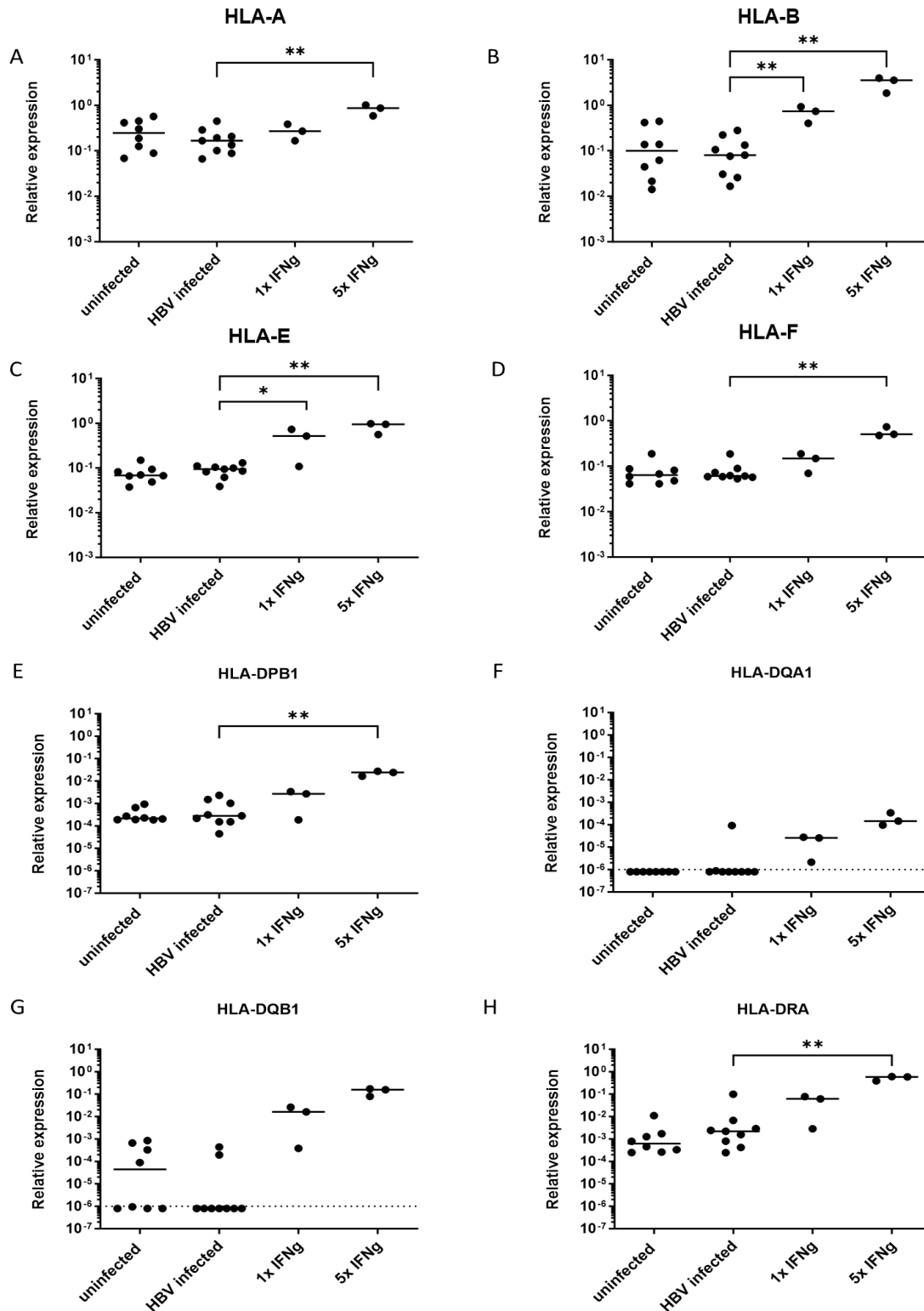


**Figure 9. Expression of different HLA class I and class II complexes on human HBV infected hepatocytes after treatment with IFN-gamma protein.**

mRNA expression levels of HLA-A (A), HLA-B (B), HLA-E(C), HLA-F(D), HLA-DPB1(E), HLA-DQA1(F), HLA-DQB1(G) and HLA-DRA(H) were determined by qPCR in mice infected with HBV ( $n=9$ ), uninfected controls ( $n=8$ ) and HBV-infected mice treated with a single dose of 500 ng IFN-gamma/mouse ( $n=3$ ) and five repeated doses of 500 ng IFN-gamma/mouse every 12 hours ( $n=3$ ). Expression levels were normalised to the mean of GAPDH and RPL30. *P* values were calculated via Mann-Whitney *U* test. \* $p<0.05$ ; \*\* $p<0.01$ .

Recently, a subset of HLA-DP molecules has been identified as novel ligands for the activating NK cell receptor NKp44 [131]. NK cells, next to CD8 T cells, have cytotoxic effects on virus infected cells indicating a potential role in early clearance of infection [107, 135]. To assess the effect of IFN-gamma released by HBV-directed T cells on the expression levels of HLA class II molecules on HBV-infected hepatocytes, transient and stable HBV-directed TCR-expressing T cells were injected into humanized USG mice as described previously [158, 159]. At the end of the experiment and as indicated above (Methods 2.2), an-

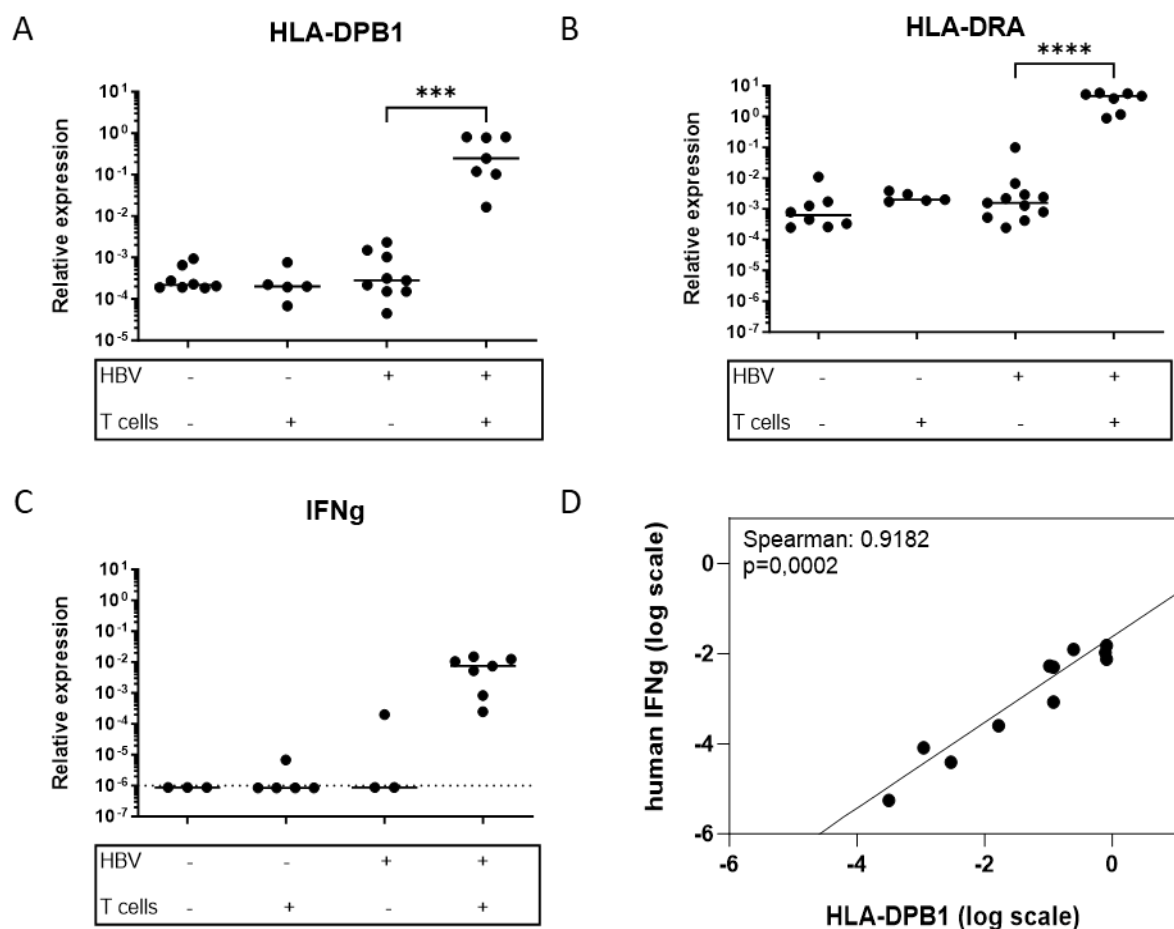


**Figure 10. Expression of different HLA class II complexes on human HBV infected hepatocytes after treatment with IFN-gamma producing T cells.**

mRNA expression levels of HLA-DPB1(A), HLA-DRA(B) and IFN-gamma (C) were determined by qPCR in mice infected with HBV (n=9), uninfected controls (n=8), HBV infected and T cell treated mice (n=7) and uninfected T cell treated mice (n=5). Expression levels were normalised to the mean of GAPDH and RPL30. A correlation of HLA-DPB1 and IFN-gamma was calculated for (n=11) mice, including 4 animals that were sacrificed shortly after T cell transfer(D). p values were calculated via Mann-Whitney U test. \*\*\*p=0.002; \*\*\*\*p<0.0001.

imals were sacrificed, livers were collected, and liver RNA was isolated. The mRNA expression data clearly demonstrate an upregulation of all four HLA class II molecules tested after transfer of engineered HBV-directed T cells into liver chimeric USG mice. In HBV-infected and T cell-treated mice, a clear and strong induction (~ 3 log) of HLA-DP expression was determined ( $p=0.002$ ), similar to HLA-DRA expression results, which showed >3 log induction ( $p<0.0001$ ) compared to untreated HBV-infected animals (**Figure 10 A+B**). Although HLA-DQA1 and HLA-DQB1 expression levels were mostly below the detection limit, an upregulation of these molecules was evident in HBV-infected and T cell-treated mice (data not shown). All HBV-uninfected and T cell recipient uninfected controls showed no induction of HLA-class II molecules. In addition, the detection of high IFN-gamma mRNA expression only in HBV-infected and T cell-recipient mice indicates the occurrence of an interaction between HBV-infected hepatocytes and T cells adoptively transferred into liver chimeric USG mice (**Figure 10 C**). Notably, HLA-DPB1 mRNA expression levels positively correlated with IFN-gamma mRNA expression in the liver (Spearman rank correlation coefficient=0.9182;  $p=0.0002$ ) (**Figure 10 D**), suggesting a direct effect of IFN-gamma levels on HLA-DPB1 expression.

For HLA class I molecules, the effect on mRNA expression was strong when mice were treated with HLA-matched and HBV-restricted T cells. HLA class I mRNA expression levels for uninfected (treated and untreated with T cells) and HBV-infected and untreated mice were similar to each other. Only HBV-infected and T cell-recipient livers of humanized mice showed a clear induction of mRNA expression for HLA-A (~ 1.5 log), HLA-B (2 log), HLA-E (~ 1log) and HLA.F (1 log) (**Figure 11 A-D**).

In summary, both IFN-gamma and administration and IFN produced by T cells significantly increased HLA class I and class II mRNA expression in a dose-dependent manner and exclusively in animals harbouring human hepatocytes infected with HBV.

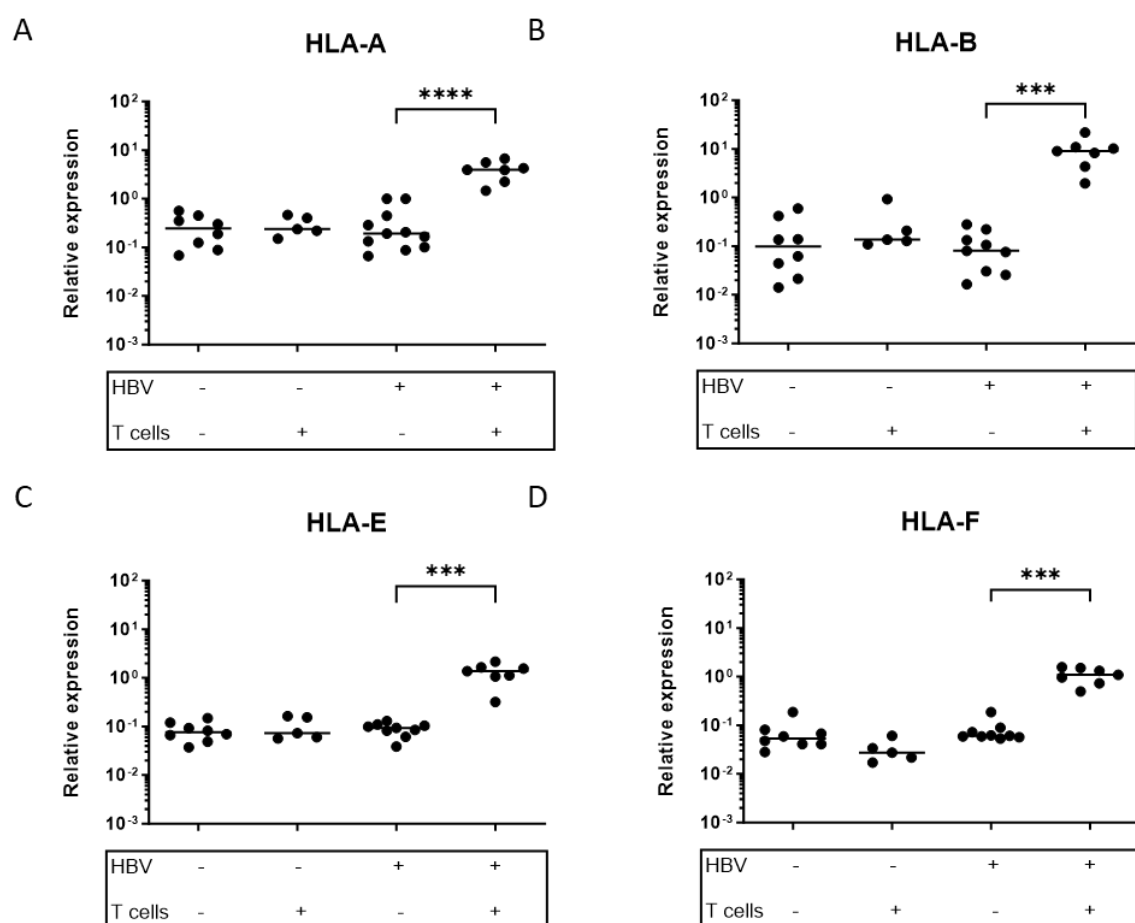


**Figure 11. Expression of different HLA complexes on human HBV infected hepatocytes after treatment with IFN-gamma producing T cells.**

mRNA expression levels of HLA-A(A), HLA-B(B), HLA-E(C), HLA-F(D) were determined by qPCR in mice infected with HBV (n=9), uninfected controls (n=8), HBV infected and T cell treated mice (n=7), and uninfected T cell treated mice (n=5). Expression levels were normalised to the mean of GAPDH and RPL30. p values were calculated via Mann-Whitney U test. \*\*\*p<0.0005; \*\*\*\*p<0.0001.

### 3.1.4 IFN-beta treatment of HBV-infected liver chimeric mice clearly induces HLA-class I and class II mRNA expression

HBV infection is currently treated with reverse transcriptase inhibitors (nucleosides or nucleotide analogues [NAs]) and interferon therapy [221]. In particular, PEG-IFN-alpha is used in anti-HBV therapy because of its immunomodulatory function in NK cell activation [222]. Various members of the interferon family, IFN-beta and IFN-lambda are also being investigated for their potential in controlling and clearing of HBV and HDV infection [223, 224]. IFN-gamma clearly induced different HLA complexes on HBV-infected hepatocytes (Figure 9 + Figure 10 + Figure 11). It is therefore interesting to investigate whether other

interferons have a similar effect on the HLA expression of infected parenchymal cells. To investigate this, liver chimeric USG mice, stably infected with HBV, were treated with either PEG-IFN-alpha (6 weeks, n = 4), PEG-IFN-beta (4 weeks, n = 5; 6 weeks, n = 2) or PEG-IFN-lambda (2 weeks, n = 3). Two of the four PEG-IFN-alpha treated mice were sacrificed after 6 weeks of treatment. The other two mice were left alive to investigate an HBV rebound. Therefore PEG-IFN-alpha therapy was stopped after 6 weeks and HBV titre was detected for additional 3 weeks. After sacrifice, livers were collected and liver RNA was isolated. mRNA expression levels of HLA-A, HLA-B, HLA-C (data not shown), HLA-E and HLA-F as well as HLA-DPB1, HLA-DQA1, HLA-DQB1 and HLA-DRA were measured using qPCR and compared to uninfected and HBV-infected and untreated controls.

Treatment of HBV-infected hepatocytes in liver chimeric mice with IFN-alpha had no effect on the expression levels of the HLA class II molecules HLA-DPB1, -DQA1, -DQB1 and -DRA (**Figure 12 E-H**). Lower viral load and antigen levels are associated with higher IFN-alpha responsiveness. However, there was a significant increase in HLA class I expression of HLA-A (0.5 log,  $p < 0.02$ ) and HLA-B (1 log,  $p = 0.002$ ) (**Figure 12 A+B**). To rule out donor-specific variations, all mice contained hepatocytes from the same donor. Within the IFN-alpha treatment group, two mice received PEG-IFN-alpha for 6 weeks and were then sacrificed, while two additional mice were used to monitor viral rebound for additional 3 weeks before being sacrificed. Also the rebound mice showed decreasing HBeAg and HBsAg levels under IFN-alpha treatment, whereas these HBV protein levels increased after rebound (data not shown), thus confirming the transient effectiveness of IFN-alpha therapy also in these mice. While HLA-E and -F mRNA expression was clearly induced in 6-week IFN-alpha-treated mice, rebound mice showed expression levels comparable to HBV-infected and untreated mice. This clearly demonstrates that the induction of mRNA expression is IFN-alpha dependent and time-limited. Withdrawal of IFN-alpha treatment reverses HBV infection parameters and the decline in HLA-E and HLA-F mRNA expression (**Figure 12 C+D**).

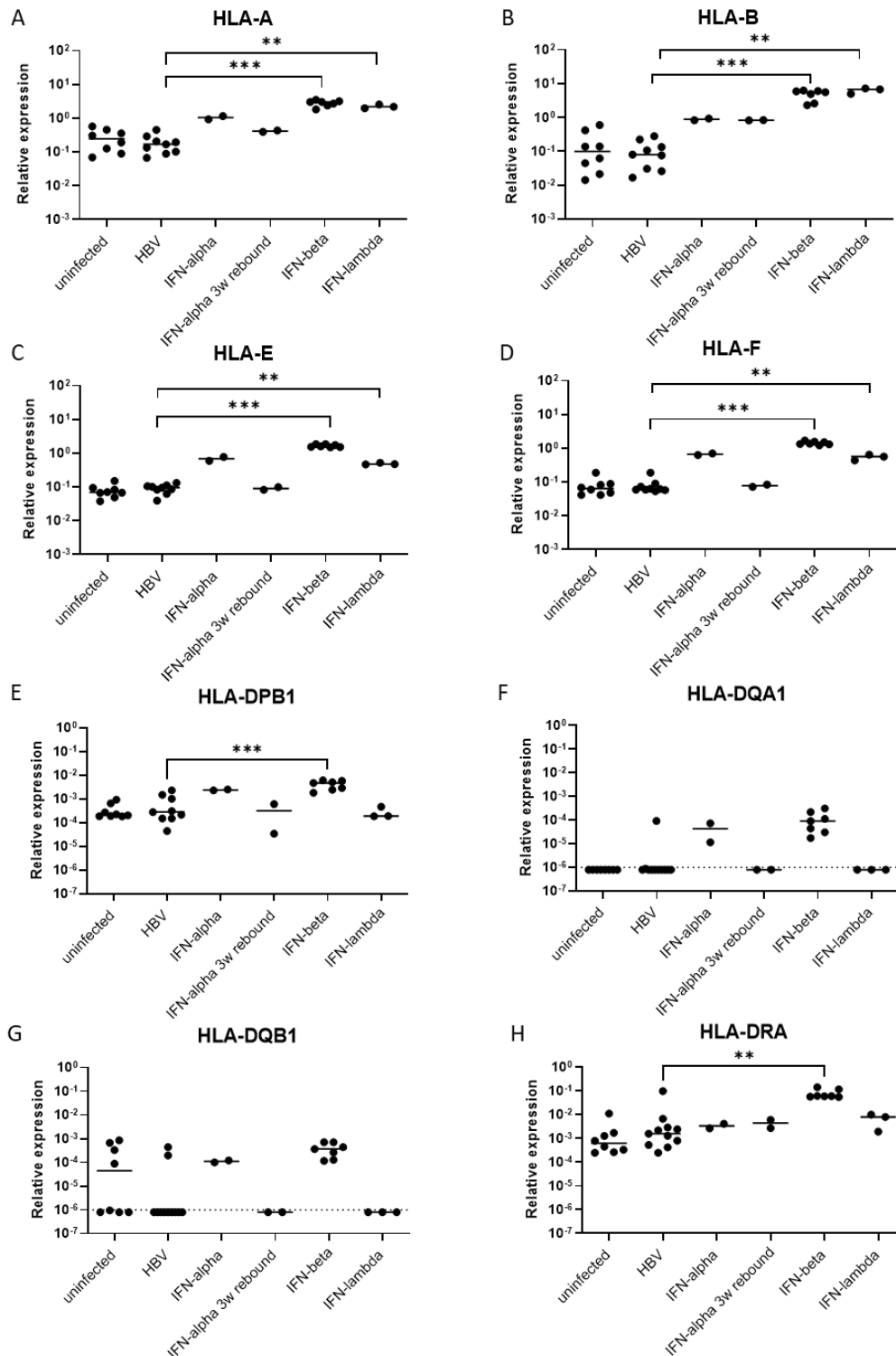


**Figure 12. Expression levels of different HLA class I and class II complexes on human HBV-infected hepatocytes after treatment with IFN alpha, beta or lambda.**

mRNA expression levels of HLA-A(A), HLA-B(B), HLA-E(C) and HLA-F(D) next to HLA DPB1(E), HLA-DQA1(F), HLA-DQB1(G) and HLA-DRA(H) were determined by qPCR in mice infected with HBV (n=9), uninfected controls (n=8) and mice infected with HBV and treated with IFN-alpha (6 weeks, n=4), IFN-beta (4 weeks, n=5; 6 weeks, n=2n) or IFN lambda (2 weeks, n=3). Expression levels were normalised to the mean of GAPDH and RPL30. P values were calculated via Mann-Whitney U test. \*p<0.02; \*\*p< 0.002; \*\*\*p=0.0003.

Interestingly, treatment of mice with PEG-IFN-beta (for either 4 or 6 weeks) significantly increased mRNA expression levels for HLA-A (~1 log; p=0.0003), HLA-B (~ 1.5 log; p=0.0003), HLA-E (>1 log; p=0.0003), HLA-F (>1 log; p=0.0003), HLA-DPB1( >1 log; p=0.0003) and HLA-DRA (~1.5 log; p=0.002) (**Figure 12**) compared to HBV-infected untreated and uninfected mice. Due to the low expression pattern of HLA-DQA1, no statistical analysis could be performed but a trend towards induction of HLA-DQA1 expression after IFN-beta treatment could be detected (**Figure 12 B**). The same was true for HLA-DQB1 mRNA expression (**Figure 12 C**). It is noteworthy that IFN-alpha and IFN-beta both belong to the same IFN family (I). They interact through the same pair of receptors (IFN-ALPHAR1 and IFN-ALPHAR2) and can initiate a remarkable number of inflammatory and antiviral pathways. Differences in receptor-affinity may in part explain the different use of IFN-alpha, predominantly for infectious diseases, whereas IFN-beta is mostly administered for the treatment of certain inflammatory diseases [225, 226]. This may also explain why IFN-gamma and IFN-beta clearly induce HLA-DPB1 and HLA-DRA mRNA expression, as both are involved in the activation of inflammatory immune responses [227].

Treatment of HBV-infected mice with PEG-IFN-lambda had no substantial impact on the mRNA expression levels of the four HLA class II molecules tested (**Figure 12 E-H**). In contrast, all HLA class I molecules were significantly induced by IFN-lambda treatment, with a ~1 log increase for HLA-A, HLA-E and HLA-F and a 1.5 log increase for HLA-B (p=0.002).

In conclusion, IFN-gamma strongly upregulated the expression of HLA-DPB1, HLA-DQA1, HLA-DQB1 and HLA-DRA within HBV-infected hepatocytes, regardless of its origin as a recombinant protein or released by T cells. In addition, HLA class I molecules were almost completely induced by IFN-alpha, IFN-beta and IFN-lambda. However, HLA class II was only upregulated after treatment with IFN-beta.

## **3.2 Analysis of non-parenchymal cell fractions isolated from different donors**

### **3.2.1 Characterisation of non-parenchymal cells shows donor dependent**

## differences in lymphocyte cell composition

The cell populations of the liver can be divided into two main groups called parenchymal cells and non-parenchymal cells [228]. The liver parenchyma consists of hepatocytes, which can act as antigen-presenting cells [229]. The smaller NPC fraction included several cell types: liver sinusoidal epithelial cells (LSECs), Kupffer cells (KCs), hepatic stellate cells (HSCs) and liver-resident lymphocytes [228]. This lymphocyte population is highly enriched in natural killer (NK) cells and natural killer T (NKT) cells, which play a critical role in innate immunity [203]. While acute HBV infection is cleared by non-cytopathic mechanisms, including the release of inflammatory cytokines [230], chronic HBV infection results in a dramatic activation of dysfunctional immune responses. Innate immune cells (DCs, macrophages, and NK cells) have both protective and pathogenic roles, whereas adaptive immune cells (T cells and B cells) recognise and kill infected cells and induce liver inflammation [231]. Various immune cell-based approaches have been investigated to reactivate a functional immune response directed against HBV.

In this study, non-parenchymal cells from different donors are analysed, in particular for their lymphocyte composition and survival, to elucidate their potential in a therapeutic setting. The main difference to T cell-based studies and a major issue is the availability of matched hepatocytes and non-parenchymal cells in adequate amounts and in a ready-to-use status. Extensive searches for possible sources of these matched cells were necessary to obtain 4 different donors with a suitable proportion of lymphocytes that could be used for this study.

Previously isolated and separated non-parenchymal cells were either thawed under “warm” conditions (pre-warmed medium at 37°C, centrifuge temperature at room temperature) or under “cold” conditions (medium temperature and centrifuge temperature at 4°C). The thawed NPCs were stained with trypan blue and live as well as dead cells were counted using a Neubauer chamber. This experiment clearly demonstrates the positive influence of “warm” thawing conditions on the survival of human NPCs. The use of warm thawing condition increased cell survival from 40.9% up to 70.3% ( $p=0.0002$ ) (**Figure 13 A**). This experiment shows the influence of temperature on NPC survival, so warm thawing conditions were used in all subsequent approaches. In this study, NPCs from different donors were thawed, live/dead stained, cell surface stained with dye-conjugated antibodies

against CD45, CD3, CD4, CD8 and CD56 (**Table 5**) and analysed by flow cytometry (donors 1, 2 and 3). The results were compared with NPCs derived from a fresh isolated liver. These NPCs had never been frozen and were also stained with the same antibodies. Flow cytometry analysis showed that freezing and thawing had a strong negative effect on the survival of NPCs. Their survival was only ~36% (donor 1-3) compared to freshly isolated NPC showing ~77% survival (**Figure 13 B**). This is an overall reduction of ~46%. The survival of the lymphocyte population appeared to be similar (~15% vs. 11%), but the large variation within donors 1-3 may confound this (**Figure 13 C**).

The observed variations in cell survival might be due to donor variations, particularly their immunological or inflammatory background. Data were only available for one donor with freshly isolated NPCs. Analysing more donors of freshly isolated NPC could determine the influence of an immunological or inflammatory background. Phenotypic flow cytometric analysis showed both very strong similarities between donors 1 and 2 and clear differences, for example to donor 3 (**Figure 13 D**). This highlights the importance of cell type analysis before using different donors for cell type-based approaches. For further investigation of T cell-mediated interactions with HBV-infected cells, donors 1, 2 and 4 are the better choice, whereas donor 3 should be used to study NK cell-mediated immune responses.

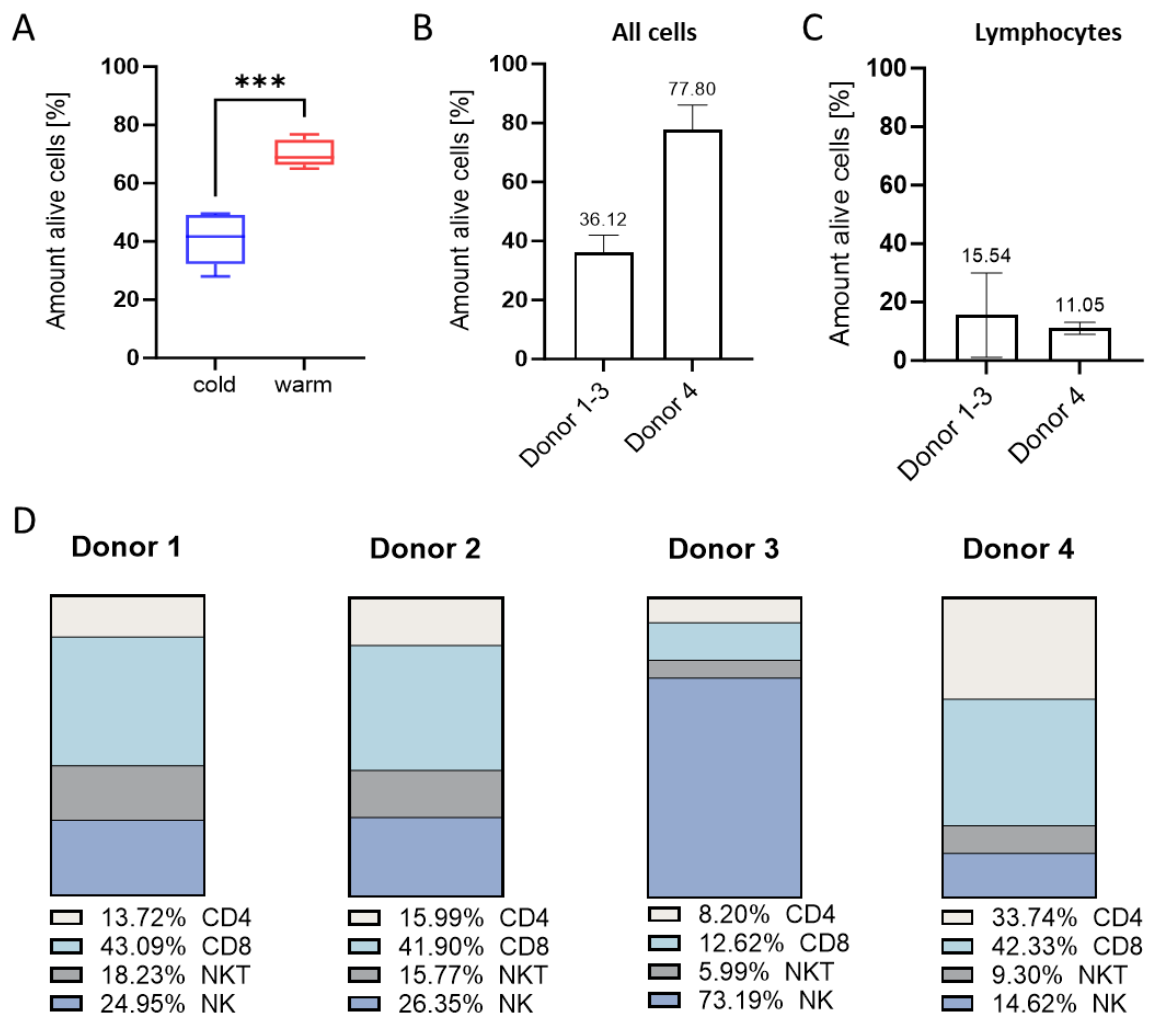


**Figure 13 Characterisation of human NPC thawed after cryopreservation.**

Comparison of NPCs derived from the same donor either thawed under warm ( $n=5$ ) or cold ( $n=5$ ) conditions (A). Dead cells were identified by trypan blue staining and counted using a Neubauer counting chamber. Flow cytometry analysis of the survival of cryopreserved NPC derived from 3 donors ( $n=5$ ) or fresh isolated NPC derived from 1 donor ( $n=2$ ) (B+C). Live/dead staining was performed using Zombie Aqua Fixable Viability Kit. Note: gate was set for all cells (B) or CD45+ (C). Representative flow cytometry analysis of the NPC lymphocyte cell composition of four different donors (D). Cells were pre-gated as described above.  $p$  values were calculated via Mann-Whitney U test. \*\*\* $p=0,0002$ .

### 3.2.2 Stimulation of NPC with IL-2 and IL-15 results in proliferation of intrahepatic lymphocytes

Isolation and cell culture of PBMC is a well-established method for investigating immunological tasks. The isolation and cell culture of specific NPC-derived cell types (Kupffer cells, stellate cells, LSECs) have been described previously [228]. Less is known about the cell

culture of the whole non-parenchymal cell fraction. Some companies offer cell culture media for specific liver-derived cell types (hepatocytes, LSECs, KCs), but no company has good experience with culturing NPCs. In addition, there are only a few companies offering isolated NPCs and most of them do not offer matched cells (hepatocytes and non-parenchymal cells from the same donor). This may be because the isolation techniques are specialized to produce large quantities of one cell type with high quality. Therefore, a large part of this work focused on establishing cell culture conditions for a complete NPC fraction. First, cell culture plates for suspension cells and adherent cells were tested and compared. For thawed human NPC, the use of suspension plates was advantageous in terms of cell growth (data not shown). In a next step, different seeding densities were investigated. It was found that fully confluent seeded cells had a higher potential to survive for more than 6 days (data not shown). For this work, the function and quality of the lymphocyte population within the NPCs was of paramount importance. Therefore, a well-established cell culture medium for human lymphocytes was used. Cells were always cultured in RPMI+10% FCS+1% pen/strep, unless otherwise stated.

Cell culture experiments usually require additives that stimulate the cells and somehow mimic the natural environment. Therefore, several simulating molecules already described for cell culture studies of PBMC-derived lymphocytes were tested. The use of interleukin-2 (IL-2) for the proliferation capacity and activation of T cells in particular has been extensively characterized (e.g. [232]). In addition, IL-15 has been shown to have a positive effect on the proliferative capacity of NK cells and was therefore used here to increase NK cell activity and proliferation [233]. After 4 days of cell culture, only cells incubated with IL-2 showed a slight increase (29.9% /29.8%) in the CD45<sup>+</sup> population compared to unstimulated cells on day 1 (22.5%) or day 4 (20.5%) (**Figure 14 A-E left**).

IL-15 alone had no effect on the amount of CD45<sup>+</sup> population. Stimulation with either IL-2 or IL-15 alone or the combined dose did not affect the proportion of CD4<sup>+</sup> T cells (**Figure 14 A-E middle right**). Similar results were shown for the CD8<sup>+</sup> T cell population (**Figure 14 A-E middle left**). Small variations might occur due to the gate setting.

Interestingly, the NK cell population increased not only in the number of cells counted, but also the fluorescence intensity was higher in interferon stimulated cells (25.3% for IL-2; 28.2% for IL-15; 26.7% for IL-2/IL-15) compared to day 1 (13.9%) and day 4 without stimulation (15%) (**Figure 14 A-E right**).

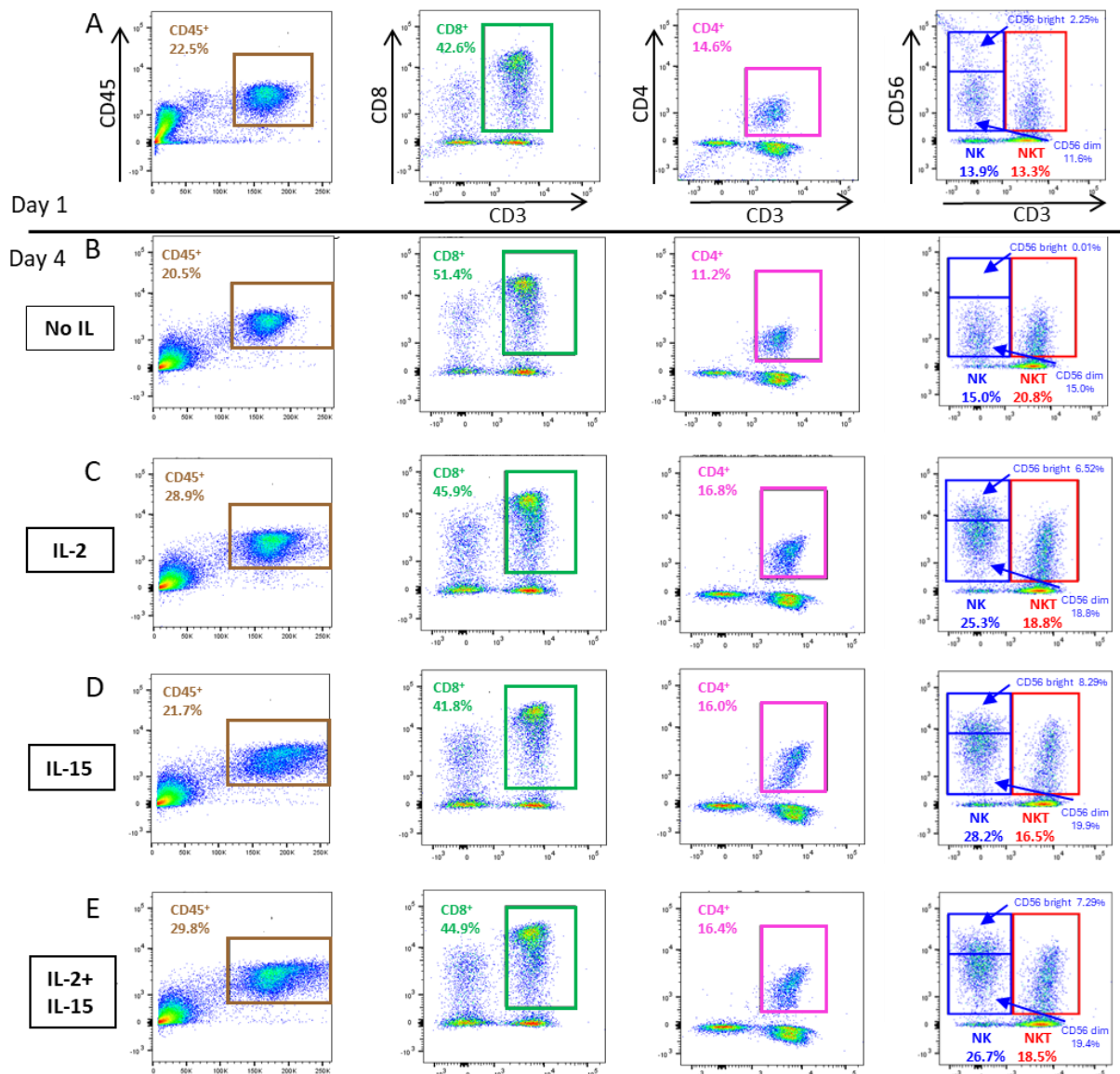


**Figure 14.** Flow cytometric analysis of lymphocyte population derived from non-parenchymal cells under different stimulation in vitro indicate differences in cell proliferation upon stimulation.

Cryopreserved NPC derived from donor 2 were thawed, seeded in RPMI+10% FCS + 1% Pen/Strep and stimulated with IL-2 (600 IU/mL) (I-L), IL-15 (100 µg/mL) (M-P) or combined with IL-2 / IL-15 (W-T) and cultured for 4 days. Unstimulated (E-H) cells as well as cell analysed at day 1 (A-D) served as control. Cells were harvested, stained with cell surface antibodies and analysed with flow cytometer. Data were analysed using FlowJo software.

Natural killer cells can be divided into CD56<sup>bright</sup> and CD56<sup>dim</sup> cells. Phenotypically, these populations are very different depending on the expression of surface receptors and therefore have different functions. CD56<sup>dim</sup> cells contain much more perforin, granzymes and cytolytic granules and are therefore much more cytotoxic than CD56<sup>bright</sup> cells. On the other hand, CD56<sup>bright</sup> cells are the most effective producers of cytokines such as IFN-

gamma, TNF-alpha, IL-10 and IL-13. Stimulation with IL-2 is reported to strongly increase the cytotoxic activity of all NK cell subsets [234, 235]. The observed CD56 shift might be due to an increase in CD56<sup>bright</sup> cells and indicates an activation of cytotoxic NK cells within the NK cell population. The population of NKT cells in cell culture appeared to increase from 13.3% on day 1 (**Figure 14 A right**) to a maximum of 20.8% on day 4 without stimulation (**Figure 14 B right**). However, this was the result of the gate setting as the CD3<sup>+</sup>/CD56<sup>+</sup> (NKT) population was not clearly separated from the CD3<sup>+</sup>/CD56<sup>-</sup> cell population. This experiment showed that for NPCs stimulated with IL-2 and/or IL-15 for 4 days, NK cells started to proliferate but T cells were not affected.

In a next step, NPCs derived from donor 3 were cultured for 8 days in RPMI + 10% FCS + 1% pen/strep to test whether cells expanded when cultured for a longer time. The cells were either stimulated with 600 IU/mL IL-2 or left unstimulated. The total cell number was calculated at the indicated time points (**Figure 15 A**). Strong effects on the cell number were not detectable until day 7. However, there was no difference between IL-2 stimulated cells and unstimulated cells (**Figure 15 A**).

The CFSE cell division tracker kit was used to demonstrate the proliferative capacity of the stimulation agents already used on NPCs. CFSE diffuses into cells and forms a strong bond by being converted into a fluorescent molecule. As cells divide, the fluorescent molecule is evenly distributed, which can be seen as a loss of fluorescence intensity. Using histogram plots, each new generation of divided cells appears as a single peak with lower CFSE fluorescence intensity. The more peaks detected, the more cell divisions have taken place. NPCs were stained with CFSE according to the manufacturer's instructions (Biolegend, **Table 4**). Cells were then cultured for 7 days in either RPMI + 10% FCS + 1% pen/strep or SCGM + 10% FCS + 1% pen/strep. SCGM is a medium commonly used to cultivate haematopoietic stem cells, progenitor cells and NK cells and was used here to test whether NPC-derived lymphocytes have a higher proliferation and survival rate.

NPCs were stimulated with 600 IU/mL IL-2 and 100 ng/mL IL-15 or left unstimulated as control. After 7 days, NPC-derived lymphocytes (CD45<sup>+</sup> population) showed the dilution of CFSE in both media (**Figure 15 B**). Cells cultured in RPMI showed three cell divisions for CD8 T cells (green) and four cell divisions for NK (blue) and CD4 T cells (pink). For NKT cells (red) and unstimulated cells (grey) no clear cell division was visible (**Figure 15 B left**). In

comparison, using SCGM as cell culture medium, CD4<sup>+</sup> T cells showed four cell divisions, NK cells showed at least two cell divisions, but CD8<sup>+</sup> T cells and NKT cells did not clearly exhibit any CFSE dilution (**Figure 15 B right**). Due to the reduced proliferative capacity of NPCs within SCGM medium, RPMI is more suitable for the culture of non-parenchymal cells *in vitro*.

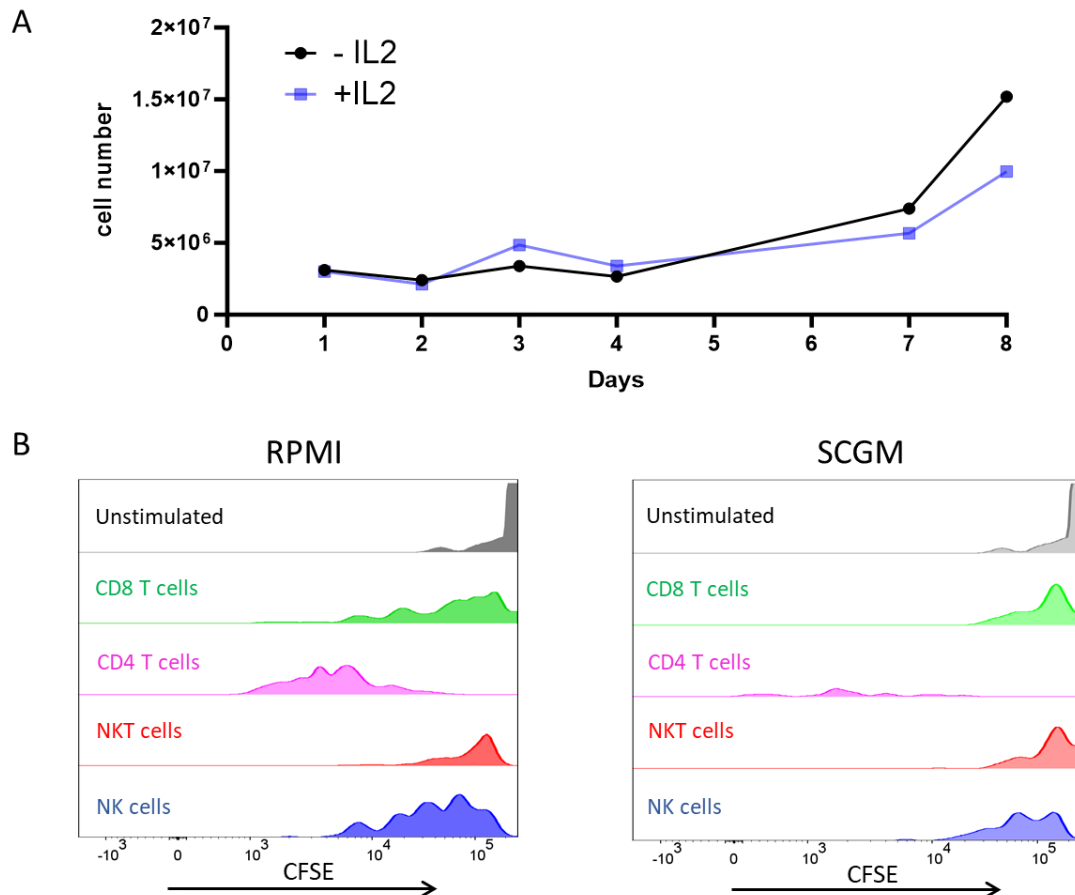


**Figure 15. Cell culture analysis of non-parenchymal cells demonstrates cell proliferation of hepatic lymphocytes.**

Cryopreserved non-parenchymal cells from donor 3 were thawed and kept in RPMI+10% FCS+1% pen/strep with or without IL-2 stimulation (600IU/mL) for 8 days (**A**). Cells were counted at indicated time points. Cryopreserved non-parenchymal cells from donor 2 were thawed and stained with CFSE proliferation marker (**B**). Then, cells were kept either in RPMI+10% FCS+1% Pen/Strep (**B left**) or in SCGM+10% FCS+1% pen/strep (**B right**) and stimulated with IL-2 (600IU/mL), IL-15 (100 ng/mL) or IL-2/IL-15 for 7 days. Unstimulated cells served as control. Then cells were stained for flow cytometric analysis. Histogram plots show the proliferation of NPC derived lymphocyte population: CD4 T cells (pink), CD8 T cells (green), NKT cells (red) and NK cells (blue), unstimulated NPCs (grey).

To sum up these data, non-parenchymal cells isolated from human livers could be cultured successfully *in vitro*. When stimulated with IL-2 and/or IL-15, NK cells began to proliferate after four days in culture, whereas CD4<sup>+</sup> T cells, CD8<sup>+</sup> T cells and NKT cells took longer to

proliferate. If stimulation had no effect on cell number, but CFSE dilution shows proliferation, this could mean that there is a balance between the generation of new cells and cell death. This would provide evidence for optimising cell culture conditions, as the amount of cell death should be significantly less than the amount of new cells generated.

### **3.2.3 NK cells can efficiently be enriched within NPC fraction using an immunomagnetic selection tool**

For immunological characterization of distinct immune cells, it is necessary to isolate specific immune cell populations. Different tools are available for this purpose. When cell populations have precise size differences, a density gradient is often used as a first separation step, for example to isolate PBMC from whole blood. For cells with similar size, immunomagnetic selection tools show successful results. Cells of interest are labelled with antibodies attached to magnetic beads and then the labelled cells are magnetically immobilised within the column. The cells are then released by removing the magnetic field. This efficiently enriches cells of interest. If cells of interest are still required for immunological tasks, negative selection tools are a better choice. All other cells are labelled and immobilised on a column, and the cells of interest pass through the column without antibodies attached. Isolation kits containing antibodies that can be released after separation steps are now available. However, their use for immunological therapeutics remains questionable. Here, the EasySep™ Human NK cell Enrichment Kit (Stemcell™ Technologies) was used to negatively select NK cells from the NPC fraction, which was originally developed to enrich NK cells from the PBMC fraction. This tool targets unwanted non-NK cells using tetrameric antibodies and dextran-coated magnetic particles. The separation process is performed in tubes, so no columns are required and the cells of interest are transferred to a new tube. Flow cytometric analysis clearly demonstrates the efficiency of the enrichment kit. Before the separation steps were performed, the NK cell population was calculated at 13.9% within the CD45<sup>+</sup> cell population and CD3<sup>+</sup> cells had an average of 63.4% (**Figure 16 A**). After NK cell enrichment, the ratio was calculated to be 87.9% and CD3<sup>+</sup> cells were calculated to be 0.32% (**Figure 16 B**). This enrichment is in line with manufacturers expected NK cell content of 73-95% within the enriched sample.

The purity may vary due to the NK cell content of the starting sample.

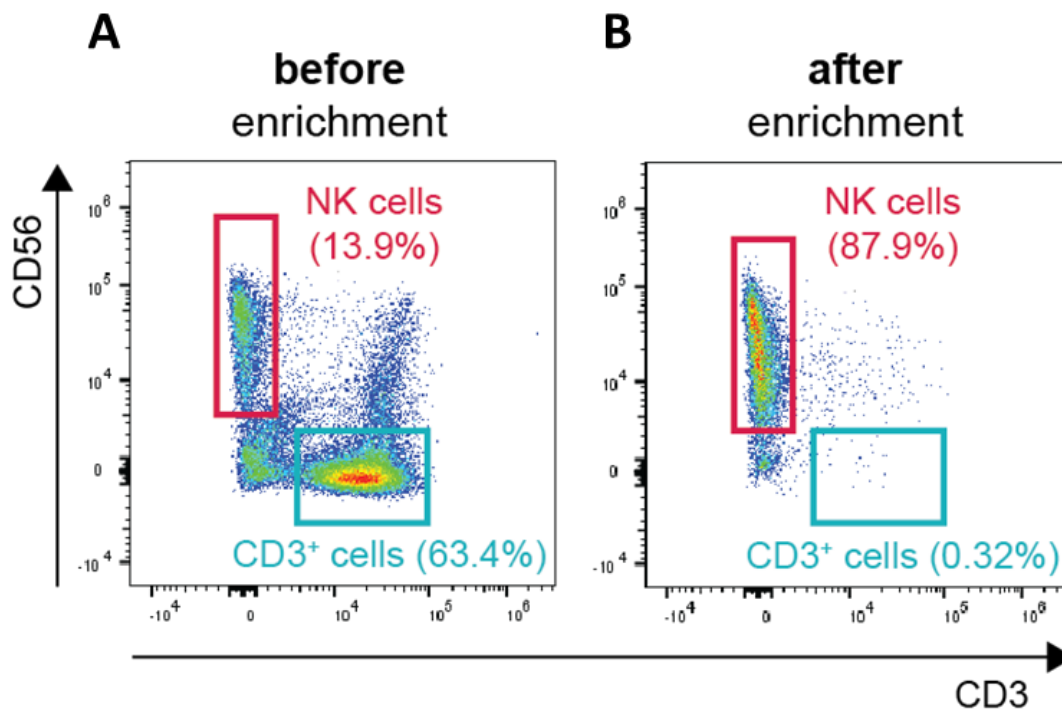


**Figure 16. Natural killer cells can be enriched from NPC fraction.**

Non-parenchymal cells derived from donor 4 were labelled using EasySep™ Human NK cell Enrichment Kit and prepared according to manufacturer's instructions. Cells were then stained with fluorescence antibodies and analysed using flow cytometry (B) and compared to cells that were not undergone separation (A).

In summary, these analyses show that NPCs from different donors can differ greatly in the composition of cell subsets. Moreover, freezing and thawing processes have a strong negative impact on cell survival. Many cells showed poor recovery after these processes, as assessed by microscopy. However, it is possible to maintain NPC in cell culture, although the most appropriate cell culture conditions still need to be investigated. To expand the lymphocyte population, stimulation of the cells is necessary. IL-2 and IL-15 stimulation resulted in strong expansion of NK and T cells after 7 days. To target NK cells, the NK cell enrichment kit provides high purity.

### **3.3 Establishment of the adoptive transfer of NPC into liver humanized mice harbouring matched hepatocytes infected with HBV**

T cells have previously been shown to reduce HBV viremia, HBV DNA and RNA and cccDNA when adoptively transferred into humanized mice harbouring HLA-matched human hepatocytes. PBMC-derived T cells were genetically modified to express HBV-specific TCRs. The expression of HBV-directed TCRs can either be transient or stable. For effective treatment of HBV infection, T cells expressing transient HBV-directed TCR require repeated administration of the generated T cells, whereas a single dose of T cells stably expressing HBV-directed TCR is effective [158, 159]. In another approach, PBMC were transferred into humanized mice infected with HBV and NK-mediated hepatocyte degeneration was observed. This was induced by Fas/Fas-ligand interaction provided by NK cells activated by dendritic cells [194]. To date, no approaches using liver-derived lymphocytes for adoptive cell transfer have been published. Both peripheral T cells and NK cells have been shown to efficiently recognise and eliminate HBV-infected hepatocytes. However, the amount of NK cells within the liver-resident lymphocytes is higher than in the periphery. In this study, liver-resident lymphocytes are transferred into humanized mice (USG) harbouring hepatocytes from the same donor. It is investigated whether NPCs are recruited to the HBV-infected liver. In addition, possible serological and intrahepatic effects between HBV infected hepatocytes and NPC -derived immune cells were to be analysed as a part of the NPC-PHH crosstalk. Therefore, a piece of liver was carefully separated into a hepatocyte and a non-parenchymal cell containing fraction. Hepatocytes were used to generate liver chimeric USG mice which were then infected i.p. with HBV infectious serum (**Figure 5 + Figure 17**). After 11 weeks, a stable HBV viremia was detected measuring HBV in blood serum. NPCs were thawed and activated with IL-15 overnight in cell culture. The flow cytometric analysis of the used NPCs for this approach revealed following lymphocyte fractions: ~ 40% T cells, ~ 28% NK cells and ~ 31% B cells. In addition, ~ 15% monocytes

were calculated within the CD45<sup>+</sup> fraction. Together with the lymphocytes monocytes display the CD45<sup>+</sup> leucocytes. Next day, NPCs were harvested and transferred interperitoneally into USG mice bearing matched HBV-infected hepatocytes (**Figure 17**). After 6 or 7 days, the mice were sacrificed and blood and livers were collected and analysed.

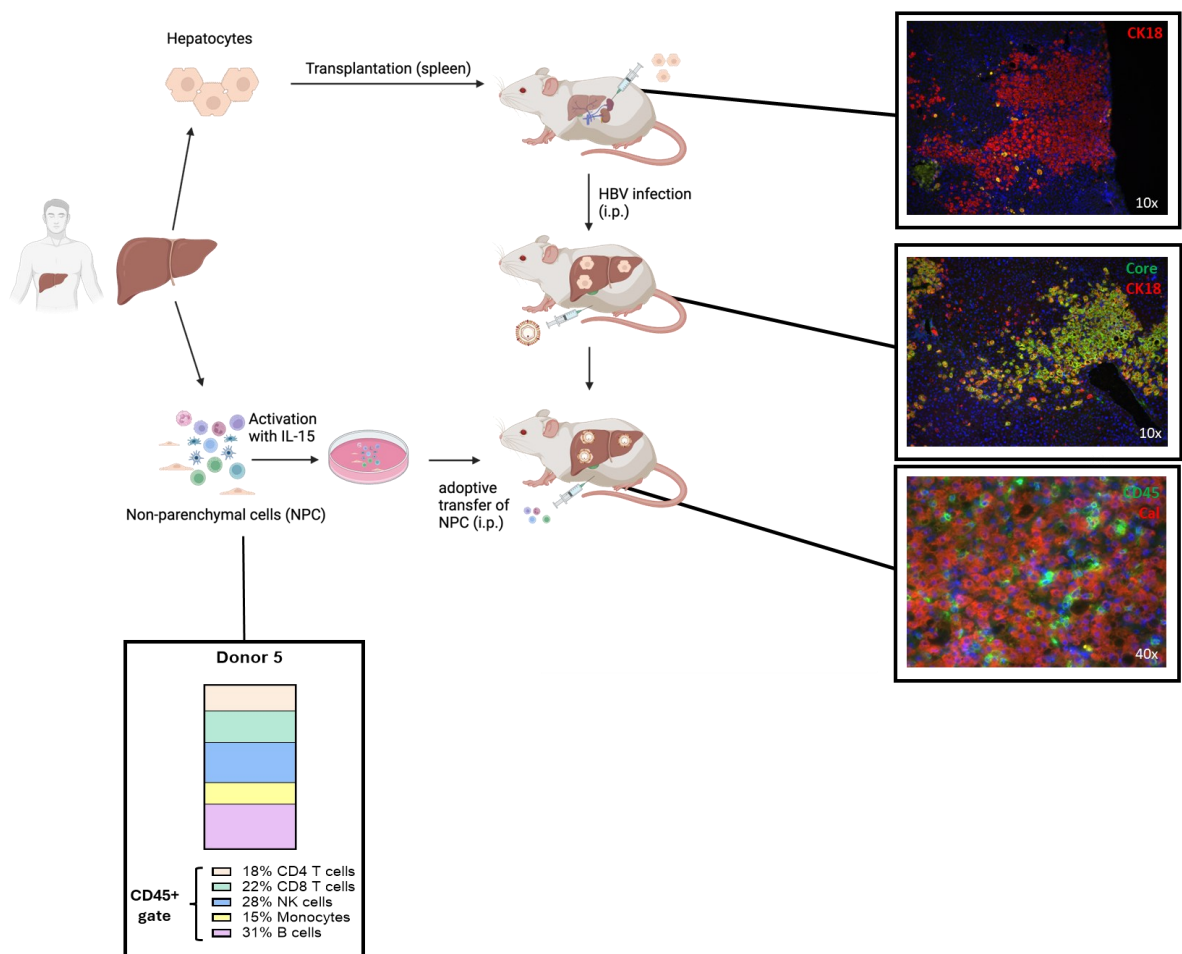


**Figure 17. Scheme of the adoptive cell transfer of NPC into liver humanized mice chronically infected with HBV.**

A piece of human liver was separated into hepatocyte and non-parenchymal cell fractions. Both were cryopreserved until use. Hepatocytes were used for transplantation of humanized mice. After 8 weeks of repopulation mouse livers show big clusters of human hepatocytes (upper histology, CK18, red). Mice were infected with passaged HBV-infectious mouse serum. After 12 weeks, a stable HBV infection was detected (middle histology, core (green), CK18 (red)). NPCs were analysed using flow cytometry and antibodies detecting phenotypical lymphocyte proteins. NPCs were thawed and activated with 100 µg/mL IL-15 over night. Next day, NPCs were harvested and transferred i.p. into humanized HBV-infected mice and uninfected control mice. Humanized mouse livers were stained for CD45 lymphocyte marker (green) and human hepatocyte marker (cal, red) (lower histology).

### 3.3.1 CD45<sup>+</sup> lymphocytes are recruited into the liver of humanized mice after adoptive transfer of NPCs

Adoptive transfer of 0.3 million NPCs into hepatocyte-matched USG mice (n=8) resulted in the reduction of HBV viremia in 3 mice compared to HBV-infected controls (n=6) (**Figure 18 A**). The majority of mice showed no changes in HBV viremia levels, only 1 untreated control mouse and 2 NPC treated mice appear to have higher HBV levels after 6 days. This may be a consequence of ongoing hepatocyte infection. In two mice that showed a decrease in HBV titre, infiltration of CD45<sup>+</sup> lymphocytes into the liver was detected by immunofluorescence staining. CD45<sup>+</sup> lymphocytes were specifically enriched in human areas (human calnexin, red) of the chimeric livers (**Figure 18 D+E**). Untreated mice were negative for CD45<sup>+</sup> immunofluorescence staining (**Figure 18 F**). Only the 2 mice positive for

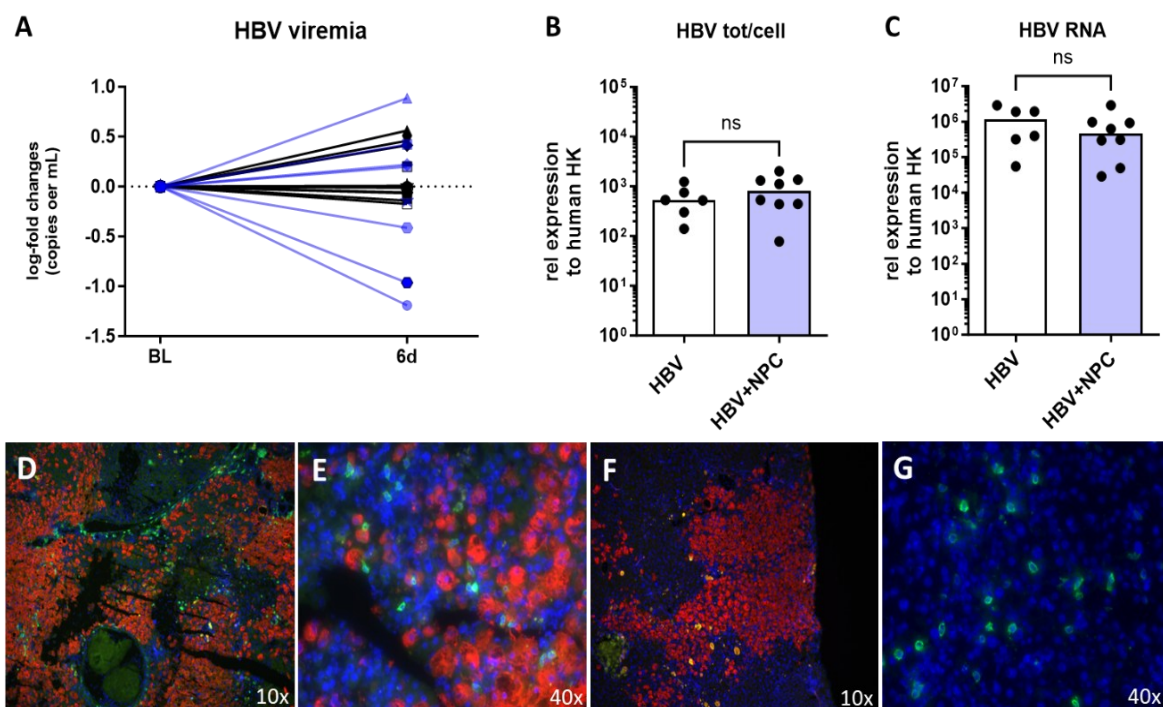


**Figure 18. NPCs can be recruited into the liver of HBV-infected USG mice and reduce HBV viremia.**

The adoptive transfer of 0.3 million NPC into hepatocyte matched USG mice (n=8) was compared with HBV infected controls (n=6). HBV DNA was extracted from mouse serum and HBV viremia was calculated using PCR technique and HBV standard curves (**A**). HBV DNA (**B**) and RNA (**C**) were extracted from mouse livers and compared to infected controls. Immune fluorescence co-staining demonstrates liver infiltrating CD45<sup>+</sup> lymphocytes (green) into HBV infected USG mice harbouring human hepatocytes (CK18 red) (**D+E**). No CD45<sup>+</sup> cells were found in untreated mice (**F**). Livers positive for human CD45 also showed CD45<sup>+</sup> lymphocytes within the spleen (**G**). Cell nuclei were stained with DAPI (blue; **D-G**). Expression levels were normalised to the mean of GAPDH and RPL30.

CD45 in the liver also showed CD45<sup>+</sup> lymphocytes in the spleen (**Figure 18 G**). This is the first part of the NPC-PHH crosstalk, showing that adoptively transferred NPCs can detect HBV-infected hepatocytes, even if only in some cases. However, intrahepatic analysis revealed no substantial changes in HBV DNA and RNA levels (**Figure 18 B+C**). Furthermore, serum levels of HBsAg and HBeAg did not vary over the 6 days (data not shown).

The secretion of cytokines involved in immune cell recruitment and direct cell killing is a major function of lymphocytes. In principle, TNF-alpha is released by macrophages and lymphocytes to initiate NF-κB activation, which then induces cell activation, cell differentiation or regulates cell apoptosis. As part of the innate immune response, IFN-gamma is responsible for the activation of cytotoxic NK and T cells. After binding to the IFN receptor, signal transduction via the JAK/STAT pathway induces the transcription of genes involved in adaptive immune responses. It also induces the expression of HLA class I and class II molecules to enhance antigen presentation. When cytotoxic lymphocytes identify infected cells, they release granzyme B (GZMB) which is a protease that induces programmed cell death by activating caspases. The release of cytokines in response to HBV

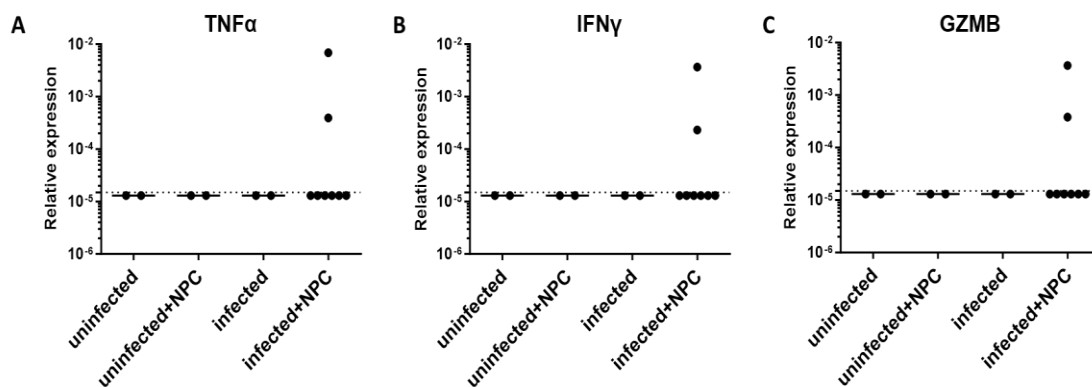


**Figure 19. Upregulation of cytokines involved in lymphocyte signalling and HBV cell killing.**

RNA was extracted from chimeric livers of mice infected with HBV and treated with NPC ( $n=8$ ). PCR amplification revealed mRNA gene expression of the cytokines TNF $\alpha$  (A), IFN-gamma (B) and GZMB (C). Expression levels were compared to untreated ( $n=2$ ), uninfected ( $n=2$ ) as well as uninfected and NPC treated ( $n=2$ ) mice. Expression levels were normalised to the mean of GAPDH and RPL30. Dashed line indicates the low limit of detection.

infection is an important step that needs to be demonstrated to prove functional crosstalk between NPC-derived immune cells and PHH. After NPC administration, RNA was extracted from mouse livers and the mRNA expression of TNF $\alpha$ , IFN-gamma and GZMB was analysed by PCR. It was shown that only the 2 livers positive for CD45 and with reduced

HBV viremia induced the expression of all 3 cytokines. In the other specimen, mRNA expression was below the detection limit (**Figure 19 A-C**). This clearly indicates the functionality of the recruited lymphocytes. The detection of released cytokines in this approach is a clear indication of a functional NPC-PHH interaction, as TNF-alpha, IFN-gamma and GzmB were only detected within HBV-infected mice after adoptive NPC transfer. The production of TGF-beta by regulatory T cells and hepatic stellate cells can suppress immune responses and promote fibrosis [236]. In this study, no changes in TGF-beta expression were detected (data not shown), suggesting that regulatory T cells are not yet activated. To identify the lymphocyte populations responsible for the observed effects, immunofluorescence staining of liver sections and mRNA expression analysis of liver samples were performed. Lymphocytes, especially NK cells, are balanced by stimulation of their activating and inhibitory receptors expressed on the cell surface. Some of these receptors are found on both NK and T cells, while others are expressed dominantly or exclusively by one cell type. Therefore, mRNA expression analysis was performed. As the mouse livers were not perfused after explants, the lymphocytes that migrated into the mouse liver were still in the tissue and could be detected by PCR. Here, only RNA from mice with CD45<sup>+</sup> lymphocytes and titre reduction were selected for visualisation.

The inhibitory receptor NKG2A was detected in both RNA samples from mice with NPC-derived liver infiltrating lymphocytes (**Figure 20 A**). Perforin was also measured in both NPC-treated mouse livers (**Figure 20 D**). Both proteins are expressed on NK cells and cytotoxic T cells. The major NK cell activating receptor NKp46, which is involved in killing of infected cells, was not expressed in NPC-treated mice, nor was NKp80, which stimulates the release of pro-inflammatory cytokines from mainly NK cells and a small subset of T cells (**Figure 20 B + C**). Unfortunately, we failed to establish functional staining to detect NK cells fixed with PFA or acetone on cryopreserved sections. Therefore, liver sections were co-stained with CD45 and CD3. Only double positive cells were found in liver sections from mice treated with NPCs (**Figure 20 F**), suggesting that T cells were recruited to the liver of humanized HBV-infected mice treated with NPCs due to their co-expression of CD45 and CD3. NK cells that do not express the CD3 receptor would have been positive for CD45 only, but these cells were not detected. Furthermore, triple staining for CD45, CD4 and CD8 showed that not only cytotoxic CD8 T cells but also CD4 T cells migrated into the liver (**Figure 20 E**).

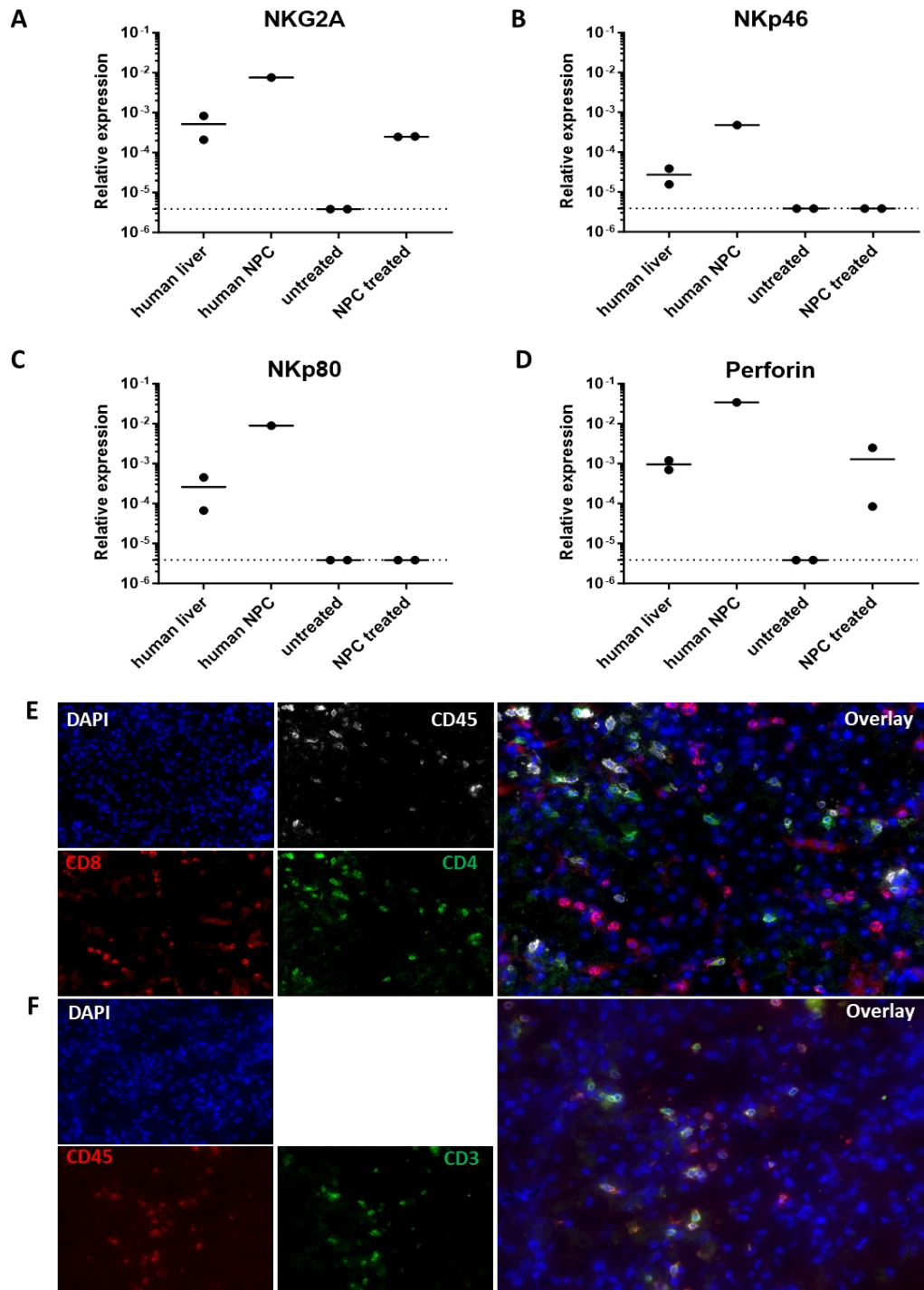


**Figure 20. Identification of lymphocyte population that infiltrates the liver of humanized mice after NPC transfer.**

mRNA expression levels of NKG2A (A), NKp46 (B), NKp80 (C) and perforin (D) were determined by qPCR in mice infected with HBV and positive for CD45 (n=2) and compared with untreated control mice (n=2), human uninfected liver sample (n=2) and human NPC (n=1). Expression levels were normalised to the mean of GAPDH and RPL30. Dashed line indicates low limit of detection. Immunofluorescence co-staining for CD45, CD8 and CD4 (E) as well as CD45 and CD3 (F) on cryopreserved liver sections derived from one of the 2 CD45+ mice after NPC transfer. Nuclei staining is shown with DAPI (blue). In conclusion, in 2 out of 8

trials, the transfer of 0.4 million NPC into liver chimeric mice with matched hepatocytes resulted in successful migration of CD45<sup>+</sup> lymphocytes into the liver and spleen. The recruited lymphocytes effectively produced IFN-gamma, TNF-alpha and GZMB, indicating a functional crosstalk between NPC and PHH. In addition, HBV viremia was reduced in these mice. CD4<sup>+</sup> and CD8<sup>+</sup> T cells were identified in the chimeric liver, while there was no evidence for the presence of NK cells.

### **Analysis of HLA class I and class II expression after NPC treatment of HBV infected liver chimeric mice**

In this study, HLA mRNA expression of class I and class II molecules already showed a clear induction after the treatment with T cells (**Figure 10 + Figure 11**) and IFN-gamma protein (**Figure 9**) in HBV-infected mice. In particular, HLA class I molecules were induced after the treatment with IFN-alpha, -beta and -lambda. HLA-DPB1 and HLA-DRA were the only members of the HLA class II group that responded to IFN-beta treatment with increased expression levels compared to untreated HBV-infected controls (**Figure 12** Fehler! Verweisquelle konnte nicht gefunden werden.). mRNA expression analysis of RNA extracted from the livers of NPC-treated mice showed clear induction of HLA class I members HLA-A (> 1 log), HLA-B (~ 1.5 log), HLA-E (1 log) and HLA-F (> 1 log) (**Figure 21 A-D**). HLA class II expression levels were also significantly upregulated following successful recruitment of liver infiltrating lymphocytes. HLA-DPB1 was significantly increased (3 log,  $p < 0.04$ ) as well as HLA-DRA (~ 3 log,  $p < 0.04$ ) (**Figure 21 E + H**). For HLA-DQA1 and HLA-DQB1, expression levels were induced after positive NPC transfer but could not be calculated due to low expression in HBV-infected untreated controls (**Figure 21 F + G**). These results are comparable to the induction of HLA class I and II expression after adoptive transfer of engineered T cells.

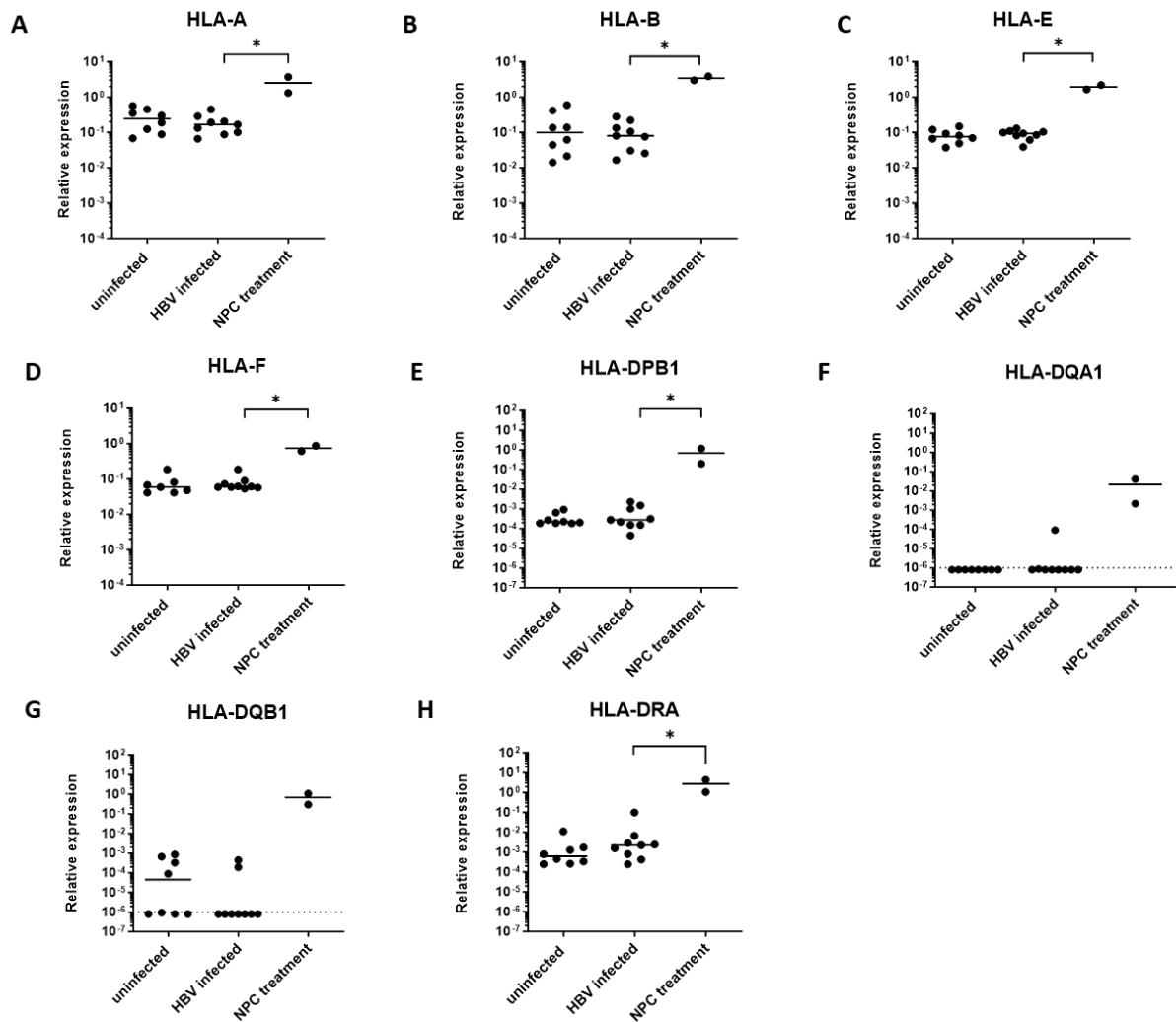


**Figure 21. HLA class I and class II were clearly induced after treatment with NPC.** mRNA expression levels of HLA-A(A), HLA-B(B), HLA-E(C) and HLA-F(D) next to HLA-DPB1(E), HLA-DQA1(F), HLA-DQB1(G) and HLA-DRA(H) were determined by qPCR in mice infected with HBV (n=9), uninfected controls (n=8) and mice infected with HBV and treated with NPC (n=2). Expression levels were normalised to the mean of GAPDH and RPL30. P values were calculated via Mann-Whitney U test. \*p<0.04. Only the 2 NPC treated mice that were proved to have CD45 lymphocytes within the humanized liver are imaged and used for calculation.

### 3.4 Mass cytometry technique opens new possibility for imaging virus infected cells in the presence of immune cells

Limited access to liver tissue samples and lack of technologies for detailed analysis have hampered investigations into the pathogenesis of human HBV. Many approaches have

focused on peripheral immune cells, liver perfusates or processed liver tissue to study the immune microenvironment of HBV-infected livers. While these techniques have provided important insights into the pathogenesis of human HBV, direct visualisation of the liver parenchyma and infiltrating immune cells and cell subtypes has not been possible. The use of CyTOF (cytometry by time of flight) lasers for the simultaneous detection of 30-40 rare earth isotope-labelled antibodies on formalin-fixed paraffin-embedded (FFPE) tissue was developed to fill this knowledge gap. This new technique, called imaging mass cytometry (IMC), has recently been reported to visualise different immune cell types (CD4 and CD8 T cells, NK cells, hepatic macrophages), hepatocytes and HBV antigens in parallel on FFPE liver tissue. This new method allows the study of associations between innate and adaptive immune cell subtypes and HBV-infected hepatocytes *in situ* [216]. However, adapting this promising new method to cryopreserved liver samples is challenging because most of the available antibodies aren't tested on cryopreserved sections. In addition, there are severe limitations due to the chimeric system. Finding antibodies that only bind to human cells fixed on cryopreserved liver tissue has been a challenge.

In this study, cryopreserved liver sections from liver chimeric mice chronically infected with HBV and treated with T cells were used to initiate the establishment of an IMC antibody panel for the detection of human immune cells within HBV-positive humanized mouse livers (workflow of IMC presented in **Figure 22**). To this end, 16 metal-conjugated antibodies (Table 5) were tested on cryopreserved liver sections for the selective binding to human cells within a liver chimeric USG mouse model. Antibodies ranging from immune cell markers (CD3, CD45, CD4, CD8, CD68) and immune checkpoint markers (PD-1, PD-L1) to hepatocyte markers (pan-keratin, keratin8/18), structural markers (collagen, CD31) and cell death associated markers (GZMB, caspase3, perforin) to general human cell markers (HLA-ABC) and proliferation markers (Ki-67). After initial binding experiments, the following antibodies were identified to fit the chimeric UBS mouse model system: HLA-ABC, CD45, CD4, CD68, CD8, CD3, GZMB, Ki-67, collagen I and keratin 8/18.

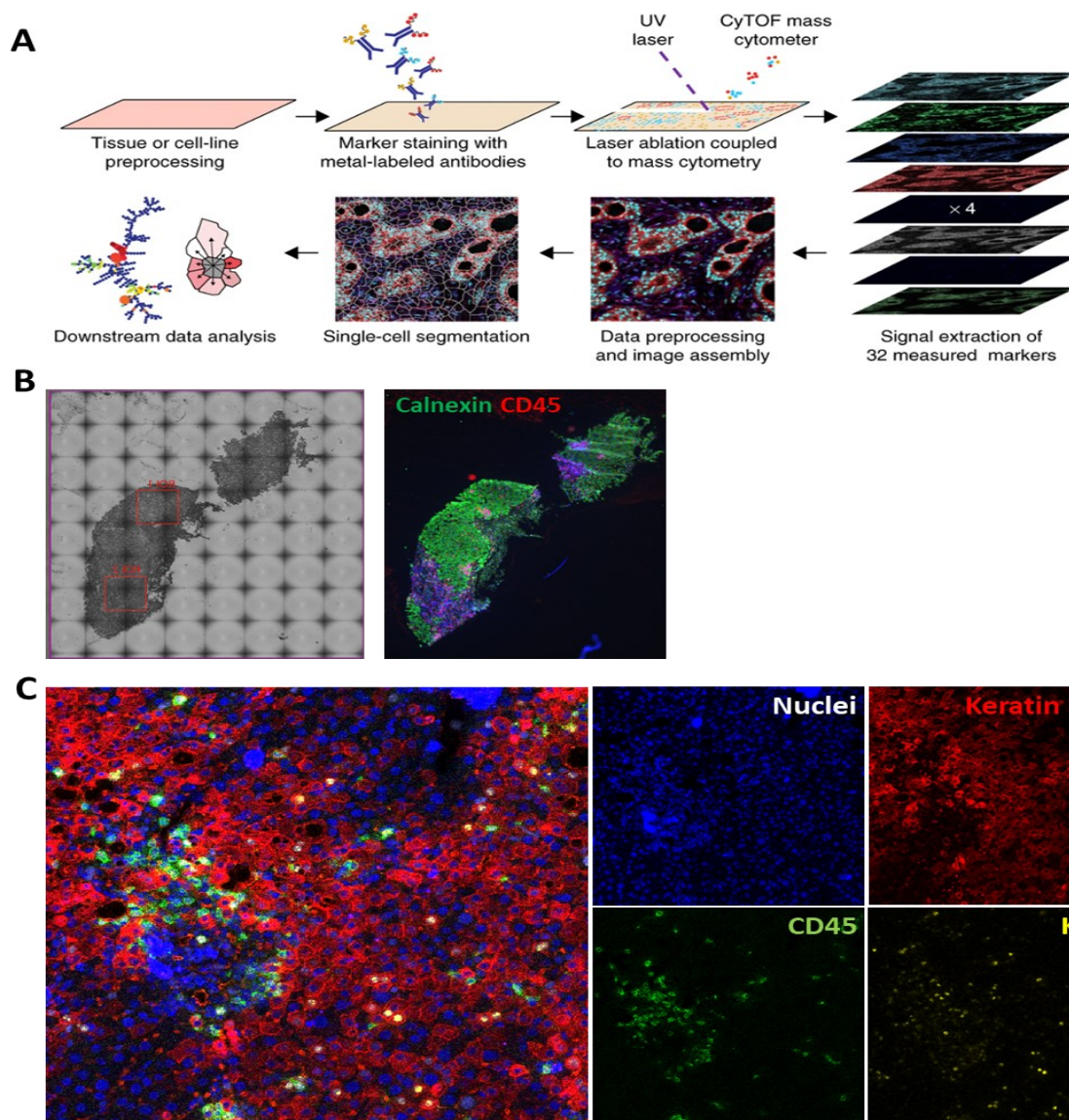


**Figure 22. Imaging mass cytometry adapted for cryopreserved chimeric liver tissue.**

Workflow of imaging mass cytometry (adapted from [216]; **A**). After staining the tissue, a panorama of the tissue on the slide was created (**B**, left). The regions of interest (ROI) were chosen using a serial slide stained with fluorescent antibodies detected by microscope. Areas including cells of interest (here CD45) were chosen for ROI (**B**, right). IMC data analysis of ablated slides derived from a liver chimeric mouse infected with HBV and treated with T cells was performed using MCD viewer. Antibody dilution 1:400 (**C**). Cells were visualized using MCD Viewer software.

The viral hepatitis B markers HBsAg and HBcAg were then additionally conjugated to metals to complete a first functional panel. With the support of Dr. Desirée Kunkel (Core Facility Berlin), the extensive process of antibody titration was planned in 4 rounds (1. DNA intercalators, 2. structural markers, 3. phenotype markers, 4. viral and other protein markers). Only a few tissue conditions have been tested so far due to the high cost and time required for instrument ablation. The panel has been validated on mouse liver (negative

control), healthy human liver tissue, HBV-infected and HBV-positive T cell treated chimeric mouse liver tissue. Using the keratin 8/18 antibody, only human hepatocytes were stained specifically and visualised (**Figure 22**). The CD45-linked antibody effectively bound to human CD45 lymphocytes that had migrated into the liver after adaptive T cell transfer (**Figure 22**). HBV infection was visualized using HBcAg and HBsAg. Hepatitis core antigen was found predominantly in the nuclei of the hepatocytes, whereas HBsAg was expressed in the cytoplasm of hepatocytes (**Figure 23**), which agrees with the literature. DNA intercalator, which stains cell nuclei, was used at 1:800 dilution. Hepatocyte markers (Keratin-8/18) and viral markers (HBcAg and HBsAg) were used at 1:400 dilution. The viral markers require further titration to avoid unspecific signals.

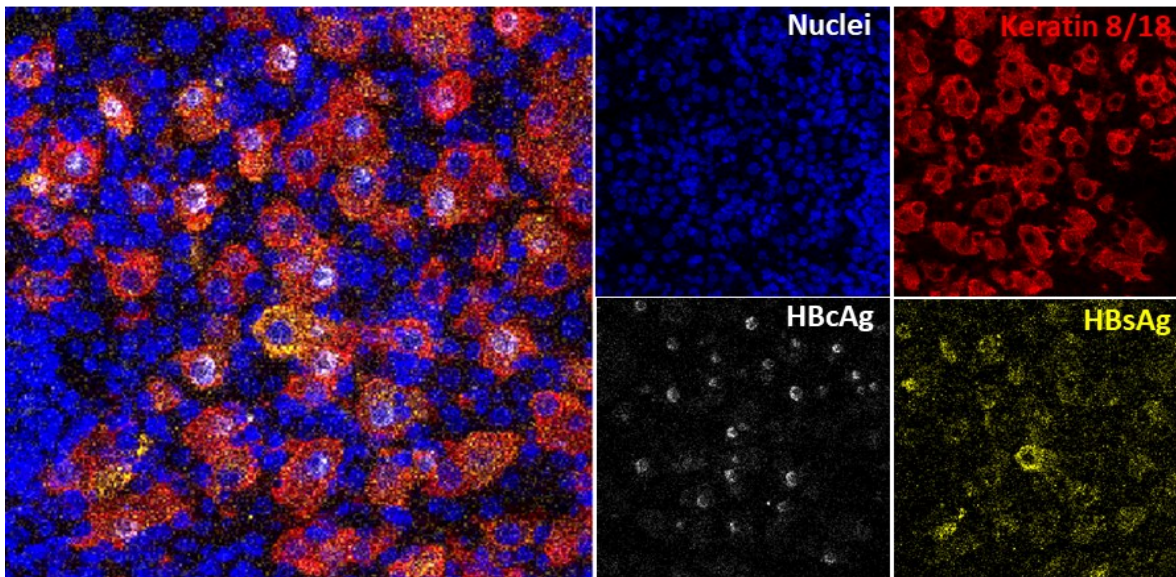


**Figure 23. IMC data analysis of HBV viral proteins within human hepatocytes.** Imaging mass cytometry data from an HBV infected liver chimeric mouse were visualised. Hepatocytes were stained with Keratin 8/18 (red), viral proteins HBcAg (white) and HBsAg (yellow) demonstrated the infection. Nuclei were stained a DNA intercalator (blue). Cells were visualized using MCD-Viewer software.

Within the panel used, both CD4 and CD8 T cells can be identified after adaptive T cell transfer (**Figure 24**). The lymphocyte marker CD45 showed a strong signal when used at a dilution of 1:400. However, a higher dilution would reduce background or non-specific signals. The T cell markers CD4 and CD8 were also used at a 1:400 dilution. While CD4 showed a good signal around the cell, CD8 was either not strongly expressed on the cell surface or the binding of the antibody to the cell surface was insufficient. The signal displayed is of variable intensity and does not completely cover the cell surface. Therefore,

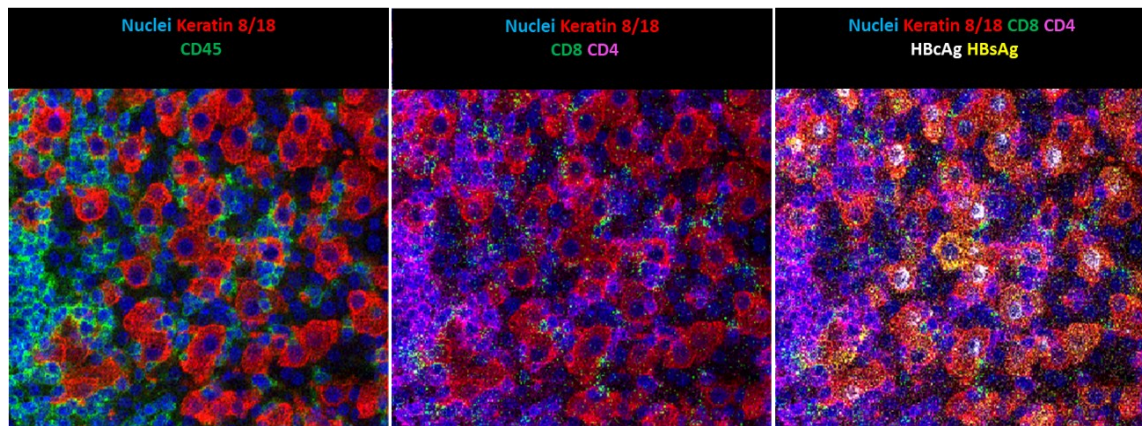


**Figure 24. IMC data analysis of HBV viral proteins within human hepatocytes.**  
 Imaging mass cytometry data from an HBV infected liver chimeric mouse. Hepatocytes were stained with Keratin 8/18 (red), viral proteins HBcAg (white) and HBsAg (yellow) demonstrate the infection. Nuclei were stained a DNA intercalator (blue). Cells were visualized using MCD Viewer software.

a different CD8 antibody derived from a different clone might give a better signal. This should be tested in the future. Overlapping of too many colours has a negative effect on the optically merged image, but for data analysis many clearly shaped cells are not a problem.

Analysis of human liver tissue revealed fewer T cells in the liver parenchyma (**Figure 25**), as CD3 (green) is rarely detected. However, this marker was less diluted (1:100) but already showed a strong signal with almost no background. In contrast, many Kupffer cells were present in the liver. These cells express both CD45 (red) and CD68 (white). The monocyte and macrophage marker CD68 showed a strong background signal and has to be

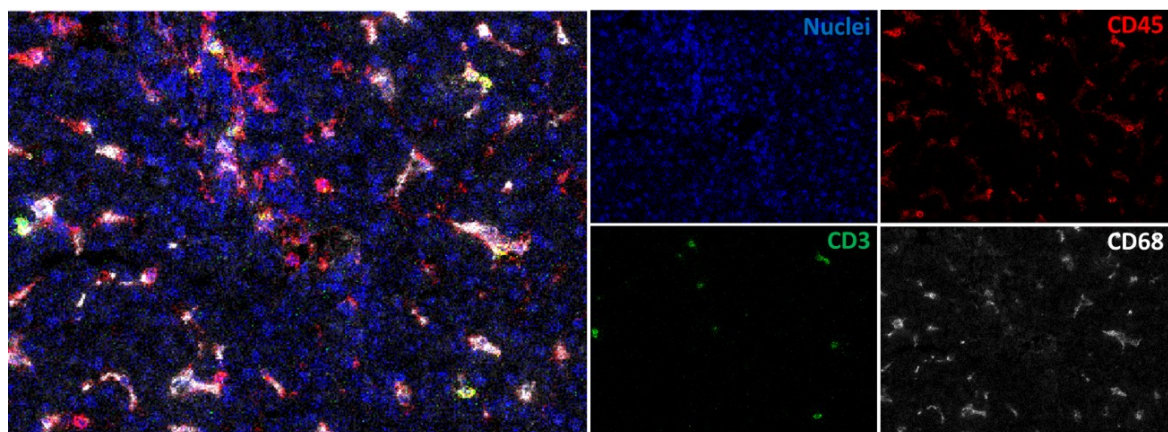


**Figure 25. IMC data analysis of human liver tissue.**  
 Lymphocytes were stained with CD45(1:100; red), CD3 T cells were stained with CD3 (1:100; green) and Kupffer cells were stained with CD68 (1:100; white). Cells were visualized using MCD-Viewer software.

further diluted.

Finally, to establish the system, HBV-infected untreated chimeric livers must be titrated, because viral markers are the strongest in HBV-infected liver. Most of the markers tested need to be further diluted to obtain optimal signals without background. This is necessary for downstream data analysis, where cells analysed with the MCD viewer, can be segmented using the Cell Profiler software, and then higher order analysis (cluster/tSNE) can be performed using the HistoCAT software.

In conclusion, imaging mass cytometry can be a useful tool to study the geographical distribution of HBV infection within human cells. It can also help to understand interactions with cells of the innate and adaptive immune system. However, the use of cryosections for the detection of HBV proteins and immune cells is challenging. Today, there are few conjugated antibodies available that effectively bind to targets on cryosections. The detection of NK cells is of great interest for answering questions related to innate immune responses. Therefore, the development of functional NK-directed antibodies is required.

## 4 Discussion

Despite being discovered in the 1960s, a cure for chronic HBV infection remains elusive. Chronic HBV causes severe liver disease, cancer, and over one million deaths annually, representing a significant global health burden. Current treatments using Nucleotide analogues are safe and very effective in controlling HBV replication, leading to improvement of liver diseases. However, they are not curative and requires lifelong use. Researchers are exploring new therapies to achieve functional cure, focusing on HBV's interaction with hepatocytes and infection pathways to develop new antiviral strategies. However, the role of antiviral signalling in HBV pathogenesis is not fully understood.

Studying HBV is challenging due to limited infection models and patient biopsy access. This study utilized chimeric liver USG mice, which lack an adaptive immune system, to investigate hepatocyte-expressed HLA molecules in HBV detection. Humanized mouse liver RNA was analysed for HLA mRNA expression using TaqMan probes. The liver's NPC fraction, rich in immune cells, is characterized for T cells, NK cells, and NKT cells from different donors. Additionally, the study will evaluate the effectiveness of NPC adoptive transfer in HBV-infected humanized mice, focusing on immune cell recruitment and antiviral effects.

### **4.1 Human leucocyte antigen molecules are not induced upon HBV infection but can be differently upregulated upon IFN stimulation**

Recently published data have shown a high variability in the innate immune response to HBV. Using a chimpanzee model, Wieland et al. found that HBV neither induces nor blocks innate antiviral responses in hepatocytes. However, other studies suggest that non-cytopathic antiviral mechanisms can clear HBV from hepatocytes before adaptive immune cells infiltrate, suggesting a potential role for innate immunity [87, 131].

Studying innate immune responses in hepatocytes is challenging due to limited models. Liver chimeric USG mice, which lack adaptive immunity, provide a valuable system to examine hepatocyte-specific responses to HBV without interference from other immune cells. Key questions include whether hepatocytes can sense HBV and if their signalling

pathways are functional [237]. Hepatocytes, the main cells of the liver, can detect and combat pathogens by expressing key IFN receptors and activating innate immune signaling upon viral infection [238, 239]. This could lead to new therapeutic strategies for curing HBV infection [237]. Immune responses to pathogens are orchestrated by HLA class I and II molecules, which present antigenic peptides to CD4<sup>+</sup> helper T cells and CD8<sup>+</sup> cytotoxic T cells, thereby activating adaptive immunity [111]. The outcome of HBV infection is critically influenced by the immune response, particularly polyclonal CTL responses, which are linked to viral clearance and may be affected by genetic factors [240-242]. Given the high polymorphism of HLA genes, they are ideal for studying HBV infection outcomes [111]. However, few studies have explored HLA class I expression on human hepatocytes infected with hepatitis viruses. This study used liver chimeric USG mice to analyse mRNA expression levels of HLA-A, -B, -E, and -F in human hepatocytes infected with HBV, HCV, and HEV. The results showed no changes in HLA class I expression on HBV-infected hepatocytes compared to uninfected controls, aligning with the dysfunctional immune responses observed in HBV-specific CTLs [243].

HBV-specific immunodominance is strongly influenced by the HLA class I profile and HBV genotypes.

HLA class I alleles associated with HBV persistence suggest that the outcome of HBV infection is influenced by HLA composition and effective epitope presentation [111]. Differences in the process of antigen presentation for HBV and HCV may be due to different life cycles. HCV, an RNA virus, is released into the cytoplasm, making it more detectable by the host's immune system. In contrast, HBV, a DNA virus, enters the nucleus of hepatocytes almost undetected to produce viral particles [29, 244].

Additionally, HLA class I mRNA expression is significantly upregulated during HEV infection, an RNA virus that shares life cycle similarities with HCV [245]. Previous studies have shown that HLA-E mRNA is induced in HBV/HDV co-infected hepatocytes in humanized mice [90], and similar increases in HLA-A, HLA-B, and HLA-C mRNA were observed in HBV/HDV co-infected primary human hepatocytes [246]. However, consistent with the findings here, HLA-A and HLA-B expression were not upregulated in HBV-infected PHHs or human liver biopsies. Tham et al. noted a slight induction of HLA-C during HBV infection, but HLA-C levels were not analysed in this study due to detection limits.

The significance of HLA genes in HBV infection was further emphasized with the discovery

of HLA-DP gene variants, which show the strongest association with chronic HBV infection [6, 129]. Despite their lower surface expression and less polymorphic structure compared to HLA-DR and HLA-DQ, HLA-DP molecules have often been overlooked in viral infection studies. [129, 247].

The mRNA expression levels of HLA-DP molecules are increasingly recognized for their role in HBV infection outcomes. Specific HLA class II alleles have been linked to either HBV clearance or persistence. O'Brien et al. found that reduced mRNA expression of HLA-DPA1 and HLA-DPB1, associated with SNPs, increases the risk of chronic HBV infection [248]. They suggested that variations in the 3' UTR might reduce mRNA stability, possibly due to regulatory factor binding or microRNA regulation [249]. This aligns with recent findings showing that lower HLA-DPB1 expression in chronic HBV patients could impair immune responses by reducing antigen presentation [250]. These insights suggest that HLA expression might influence viral control, prompting further analysis of HLA class II expression in hepatocytes infected with different hepatitis viruses using liver chimeric USG mice.

Compared to uninfected controls, HBV- and HEV-infected hepatocytes showed no changes in HLA-DPB1 and HLA-DRA expression levels. Only HCV infection significantly increased HLA-DPB1 expression. The study did not assess different HLA allele variants, and the donors for hepatocyte transplantation were not further HLA typed. This suggests that HLA molecule expression levels are generally distributed, regardless of specific protective or risk factors. Hepatocyte donors did not affect HLA-DPB1 expression levels, as different donors were used for HBV control and infection groups. The SCID model used for HBV infection lacks both innate and adaptive immune responses, including IFN-gamma, which is crucial for inducing HLA class I and II expression. The data indicate that HBV alone does not induce HLA class II expression on human hepatocytes without inflammatory stimuli, reinforcing the notion that HBV evades detection by not activating innate immune genes in infected hepatocytes.

Published studies on altered HLA expression are based on human samples, reflecting natural immune responses. However, administering IFN-gamma to HBV-infected humanized mice significantly increased mRNA expression of several HLA genes. Although statistical analysis wasn't feasible due to low control detection, these findings support IFN-gamma's ability to induce HLA class II expression on non-hematopoietic cells, while HLA class I is

universally expressed [219, 251]. If IFN-gamma can induce HLA expression on HBV-infected hepatocytes linked to viral clearance, it may offer a therapeutic approach, though further studies are needed to assess its effectiveness and manage the risk of immune-triggered liver damage in chronic HBV.

Analysis of HLA expression after HBV-directed T cell treatment showed clear induction of HLA class I and II, with detectable IFN-gamma only after T cell transfer. The correlation between HLA-DPB1 induction and IFN-gamma is noted, but it's unclear if HLA expression is driven by IFN-gamma or direct T cell-hepatocyte interaction, requiring further investigation. Since PCR was performed on total liver RNA, mRNA expression differences can't be solely attributed to hepatocytes. Control groups showed no HLA expression change without T cell infiltration. Future studies using immunofluorescence microscopy and flow cytometry could clarify these findings. Additionally, the interaction between T cells and HLA molecules is crucial, but NK cells, which also release IFN-gamma, play a significant role in this immune response.

Niehhs et al. recently demonstrated that protective HLA-DPB1 alleles interact with the activating receptor NKp44 on NK cells, triggering innate immune responses [134]. This discovery, similar to the identification of KIR3DS1 as a ligand for HLA-F, suggests that HLA class II plays a role in the innate immune response [134, 250]. The authors propose a mechanism during acute HBV infection where NKp44 binding to HLA-DP on HBV-infected hepatocytes, along with IFN-gamma release by NK cells and CD4 T cells, leads to the lysis of infected hepatocytes [252]. However, NKp44 cannot bind to HLA-DP with risk alleles, leading to inefficient lysis and an increased risk of chronic HBV infection [250, 252]. These findings highlight the synergy between adaptive and innate immunity in controlling viral infections and suggest new therapeutic approaches that exploit the interaction between HLA class II and immune cells to eliminate HBV infection.

This study, along with previous research, confirms that IFN-gamma induces HLA class I and II expression, whether as a recombinant protein or released from immune cells. However, the effects of other type I and III interferons on HLA expression remain less understood. PEG-IFN-alpha therapy, combined with nucleoside/nucleotide analogues, is the standard treatment for chronic HBV infection, though only 30-40% of patients respond to it [146]. The study aimed to investigate how interferons influence HLA class I and II expression to enhance viral sensing and peptide presentation. After 6 weeks of IFN-alpha treatment,

mRNA expression of HLA class I molecules was induced, but HLA class II molecules were not. Donor-specific variation was eliminated as all IFN-alpha-treated subjects contained hepatocytes from the same donor as the control groups. The rebound mice showed decreasing HBeAg and HBsAg levels under IFN-alpha treatment, which increased after treatment withdrawal (data not shown), indicating IFN-alpha's effectiveness. While HLA class I expression was clearly induced during IFN-alpha treatment, their levels returned to those of untreated mice after rebound, demonstrating that mRNA induction is dependent on IFN-alpha and that withdrawing treatment reverses both HBV infection markers and HLA expression.

IFN-alpha and -beta share the same receptor pair for binding (IFNRA1/A2), but IFN-beta appears to have a higher affinity for its receptor [225]. Treatment with IFN-beta for 4 and 6 weeks significantly induced all HLA class I molecules and also upregulated HLA-DPB1 and HLA-DRA, suggesting a stronger effect on HLA induction in HBV-infected hepatocytes compared to IFN-alpha. IFN-lambda, a member of the IFN III family using a different receptor for signal transduction, also induced HLA class I mRNA expression, but HLA class II expression remained unchanged compared to control groups. It remains to be determined whether the increased HLA class I expression improves immune responses via enhanced peptide presentation. Due to the lack of immune cells in the study model, further research, potentially involving immune cell transfer or alternative models, is needed to explore this. Additionally, the relationship between HLA induction and interferon treatment, independent of HBV status, should be investigated by treating HBV-uninfected mice with interferons and analysing their liver mRNA expression of HLA class I and II.

In conclusion, HBV does not alter the expression levels of HLA class I and II proteins on infected hepatocytes in vivo. IFN-gamma, whether from T cells or as a recombinant protein, can significantly induce HLA class I (HLA-A and -B) and class II (HLA-DPB1 and -DRA) expression on human hepatocytes, potentially enhancing immune detection in cases with protective alleles. While IFN-alpha, IFN-beta, and IFN-lambda all induce HLA class I molecule expression on human hepatocytes, only IFN-beta induces HLA class II molecules.

## **4.2 Liver-derived non-parenchymal cells can be stimulated to proliferate in cell culture after cryopreservation**

The importance of pathogen non-specific innate immune responses is gaining increasing attention in the context of HBV pathogenesis. With respect to host defence mechanisms in general, the liver is particularly enriched in innate immune cells [202]. In hepatitis infections, the intrinsic innate immune responses provided by these cells involve both protective direct antiviral and inflammatory pathways [239]. Studying HBV-hepatocyte interactions, particularly cell-intrinsic innate immune responses, has been challenging due to the lack of suitable infection models. Effective models must include functional host defence pathways and non-parenchymal cells to be biologically relevant [237]. These conditions aren't available in standard cell culture. This study analysed non-parenchymal cells (NPCs) from different donors for their composition, survival, and ability to proliferate after cryopreservation, aiming to find the best cell culture conditions for potential adoptive transfer into HBV-infected humanized mice. Cryopreserved NPCs were used instead of fresh cells due to the long timeframe required for the humanized mouse infection model, with only donor-matched hepatocytes and NPCs used to prevent immune activation from mismatched cells.

Due to the limited NPC supply from a single donor, the study involved NPCs from 5 different donors. Survival was analysed in cryopreserved cells from 3 donors and compared to fresh NPCs from a fourth donor. Flow cytometry revealed about a 46% reduction in total cell survival post-thawing. While CD45<sup>+</sup> lymphocyte survival rates were similar, significant variability was noted in cryopreserved NPCs, possibly due to general variability or the cryopreservation process. Variability in the fresh NPC group could not be assessed due to a single donor. The liver contains 30-40% non-parenchymal cells, including liver sinusoidal endothelial cells (50%), Kupffer cells (20%), lymphocytes (25%), biliary cells (5%), and hepatic stellate cells (1%) [202, 203, 213]. Comparing NPC data from this study with other analyses shows an 11-15% reduction in the CD45<sup>+</sup> lymphocyte population. This discrepancy might stem from differences in isolation protocols, as NPCs were obtained from two companies and an internal lab, which may have optimized protocols for hepatocyte isola-

tion. Additionally, cell death during thawing, a common issue with PBMC-derived lymphocytes, could also contribute to the reduced lymphocyte population in thawed NPCs.

A lymphocyte ratio of 10-15% in NPCs is typical for cell culture or transfer applications, given the higher number of non-target cells. This study analysed four NPC fractions from different sources, comparing cell surface protein expression (CD4 T cells, CD8 T cells, NKT cells, NK cells) using flow cytometry. NPCs from two companies showed nearly identical lymphocyte distributions, likely due to similar isolation protocols, though this needs further investigation including more donors. All NPC fractions had more NK cells and a higher CD8<sup>+</sup> T cell proportion compared to CD4<sup>+</sup> T cells. Significant variation in CD45<sup>+</sup> lymphocyte composition among donors is expected due to the greater tissue variability in human liver compared to standardized laboratory animals and the influence of factors like diet, lifestyle, and disease status [228].

Liver resections often performed due to disease, tumours, or inflammation, lead to variability in lymphocyte composition among donors. Ideally, research would use rejected livers from transplantation, but these are rarely available. Aizarani et al. observed differences in composition between fresh and cryopreserved liver samples from the same donor, as well as among different samples, due to variability in cell viability and types [65]. The study aimed to determine if non-parenchymal lymphocytes from liver tissue could proliferate and expand in culture. Various cell culture media (RPMI and SCGM) and interleukins (IL-2 and IL-15) were tested for stimulation. Unlike typical methods that isolate specific cell types, this study aimed to culture NPCs in their natural environment without separation. Despite efforts, the culture methods were insufficient for enriching the CD45<sup>+</sup> lymphocyte population. However, IL-15 stimulation increased the NK cell fraction within CD45<sup>+</sup> cells. NK cells were categorized based on CD56 expression into CD56<sup>dim</sup>, CD56<sup>bright</sup>, and CD56<sup>superbright</sup> subsets. Both IL-2 and IL-15 treatments elevated CD56 expression from CD56<sup>dim</sup> to CD56<sup>bright</sup>. CD56<sup>bright</sup> NK cells, which play a regulatory role and can develop antiviral cytotoxicity, showed expansion in CHB patients treated with PEG-IFN-alpha, particularly in responders. PEG-IFN-alpha also enhanced the expression of activating receptors, IFN-gamma production, and degranulation in CD56<sup>bright</sup> NK cells [253, 254]. Further research is needed to explore if CD56 expression levels correlate with increased NK cell activation and functional potential. It is hypothesized that NK cell subsets with higher CD56 expression might offer the most potential for therapeutic modulation [255].

Based on these findings, priming NK cells in culture may boost their antiviral potential for adoptive transfer. Cells stained with CFSE and cultured for 6 days showed NK cell activation and expansion, but no T cell expansion. Flow cytometry revealed NK, CD4 T, and CD8 T cells divided, while NKT cells did not. NK cell divisions aligned with previous data, but CD4 and CD8 T cells showed no increased numbers after 4 days, possibly due to balancing division and death rates or insufficient time for T cell division.

CD4 T cell divisions peaked with lower CFSE levels than NK, NKT, and CD8 T cells, likely due to faster division or lower initial CFSE uptake. Peaks were unclear due to uneven staining and low lymphocyte numbers. Despite proliferation in CD4, CD8, and NK cells, there was no clear lymphocyte enrichment, suggesting concurrent cell death possibly from culture conditions or cryopreservation issues.

In conclusion, understanding the variable composition of NPCs from hepatocytes is essential for experiments. Further separation of NPC-derived lymphocytes can increase target cell numbers and improve culture survival by allowing higher cell densities. Although NPCs in this study were responsive to stimulation and proliferation, optimizing cell culture protocols by pre-separating lymphocytes is recommended. Using density gradients to remove dead cells and debris, and consistent cell separation techniques, will help reduce composition variability. Donor health status, including HBV vaccination and liver immune status, is also crucial but often unavailable, especially when NPCs are sourced from companies.

### **4.3 Lymphocytes can be recruited into the liver of HBV-infected humanized mice after adoptive transfer of non-parenchymal cells**

Today, HBV is treated with nucleos(t)ide analogues (NAs) and PEGylated IFN-alpha. But strategies aiming at restoring immune cell function are also under intense investigation. Adoptive cell therapy, which has revolutionized cancer treatment, is now being explored for HBV [256]. T cells play a crucial role in the adaptive immune response. CD4 T cells activate B cells, stimulate CD8 T cells, and secrete cytokines to support APCs and effector T cells. CD8 T cells kill infected cells but often become exhausted and anergic in chronic HBV infections, marked by high levels of exhaustion markers (PD-1, CTLA-4), leading to

reduced HBV-specific T cell activity and lower antiviral responses [257, 258]. A breakthrough came with allogeneic bone marrow transplantation from HBV-cleared donors, resulting in HBsAg clearance, suggesting that donor HBV-specific T cells can overcome immunological exhaustion [257, 259]. Recent experimental approaches focus on restoring HBV-specific immunity with genetically engineered T cells, including chimeric antigen receptor (CAR) T cells [260] or a natural T cell receptor [261] targeting HBV surface proteins. These methods can detect and destroy HBV-infected cells and target cccDNA and integrated HBV DNA, offering advantages over immune checkpoint treatments [260, 261].

Adoptive transfer of engineered T cells into HBV-infected humanized mice effectively controlled viral replication and significantly reduced viral markers. Additionally, the HBV entry inhibitor bulevirtide (Myrcludex B) achieved long-term control of HBV infection [159]. However, T cell therapy can also cause liver damage, necessitating extensive preclinical research to understand its immunological impacts [257, 260].

Koh et al. and Kah et al. developed a method to create transient TCR-expressing T cells by electroporating T cells with mRNA for HBV-specific TCRs. These T cells, when transferred into HBV-infected humanized mice, produced IFN-gamma but lacked cytolytic activity, minimizing ongoing T cell proliferation and reducing liver inflammation [158, 262]. Currently, there are 9 clinical trials (phases 1 and 2) assessing the efficacy, dose, and safety of TCR-engineered T cells for HBV-related HCC [263].

Fergusson et al. developed "Immune Mobilising Monoclonal T cell Receptors against Virus" (ImmTAV), a fusion protein that combines an enhanced TCR with a humanized anti-CD3 antibody [264]. ImmTAV binds HBV epitopes on infected hepatocytes and redirects non-HBV-specific T cells to these targets via CD3 attachment [264, 265]. This method reprograms conventional CD8 T cells, inducing cytokine release and cytolysis of HBV-infected cells without the need for prior T cell expansion [264].

In this study, NPCs from a healthy liver that was transplanted but rejected were used for adoptive transfer into humanized USG mice chronically infected with HBV. Hepatocytes for liver repopulation came from the same donor. This study focussed on the understanding of interactions occurring between HBV-infected hepatocytes and immune cells derived from NPCs.

HBV viremia was reduced in 3 out of 8 mice, while one mouse showed an increase in HBV titre (>0.5 log). This small increase may also be due to some cell lysis or natural variations.

The increase in serum HBV DNA levels in some NPC-treated and untreated mice could be attributed to several factors. The virus may still be in the spreading phase, as full hepatocyte infection typically takes 12 weeks, and uneven distribution of human cells in low repopulation mice could prolong this phase. Additionally, hepatocyte cell lysis could release HBV, HBV DNA, HBV RNA, and viral proteins into the blood, with the impact depending on the extent of hepatocyte damage.

However, immunofluorescence for CD45 indicated that NPC-derived lymphocytes were recruited to the liver in only 2 of the mice with reduced HBV titre.

One HBV-infected mouse treated with NPCs showed an increased HBV titre and a significant rise in the hepatocyte marker CK18, suggesting severe liver injury. However, no significant changes in HBV RNA and DNA levels were observed, even with CD45 lymphocyte recruitment. The 6-day post-NPC transfer period may have been too short to detect more substantial changes in HBV DNA and RNA levels, unlike studies where T cells were analysed after 12 days [158] to 8 weeks [159] showing reductions in these levels.

Human GZMB, IFN-gamma, and TNF-alpha were detected in the liver only in animals with CD45<sup>+</sup> lymphocytes, indicating inflammation, but no evidence of immune cell-induced cell death was found, possibly due to the short duration of the experiment.

The *in vivo* experiments indicated that off-target cytotoxic effects from adoptively transferred NPCs did not occur in uninfected mice, suggesting preferential recognition of infected PHHs.

The crosstalk between immune cells and HBV-infected hepatocytes is a complex and dynamic process involving, as first steps, HBV infection and antigen presentation by HLA class I molecules, T cell activation and the release of cytokines that help to enhance the antiviral state within the hepatocytes and recruit additional immune cells to the site of infection [73, 74]. The data here show the recruitment of CD45 cells exclusively in infected mice, and the gene expression analyses here show that the cytokines IFN-gamma and TNF-alpha are released. Thus, the first steps of crosstalk between NPC-derived immune cells and hepatocytes have been demonstrated. Whether the released cytokines were able to recruit other immune cells to the site of infection cannot be determined here, as NK cells could not be detected and Kupffer cells as well as dendritic cells have not yet been attempted to be detected.

Unlike engineered T cell therapy, NPC-based HBV treatment involves NK cells, which make

up about 30% of NPCs, similar to T cells (~40%). In HBV-infected humanized USG mice, PBMC treatment caused severe hepatocyte degeneration via Fas/Fas-ligand interactions, attributed to DC-activated NK cells, as shown by anti-Fas antibody and DC depletion experiments [194].

In summary, the interaction between HBV-infected hepatocytes and T cells is a dynamic process involving antigen presentation, T cell activation, cytokine release and immune evasion. The balance of these interactions can determine the outcome of HBV infection, ranging from clearance to chronic disease. However, in these experiments, the chronic state of infection was already established before immune cells were adoptively transferred into humanized mice.

Niehrs et al. discovered a novel interaction between NK cells and HLA class II-expressing immune cells, where HLA-DP molecules act as ligands for NKp44 on NK cells. This finding suggests a mechanism linking HLA-DP molecules with HBV infection outcomes [134, 252]. Further research is needed to clarify NK cells' role in HBV recognition and control. The data indicate that IFN-gamma from T cells upregulates HLA-DP, potentially enhancing NK cell responses through NKp44-HLA-DP binding, highlighting a synergistic interaction between adaptive and innate immune cells in viral infection control.

Unlike adoptive T cell transfer, where T cells are enriched and activated *in vitro*, NPCs were briefly cultured with IL-15 before transfer. Effects observed in 2 out of 8 mice could be due to a single or multiple immune cell type. To identify recruited cell types in the liver of humanized mice, PCR gene expression analysis and immunofluorescence staining were performed. NKp46 and NKp80, activating receptors found on NK cells, were present in human liver biopsies and isolated NPCs but not in treated or infected mouse livers. This suggests NK cells either didn't migrate into the mouse liver or were suppressed by down-regulation of activating receptors and upregulation of inhibitory receptors due to HBV contact. Additionally, NKG2A, which inhibits NK cell function during chronic infections, and perforin were detected in both human samples and NPC-treated humanized livers, complicating the identification of NK cells due to overlap with T cell markers.

Identifying NK cells in liver sections usually requires co-expression of markers like CD56<sup>+</sup>/CD3<sup>+</sup> or CD56<sup>+</sup>/CD16<sup>+</sup> via immunofluorescence staining. However, this study could not find an antibody to bind CD56 on NK cells in liver cryosections from human biopsies. In this study, only CD45<sup>+</sup>/CD3<sup>+</sup> double-positive T cells were detected in the liver after NPC

transfer, suggesting recruitment of T cells rather than NK cells. Markers for CD4<sup>+</sup> and CD8<sup>+</sup> T cells, along with perforin gene expression, indicated the presence of cytotoxic CD8 T cells. In mice with infiltrating lymphocytes, HLA class I and II markers were significantly induced, similar to T cell transfer experiments, despite fewer immune cells being transferred. The small sample size ( $p < 0.04$ ) limited statistical power, as only mice with infiltrating lymphocytes were analysed.

These results suggest that human non-parenchymal cells can enter the intrahepatic environment, recognise HBV-infected human hepatocytes, and initiate a pathway of viral control mediated by antigen-specific T cell recognition. However, the transient or stable nature of these effects requires further investigation. Notably, only 2 out of 8 mice treated with NPCs showed T cell migration into the liver, and this variability was not linked to the mice's sex, age, or viremia. The lower-than-expected quality of NPCs might be a factor. Cells were stained with trypan blue, which revealed dead cells, but did not provide information about apoptosis. The low lymphocyte percentage within NPCs necessitates a large number of unwanted cells to reach the desired count. Future studies should focus on purifying the NPC fraction to remove dead cells and debris and improving lymphocyte isolation techniques to ensure viable cells post-thawing and activation. This approach should consider whether transferring the entire NPC fraction or purifying lymphocytes is more effective for creating a liver environment close to its natural state.

Additionally, this study used conventional cells for transfer, unlike other studies employing engineered HBV-targeted cells.

Okazaki et al. transferred  $4 \times 10^7$  PBMCs from HBV-vaccinated and non-vaccinated donors into humanized mice a much higher number than the engineered T cells ( $0.5 \times 10^6$  for transient TCR expression [158] and  $2 \times 10^6$  for stable TCR expression [159]) or the number of cells used in this study ( $0.4 \times 10^6$ ). Vaccinated PBMC donors showed a stronger antiviral effect, reducing HBV viremia more effectively. Notably, FasL-positive activated NK cells were detected 4 days post-PBMC injection but not at 2 or 7 days, and HBV-specific CD8 T cells were not observed [194]. NK cell function was effective only when activated by dendritic cells, highlighting the need for a more natural liver environment to explore new HBV cure strategies.

In conclusion, the use of the complete NPC fraction for adoptive cell transfer into humanized mice apparently resulted in the recruitment of T cells, whereas NK cells could not be detected. These cells were not specifically stimulated to recognize HBV. Thus, further studies are needed to dissect the nature of the weak antiviral effect determined. This approach faces two major challenges: limited access to matched human hepatocytes and NPCs, and the quality of cryopreserved NPCs. Obtaining suitable liver samples requires collaboration with transplant centres, and immediate preparation is crucial for cell viability. Few companies offer matched NPCs and hepatocytes, and those that do often provide poorly characterized NPC fractions, leading to high costs and extensive analysis. Further research on immune cell effects in HBV-infected models and patients is essential to guide new experimental and clinical trials take into account the balance and different roles of infiltrating immune cells.

#### **4.4 Immune cell recruitment can be monitored in the presence of viral markers using imaging mass cytometry technique**

Research on immune cell interactions with HBV-infected hepatocytes is limited by the scarcity of infected liver tissue and the need for simultaneous analysis of multiple markers. Imaging mass cytometry (IMC) addresses these challenges by combining fluorescence microscopy and flow cytometry. IMC enables the visualization and quantification of infected liver tissue and surrounding immune cells with up to 30 viral, immune, and structural markers, facilitating detailed correlation studies. Traum et al. demonstrated IMC's effectiveness on FFPE-fixed human liver biopsies, uncovering correlations between adaptive and innate immune cell frequencies and phenotypes [216].

This study aimed to optimize imaging mass cytometry (IMC) for cryopreserved chimeric liver tissue by analysing structural, phenotypic, and viral markers specific to human liver areas, immune cells, and HBV proteins. The antibody panel was validated using cryopreserved mouse liver as a negative control, human liver biopsy as a positive control, and HBV-infected chimeric liver mice treated with T cells as a viral and immune marker control. Titration studies identified optimal antibody dilutions by maximizing the contrast between positive and negative signals while keeping background noise low.

Keratin 8/18 was confirmed as a reliable marker for human hepatocytes, with a 1:400 dilution providing a clear signal despite strong channel bleed. The nuclear marker was optimally titrated at 1:800 for staining chimeric liver tissue. HBcAg effectively identified HBV-infected hepatocytes with a 1:400 dilution showing clear nuclear and cytoplasmic staining. The HBsAg marker also at 1:400, stained the cytoplasm of infected cells, but further titration is needed due to strong signals in negative areas. An ideal HBV protein titration would use a highly viraemic HBV-infected mouse. CD45, used at a 1:400 dilution, clearly identified immune cells, which is essential for data processing and analysis. To reduce spill over into other channels, a higher dilution might be necessary. CD4 and CD8 antibodies, also at 1:400, differentiated T cell types. Most T cells were CD4<sup>+</sup>, while CD8<sup>+</sup> signals were strong but unevenly distributed. Further immunofluorescence microscopy may clarify if this unevenness is due to low CD8 expression or insufficient antibody affinity. Visualizing CD8, CD4, HBcAg, and HBsAg together produced pixelated images due to improper titration and unclear marker expression, highlighting the need for precise titration and thin (8 µm) tissue sections. Waves in thicker sections can negatively impact analysis, so cutting serial sections and using immunofluorescence staining may help identify usable areas. The study failed to find an effective antibody for human NK cells in cryopreserved liver tissue. Despite testing various markers and collaborating with antibody providers, no functional antibody was found.

In conclusion, imaging mass cytometry (IMC) is a valuable tool for simultaneously identifying multiple cell markers at the single-cell level. It enhances both visualization and bioinformatic analysis of cell enrichment and density, offering deeper insights into HBV pathogenesis and immune interactions. In the chimeric mouse liver model, IMC maximizes data extraction from limited samples, which is crucial given the scarcity of such material.

## **4.5 Final conclusions**

Overall, this thesis provides insights into the crosstalk of immune cells and hepatocytes in HBV infection. In addition, the role of HLA molecules in HBV infection and treatment is considered.

HBV does not affect HLA class I and II mRNA expression on infected hepatocytes, suggesting these molecules may not play a direct role in CTL dysfunction. Moreover, type I-III interferons boost HLA class I mRNA expression, indicating that these molecules allow the recognition of HBV infection by virus-specific adaptive immune cells. On the other hand, IFN-beta triggered also the increase of HLA class II expression on human hepatocytes. These findings highlight the potential of enhancing specific HLA molecules to improve antiviral responses and inform new therapies combining interferons with adoptively transferred immune cells for HBV treatment.

*In vivo* experiments, based on adoptive transfer of human non-parenchymal cells into USG mice harbouring donor matched hepatocytes, showed no off-target cytotoxicity. This suggests that human NPCs can enter the murine liver, recognize infected human hepatocytes, and control the virus through antigen-specific T cell recognition. However, our pilot experiments showed that cell migration occurred substantially in only 2/8 animals receiving NPCs. Further research on immune cell effects in animal models and HBV-infected patients is essential for designing new trials. To optimize human NPC use, it's important to enhance lymphocyte yield and improve cell culture stimulation. Additionally, donor diversity can affect cell composition, making it crucial to consider the donor's health status, HBV vaccination history, and the immune status of the liver used for isolation. Unfortunately, such information is often not available and purchase of matched NPC-PHH still very limited.

Imaging mass cytometry provides a new powerful method for the simultaneous identification of cells, especially those expressing multiple markers, at the single cell level. Particularly in the complex chimeric mouse liver model used in this study, IMC could enhance data analysis given the scarcity of mouse material and the urgent need for methods that maximise information using minimal biological samples and tissues.

Despite advances, this study faced limitations. First, and as mentioned above, the very limited amount of matched NPC and PHH batches available, as well as time limitations due to the need of generating human liver chimeric and infected mice before performing adoptive transfer of matched NPCs. Both factors have limited our possibilities to explore a broader range of experimental settings (i.e. ablation of murine macrophages; selection of subpopulation of NPCs and amounts). Future research should address these limitations

to enhance understanding of the immune response to HBV. Overall, this work offers valuable insights that could lead to new therapies and research avenues, ultimately aiming to reduce the global burden of HBV infection and contribute to curing chronic HBV patients.

## 5 References

1. Pisano, M.B., et al., *Viral hepatitis update: Progress and perspectives*. World J Gastroenterol, 2021. **27**(26): p. 4018-4044.
2. Rasche, A., A.L. Sander, V.M. Corman, and J.F. Drexler, *Evolutionary biology of human hepatitis viruses*. J Hepatol, 2019. **70**(3): p. 501-520.
3. Manns, M.P. and B. Maasoumy, *Breakthroughs in hepatitis C research: from discovery to cure*. Nat Rev Gastroenterol Hepatol, 2022. **19**(8): p. 533-550.
4. Giersch, K. and M. Dandri, *In Vivo Models of HDV Infection: Is Humanizing NTCP Enough?* Viruses, 2021. **13**(4).
5. Caviglia, G.P., A. Ciancio, and M. Rizzetto, *A Review of HDV Infection*. Viruses, 2022. **14**(8).
6. Kamatani, Y., et al., *A genome-wide association study identifies variants in the HLA-DP locus associated with chronic hepatitis B in Asians*. Nat Genet, 2009. **41**(5): p. 591-5.
7. Tseng, T.C. and L.R. Huang, *Immunopathogenesis of Hepatitis B Virus*. J Infect Dis, 2017. **216**(suppl\_8): p. S765-S770.
8. Blumberg, B.S., *Australia antigen and the biology of hepatitis B*. Science, 1977. **197**(4298): p. 17-25.
9. Polaris Observatory, C., *Global prevalence, treatment, and prevention of hepatitis B virus infection in 2016: a modelling study*. Lancet Gastroenterol Hepatol, 2018. **3**(6): p. 383-403.
10. Hsu, Y.C., D.Q. Huang, and M.H. Nguyen, *Global burden of hepatitis B virus: current status, missed opportunities and a call for action*. Nat Rev Gastroenterol Hepatol, 2023. **20**(8): p. 524-537.
11. McMahon, B.J., et al., *Acute hepatitis B virus infection: relation of age to the clinical expression of disease and subsequent development of the carrier state*. J Infect Dis, 1985. **151**(4): p. 599-603.
12. Lee, H.A., et al., *The clinical effect of antiviral therapy in patients with hepatitis B virus-related decompensated cirrhosis and undetectable DNA*. J Gastroenterol Hepatol, 2023. **38**(5): p. 716-723.
13. Borgia, G., M.A. Carleo, G.B. Gaeta, and I. Gentile, *Hepatitis B in pregnancy*. World J Gastroenterol, 2012. **18**(34): p. 4677-83.
14. Lavanchy, D., *Chronic viral hepatitis as a public health issue in the world*. Best Pract Res Clin Gastroenterol, 2008. **22**(6): p. 991-1008.
15. Nelson, N.P., P.J. Easterbrook, and B.J. McMahon, *Epidemiology of Hepatitis B Virus Infection and Impact of Vaccination on Disease*. Clin Liver Dis, 2016. **20**(4): p. 607-628.
16. World Health Organisation (WHO). 2023.
17. Hyams, K.C., *Risks of chronicity following acute hepatitis B virus infection: a review*. Clin Infect Dis, 1995. **20**(4): p. 992-1000.
18. Shikata, T., et al., *Hepatitis B e antigen and infectivity of hepatitis B virus*. J Infect Dis, 1977. **136**(4): p. 571-6.
19. Lok, A.S. and B.J. McMahon, *Chronic hepatitis B*. Hepatology, 2007. **45**(2): p. 507-39.
20. Raimondo, G., et al., *Update of the statements on biology and clinical impact of occult hepatitis B virus infection*. J Hepatol, 2019. **71**(2): p. 397-408.
21. Collaborators, G.B.D.H.B., *Global, regional, and national burden of hepatitis B*,

- 1990-2019: a systematic analysis for the Global Burden of Disease Study 2019. *Lancet Gastroenterol Hepatol*, 2022. **7**(9): p. 796-829.
22. Velkov, S., J.J. Ott, U. Protzer, and T. Michler, *The Global Hepatitis B Virus Genotype Distribution Approximated from Available Genotyping Data*. *Genes* (Basel), 2018. **9**(10).
  23. Tatematsu, K., et al., *A genetic variant of hepatitis B virus divergent from known human and ape genotypes isolated from a Japanese patient and provisionally assigned to new genotype J*. *J Virol*, 2009. **83**(20): p. 10538-47.
  24. Iannacone, M. and L.G. Guidotti, *Immunobiology and pathogenesis of hepatitis B virus infection*. *Nat Rev Immunol*, 2022. **22**(1): p. 19-32.
  25. Walter, E., et al., *Hepatitis B virus infection of tupaia hepatocytes in vitro and in vivo*. *Hepatology*, 1996. **24**(1): p. 1-5.
  26. Dane, D.S., C.H. Cameron, and M. Briggs, *Virus-like particles in serum of patients with Australia-antigen-associated hepatitis*. *Lancet*, 1970. **1**(7649): p. 695-8.
  27. Jiang, B. and E. Hildt, *Intracellular Trafficking of HBV Particles*. *Cells*, 2020. **9**(9).
  28. Hu, J. and K. Liu, *Complete and Incomplete Hepatitis B Virus Particles: Formation, Function, and Application*. *Viruses*, 2017. **9**(3).
  29. Tsukuda, S. and K. Watashi, *Hepatitis B virus biology and life cycle*. *Antiviral Res*, 2020. **182**: p. 104925.
  30. Herrscher, C., P. Roingard, and E. Blanchard, *Hepatitis B Virus Entry into Cells*. *Cells*, 2020. **9**(6).
  31. Glebe, D. and C.M. Bremer, *The molecular virology of hepatitis B virus*. *Semin Liver Dis*, 2013. **33**(2): p. 103-12.
  32. Summers, J., A. O'Connell, and I. Millman, *Genome of hepatitis B virus: restriction enzyme cleavage and structure of DNA extracted from Dane particles*. *Proc Natl Acad Sci U S A*, 1975. **72**(11): p. 4597-601.
  33. Gerlich, W.H. and W.S. Robinson, *Hepatitis B virus contains protein attached to the 5' terminus of its complete DNA strand*. *Cell*, 1980. **21**(3): p. 801-9.
  34. Cattaneo, R., H. Will, and H. Schaller, *Hepatitis B virus transcription in the infected liver*. *EMBO J*, 1984. **3**(9): p. 2191-6.
  35. Nassal, M., *The arginine-rich domain of the hepatitis B virus core protein is required for pregenome encapsidation and productive viral positive-strand DNA synthesis but not for virus assembly*. *J Virol*, 1992. **66**(7): p. 4107-16.
  36. Eble, B.E., V.R. Lingappa, and D. Ganem, *Hepatitis B surface antigen: an unusual secreted protein initially synthesized as a transmembrane polypeptide*. *Mol Cell Biol*, 1986. **6**(5): p. 1454-63.
  37. Yan, H., et al., *Sodium taurocholate cotransporting polypeptide is a functional receptor for human hepatitis B and D virus*. *Elife*, 2012. **3**.
  38. Hagenbuch, B. and P.J. Meier, *Molecular cloning, chromosomal localization, and functional characterization of a human liver Na<sup>+</sup>/bile acid cotransporter*. *J Clin Invest*, 1994. **93**(3): p. 1326-31.
  39. Leistner, C.M., S. Gruen-Bernhard, and D. Glebe, *Role of glycosaminoglycans for binding and infection of hepatitis B virus*. *Cell Microbiol*, 2008. **10**(1): p. 122-33.
  40. Schulze, A., P. Gripon, and S. Urban, *Hepatitis B virus infection initiates with a large surface protein-dependent binding to heparan sulfate proteoglycans*. *Hepatology*, 2007. **46**(6): p. 1759-68.
  41. Ni, Y., et al., *Hepatitis B and D viruses exploit sodium taurocholate co-transporting polypeptide for species-specific entry into hepatocytes*. *Gastroenterology*, 2014. **146**(4): p. 1070-83.
  42. Hao, X., et al., *Single-particle tracking of hepatitis B virus-like vesicle entry into*

- cells. *Small*, 2011. **7**(9): p. 1212-8.
43. Huang, H.C., et al., *Entry of hepatitis B virus into immortalized human primary hepatocytes by clathrin-dependent endocytosis*. *J Virol*, 2012. **86**(17): p. 9443-53.
  44. Iwamoto, M., et al., *Epidermal growth factor receptor is a host-entry cofactor triggering hepatitis B virus internalization*. *Proc Natl Acad Sci U S A*, 2019. **116**(17): p. 8487-8492.
  45. Iwamoto, M., et al., *The machinery for endocytosis of epidermal growth factor receptor coordinates the transport of incoming hepatitis B virus to the endosomal network*. *J Biol Chem*, 2020. **295**(3): p. 800-807.
  46. Rabe, B., et al., *Nuclear import of hepatitis B virus capsids and release of the viral genome*. *Proc Natl Acad Sci U S A*, 2003. **100**(17): p. 9849-54.
  47. Rabe, B., D. Glebe, and M. Kann, *Lipid-mediated introduction of hepatitis B virus capsids into nonsusceptible cells allows highly efficient replication and facilitates the study of early infection events*. *J Virol*, 2006. **80**(11): p. 5465-73.
  48. Qi, Y., et al., *DNA Polymerase kappa Is a Key Cellular Factor for the Formation of Covalently Closed Circular DNA of Hepatitis B Virus*. *PLoS Pathog*, 2016. **12**(10): p. e1005893.
  49. Sheraz, M., et al., *Cellular DNA Topoisomerases Are Required for the Synthesis of Hepatitis B Virus Covalently Closed Circular DNA*. *J Virol*, 2019. **93**(11).
  50. Long, Q., et al., *The role of host DNA ligases in hepadnavirus covalently closed circular DNA formation*. *PLoS Pathog*, 2017. **13**(12): p. e1006784.
  51. Wei, L. and A. Ploss, *Core components of DNA lagging strand synthesis machinery are essential for hepatitis B virus cccDNA formation*. *Nat Microbiol*, 2020. **5**(5): p. 715-726.
  52. Quasdorff, M. and U. Protzer, *Control of hepatitis B virus at the level of transcription*. *J Viral Hepat*, 2010. **17**(8): p. 527-36.
  53. Allweiss, L. and M. Dandri, *Experimental in vitro and in vivo models for the study of human hepatitis B virus infection*. *J Hepatol*, 2016. **64**(1 Suppl): p. S17-S31.
  54. Liang, T.J., *Hepatitis B: the virus and disease*. *Hepatology*, 2009. **49**(5 Suppl): p. S13-21.
  55. Wang, J., et al., *HBV Genome and Life Cycle*. *Adv Exp Med Biol*, 2020. **1179**: p. 17-37.
  56. Bartenschlager, R. and H. Schaller, *Hepadnaviral assembly is initiated by polymerase binding to the encapsidation signal in the viral RNA genome*. *EMBO J*, 1992. **11**(9): p. 3413-20.
  57. Bottcher, B., S.A. Wynne, and R.A. Crowther, *Determination of the fold of the core protein of hepatitis B virus by electron cryomicroscopy*. *Nature*, 1997. **386**(6620): p. 88-91.
  58. Watanabe, T., et al., *Involvement of host cellular multivesicular body functions in hepatitis B virus budding*. *Proc Natl Acad Sci U S A*, 2007. **104**(24): p. 10205-10.
  59. Summers, J. and W.S. Mason, *Replication of the genome of a hepatitis B--like virus by reverse transcription of an RNA intermediate*. *Cell*, 1982. **29**(2): p. 403-15.
  60. Patient, R., et al., *Hepatitis B virus subviral envelope particle morphogenesis and intracellular trafficking*. *J Virol*, 2007. **81**(8): p. 3842-51.
  61. Dandri, M., A. Bertoletti, and M. Lutgehetmann, *Innate immunity in hepatitis B and D virus infection: consequences for viral persistence, inflammation, and T cell recognition*. *Semin Immunopathol*, 2021. **43**(4): p. 535-548.
  62. Robinson, M.W., C. Harmon, and C. O'Farrelly, *Liver immunology and its role in inflammation and homeostasis*. *Cell Mol Immunol*, 2016. **13**(3): p. 267-76.
  63. Shin, E.C., P.S. Sung, and S.H. Park, *Immune responses and immunopathology in*

- acute and chronic viral hepatitis*. Nat Rev Immunol, 2016. **16**(8): p. 509-23.
64. Suslov, A., S. Wieland, and S. Menne, *Modulators of innate immunity as novel therapeutics for treatment of chronic hepatitis B*. Curr Opin Virol, 2018. **30**: p. 9-17.
  65. Aizarani, N., et al., *A human liver cell atlas reveals heterogeneity and epithelial progenitors*. Nature, 2019. **572**(7768): p. 199-204.
  66. Megahed, F.A.K., X. Zhou, and P. Sun, *The Interactions between HBV and the Innate Immunity of Hepatocytes*. Viruses, 2020. **12**(3).
  67. Takeuchi, O. and S. Akira, *Innate immunity to virus infection*. Immunol Rev, 2009. **227**(1): p. 75-86.
  68. Lanier, L.L., *Evolutionary struggles between NK cells and viruses*. Nat Rev Immunol, 2008. **8**(4): p. 259-68.
  69. Pluddemann, A., S. Mukhopadhyay, and S. Gordon, *Innate immunity to intracellular pathogens: macrophage receptors and responses to microbial entry*. Immunol Rev, 2011. **240**(1): p. 11-24.
  70. Swiecki, M. and M. Colonna, *The multifaceted biology of plasmacytoid dendritic cells*. Nat Rev Immunol, 2015. **15**(8): p. 471-85.
  71. Knolle, P.A. and R. Thimme, *Hepatic immune regulation and its involvement in viral hepatitis infection*. Gastroenterology, 2014. **146**(5): p. 1193-207.
  72. Yang, G., et al., *Innate Immunity, Inflammation, and Intervention in HBV Infection*. Viruses, 2022. **14**(10).
  73. Busca, A. and A. Kumar, *Innate immune responses in hepatitis B virus (HBV) infection*. Virol J, 2014. **11**: p. 22.
  74. Schuch, A., A. Hoh, and R. Thimme, *The role of natural killer cells and CD8(+) T cells in hepatitis B virus infection*. Front Immunol, 2014. **5**: p. 258.
  75. Gong, J., W. Tu, J. Liu, and D. Tian, *Hepatocytes: A key role in liver inflammation*. Front Immunol, 2022. **13**: p. 1083780.
  76. Bertoletti, A. and C. Ferrari, *Innate and adaptive immune responses in chronic hepatitis B virus infections: towards restoration of immune control of viral infection*. Gut, 2012. **61**(12): p. 1754-64.
  77. Guidotti, L.G. and F.V. Chisari, *Noncytolytic control of viral infections by the innate and adaptive immune response*. Annu Rev Immunol, 2001. **19**: p. 65-91.
  78. Kennedy, P.T.F., et al., *Preserved T-cell function in children and young adults with immune-tolerant chronic hepatitis B*. Gastroenterology, 2012. **143**(3): p. 637-645.
  79. Chang, J., T.M. Block, and J.T. Guo, *The innate immune response to hepatitis B virus infection: implications for pathogenesis and therapy*. Antiviral Res, 2012. **96**(3): p. 405-13.
  80. Faure-Dupuy, S., et al., *Characterization of Pattern Recognition Receptor Expression and Functionality in Liver Primary Cells and Derived Cell Lines*. J Innate Immun, 2018. **10**(4): p. 339-348.
  81. Bigger, C.B., K.M. Brasky, and R.E. Lanford, *DNA microarray analysis of chimpanzee liver during acute resolving hepatitis C virus infection*. J Virol, 2001. **75**(15): p. 7059-66.
  82. Marukian, S., et al., *Hepatitis C virus induces interferon-lambda and interferon-stimulated genes in primary liver cultures*. Hepatology, 2011. **54**(6): p. 1913-23.
  83. Wieland, S.F. and F.V. Chisari, *Stealth and cunning: hepatitis B and hepatitis C viruses*. J Virol, 2005. **79**(15): p. 9369-80.
  84. Sato, S., et al., *The RNA sensor RIG-I dually functions as an innate sensor and direct antiviral factor for hepatitis B virus*. Immunity, 2015. **42**(1): p. 123-32.
  85. Seeger, C. and W.S. Mason, *Molecular biology of hepatitis B virus infection*.

- Virology, 2015. **479-480**: p. 672-86.
86. Maini, M.K. and A.J. Gehring, *The role of innate immunity in the immunopathology and treatment of HBV infection*. J Hepatol, 2016. **64**(1 Suppl): p. S60-S70.
  87. Wieland, S., R. Thimme, R.H. Purcell, and F.V. Chisari, *Genomic analysis of the host response to hepatitis B virus infection*. Proc Natl Acad Sci U S A, 2004. **101**(17): p. 6669-74.
  88. Dunn, C., et al., *Temporal analysis of early immune responses in patients with acute hepatitis B virus infection*. Gastroenterology, 2009. **137**(4): p. 1289-300.
  89. Fletcher, S.P., et al., *Identification of an intrahepatic transcriptional signature associated with self-limiting infection in the woodchuck model of hepatitis B*. Hepatology, 2013. **57**(1): p. 13-22.
  90. Giersch, K., et al., *Hepatitis Delta co-infection in humanized mice leads to pronounced induction of innate immune responses in comparison to HBV mono-infection*. J Hepatol, 2015. **63**(2): p. 346-53.
  91. Cheng, X., et al., *Hepatitis B virus evades innate immunity of hepatocytes but activates cytokine production by macrophages*. Hepatology, 2017. **66**(6): p. 1779-1793.
  92. Mutz, P., et al., *HBV Bypasses the Innate Immune Response and Does Not Protect HCV From Antiviral Activity of Interferon*. Gastroenterology, 2018. **154**(6): p. 1791-1804 e22.
  93. Luangsay, S., et al., *Early inhibition of hepatocyte innate responses by hepatitis B virus*. J Hepatol, 2015. **63**(6): p. 1314-22.
  94. Wu, J., et al., *Hepatitis B virus suppresses toll-like receptor-mediated innate immune responses in murine parenchymal and nonparenchymal liver cells*. Hepatology, 2009. **49**(4): p. 1132-40.
  95. Lutgehetmann, M., et al., *Hepatitis B virus limits response of human hepatocytes to interferon-alpha in chimeric mice*. Gastroenterology, 2011. **140**(7): p. 2074-83, 2083 e1-2.
  96. Ma, Z., et al., *Interaction between Hepatitis B Virus and Toll-Like Receptors: Current Status and Potential Therapeutic Use for Chronic Hepatitis B*. Vaccines (Basel), 2018. **6**(1).
  97. Lang, T., et al., *The hepatitis B e antigen (HBeAg) targets and suppresses activation of the toll-like receptor signaling pathway*. J Hepatol, 2011. **55**(4): p. 762-9.
  98. Visvanathan, K., et al., *Regulation of Toll-like receptor-2 expression in chronic hepatitis B by the precore protein*. Hepatology, 2007. **45**(1): p. 102-10.
  99. Deng, F., et al., *Hepatitis B Surface Antigen Suppresses the Activation of Nuclear Factor Kappa B Pathway via Interaction With the TAK1-TAB2 Complex*. Front Immunol, 2021. **12**: p. 618196.
  100. Kim, G.W., H. Imam, M. Khan, and A. Siddiqui, *N(6)-Methyladenosine modification of hepatitis B and C viral RNAs attenuates host innate immunity via RIG-I signaling*. J Biol Chem, 2020. **295**(37): p. 13123-13133.
  101. Kim, G.W., et al., *HBV-Induced Increased N6 Methyladenosine Modification of PTEN RNA Affects Innate Immunity and Contributes to HCC*. Hepatology, 2021. **73**(2): p. 533-547.
  102. Jiang, M., et al., *Toll-like receptor-mediated immune responses are attenuated in the presence of high levels of hepatitis B virus surface antigen*. J Viral Hepat, 2014. **21**(12): p. 860-72.
  103. Liu, D., et al., *Hepatitis B virus polymerase suppresses NF-kappaB signaling by inhibiting the activity of IKKs via interaction with Hsp90beta*. PLoS One, 2014. **9**(3): p. e91658.

104. Liu, Y., et al., *Hepatitis B virus polymerase disrupts K63-linked ubiquitination of STING to block innate cytosolic DNA-sensing pathways*. J Virol, 2015. **89**(4): p. 2287-300.
105. Rosmorduc, O., et al., *Inhibition of interferon-inducible MxA protein expression by hepatitis B virus capsid protein*. J Gen Virol, 1999. **80** ( Pt 5): p. 1253-1262.
106. Stacey, A.R., et al., *Induction of a striking systemic cytokine cascade prior to peak viremia in acute human immunodeficiency virus type 1 infection, in contrast to more modest and delayed responses in acute hepatitis B and C virus infections*. J Virol, 2009. **83**(8): p. 3719-33.
107. Bjorkstrom, N.K., B. Strunz, and H.G. Ljunggren, *Natural killer cells in antiviral immunity*. Nat Rev Immunol, 2022. **22**(2): p. 112-123.
108. Choo, S.Y., *The HLA system: genetics, immunology, clinical testing, and clinical implications*. Yonsei Med J, 2007. **48**(1): p. 11-23.
109. Coupel, S., et al., *Expression and release of soluble HLA-E is an immunoregulatory feature of endothelial cell activation*. Blood, 2007. **109**(7): p. 2806-14.
110. Carosella, E.D., P. Paul, P. Moreau, and N. Rouas-Freiss, *HLA-G and HLA-E: fundamental and pathophysiological aspects*. Immunol Today, 2000. **21**(11): p. 532-4.
111. Thio, C.L., et al., *Comprehensive analysis of class I and class II HLA antigens and chronic hepatitis B virus infection*. J Virol, 2003. **77**(22): p. 12083-7.
112. Srivastava, M., et al., *Proteogenomic identification of Hepatitis B virus (HBV) genotype-specific HLA-I restricted peptides from HBV-positive patient liver tissues*. Front Immunol, 2022. **13**: p. 1032716.
113. Singh, R., R. Kaul, A. Kaul, and K. Khan, *A comparative review of HLA associations with hepatitis B and C viral infections across global populations*. World J Gastroenterol, 2007. **13**(12): p. 1770-87.
114. Little, A.M. and P. Parham, *Polymorphism and evolution of HLA class I and II genes and molecules*. Rev Immunogenet, 1999. **1**(1): p. 105-23.
115. Wang, L., Z.Q. Zou, and K. Wang, *Clinical Relevance of HLA Gene Variants in HBV Infection*. J Immunol Res, 2016. **2016**: p. 9069375.
116. Chen, X., et al., *An immunodominant HLA-A\*1101-restricted CD8+ T-cell response targeting hepatitis B surface antigen in chronic hepatitis B patients*. J Gen Virol, 2013. **94**(Pt 12): p. 2717-2723.
117. Liu, Q., et al., *Identification of HLA-A\*0201-restricted CD8+ T-cell epitope C(6)(4)(-)(7)(2) from hepatitis B virus core protein*. Int Immunopharmacol, 2012. **13**(2): p. 141-7.
118. Miao, F., et al., *Association of human leukocyte antigen class I polymorphism with spontaneous clearance of hepatitis B surface antigen in Qidong Han population*. Clin Dev Immunol, 2013. **2013**: p. 145725.
119. Ramezani, A., et al., *Association of human leukocyte antigen polymorphism with outcomes of hepatitis B virus infection*. J Gastroenterol Hepatol, 2008. **23**(11): p. 1716-21.
120. Hwang, S.H., et al., *Human leukocyte antigen alleles and haplotypes associated with chronicity of hepatitis B virus infection in Koreans*. Arch Pathol Lab Med, 2007. **131**(1): p. 117-21.
121. Tan, A.T., et al., *Host ethnicity and virus genotype shape the hepatitis B virus-specific T-cell repertoire*. J Virol, 2008. **82**(22): p. 10986-97.
122. Luxenburger, H., C. Neumann-Haefelin, R. Thimme, and T. Boettler, *HCV-Specific T Cell Responses During and After Chronic HCV Infection*. Viruses, 2018. **10**(11).
123. Dazert, E., et al., *Loss of viral fitness and cross-recognition by CD8+ T cells limit*

- HCV escape from a protective HLA-B27-restricted human immune response.* J Clin Invest, 2009. **119**(2): p. 376-86.
124. Schmidt, J., et al., *Rapid antigen processing and presentation of a protective and immunodominant HLA-B\*27-restricted hepatitis C virus-specific CD8+ T-cell epitope.* PLoS Pathog, 2012. **8**(11): p. e1003042.
  125. Lunemann, S., et al., *Interactions Between KIR3DS1 and HLA-F Activate Natural Killer Cells to Control HCV Replication in Cell Culture.* Gastroenterology, 2018. **155**(5): p. 1366-1371 e3.
  126. Zhang, Y., et al., *Correlation of HLA-DQB1 gene polymorphism of Xinjiang Uygur with outcome of HBV infection.* Int J Clin Exp Med, 2015. **8**(4): p. 6067-72.
  127. Correa Bde, M., E.P. Lopes, F. Albuquerque Mde, and L. Dourado, *Association between HLA-DRB1\* polymorphisms and hepatitis B infection in a brazilian population.* Rev Assoc Med Bras (1992), 2012. **58**(5): p. 537-42.
  128. Matsuura, K., M. Isogawa, and Y. Tanaka, *Host genetic variants influencing the clinical course of hepatitis B virus infection.* J Med Virol, 2016. **88**(3): p. 371-9.
  129. Thomas, R., et al., *A novel variant marking HLA-DP expression levels predicts recovery from hepatitis B virus infection.* J Virol, 2012. **86**(12): p. 6979-85.
  130. Xia, Y., et al., *Interferon-gamma and Tumor Necrosis Factor-alpha Produced by T Cells Reduce the HBV Persistence Form, cccDNA, Without Cytolysis.* Gastroenterology, 2016. **150**(1): p. 194-205.
  131. Guidotti, L.G., et al., *Viral clearance without destruction of infected cells during acute HBV infection.* Science, 1999. **284**(5415): p. 825-9.
  132. Zino, E., et al., *A T-cell epitope encoded by a subset of HLA-DPB1 alleles determines nonpermissive mismatches for hematologic stem cell transplantation.* Blood, 2004. **103**(4): p. 1417-24.
  133. van Balen, P., et al., *Immunopeptidome Analysis of HLA-DPB1 Allelic Variants Reveals New Functional Hierarchies.* J Immunol, 2020. **204**(12): p. 3273-3282.
  134. Niehrs, A., et al., *A subset of HLA-DP molecules serve as ligands for the natural cytotoxicity receptor NKp44.* Nat Immunol, 2019. **20**(9): p. 1129-1137.
  135. Jost, S. and M. Altfeld, *Control of human viral infections by natural killer cells.* Annu Rev Immunol, 2013. **31**: p. 163-94.
  136. Ahlenstiel, G., et al., *Natural killer cells are polarized toward cytotoxicity in chronic hepatitis C in an interferon-alfa-dependent manner.* Gastroenterology, 2010. **138**(1): p. 325-35 e1-2.
  137. Dunn, C., et al., *Cytokines induced during chronic hepatitis B virus infection promote a pathway for NK cell-mediated liver damage.* J Exp Med, 2007. **204**(3): p. 667-80.
  138. Nel, I., et al., *Accumulation of Intrahepatic TNF-alpha-Producing NKp44+ NK Cells Correlates With Liver Fibrosis and Viral Load in Chronic HCV Infection.* Medicine (Baltimore), 2016. **95**(19): p. e3678.
  139. Bertoletti, A. and N. Le Bert, *Immunotherapy for Chronic Hepatitis B Virus Infection.* Gut Liver, 2018. **12**(5): p. 497-507.
  140. Gish, R.G., et al., *Chronic hepatitis B: Virology, natural history, current management and a glimpse at future opportunities.* Antiviral Res, 2015. **121**: p. 47-58.
  141. Chang, J., F. Guo, X. Zhao, and J.T. Guo, *Therapeutic strategies for a functional cure of chronic hepatitis B virus infection.* Acta Pharm Sin B, 2014. **4**(4): p. 248-57.
  142. Block, T.M., et al., *Chronic hepatitis B: what should be the goal for new therapies?* Antiviral Res, 2013. **98**(1): p. 27-34.

143. Lim, S.G., et al., *The scientific basis of combination therapy for chronic hepatitis B functional cure*. Nat Rev Gastroenterol Hepatol, 2023. **20**(4): p. 238-253.
144. Belloni, L., et al., *IFN-alpha inhibits HBV transcription and replication in cell culture and in humanized mice by targeting the epigenetic regulation of the nuclear cccDNA minichromosome*. J Clin Invest, 2012. **122**(2): p. 529-37.
145. Lau, G.K., et al., *Peginterferon Alfa-2a, lamivudine, and the combination for HBeAg-positive chronic hepatitis B*. N Engl J Med, 2005. **352**(26): p. 2682-95.
146. Perrillo, R., *Benefits and risks of interferon therapy for hepatitis B*. Hepatology, 2009. **49**(5 Suppl): p. S103-11.
147. Janssen, H.L., et al., *Pegylated interferon alfa-2b alone or in combination with lamivudine for HBeAg-positive chronic hepatitis B: a randomised trial*. Lancet, 2005. **365**(9454): p. 123-9.
148. Konerman, M.A. and A.S. Lok, *Interferon Treatment for Hepatitis B*. Clin Liver Dis, 2016. **20**(4): p. 645-665.
149. Kim, G.A., et al., *HBsAg seroclearance after nucleoside analogue therapy in patients with chronic hepatitis B: clinical outcomes and durability*. Gut, 2014. **63**(8): p. 1325-32.
150. Urban, S., R. Bartenschlager, R. Kubitz, and F. Zoulim, *Strategies to inhibit entry of HBV and HDV into hepatocytes*. Gastroenterology, 2014. **147**(1): p. 48-64.
151. Agency, E.M. *Hepcludex*. 2024 25/07/2023; Available from: <https://www.ema.europa.eu/en/medicines/human/EPAR/hepcludex>.
152. Fanning, G.C., F. Zoulim, J. Hou, and A. Bertoletti, *Author Correction: Therapeutic strategies for hepatitis B virus infection: towards a cure*. Nat Rev Drug Discov, 2020. **19**(4): p. 291.
153. Zhang, H., et al., *Antiviral Activity and Pharmacokinetics of the Hepatitis B Virus (HBV) Capsid Assembly Modulator GLS4 in Patients With Chronic HBV Infection*. Clin Infect Dis, 2021. **73**(2): p. 175-182.
154. Yuen, M.F., et al., *Safety, pharmacokinetics, and antiviral effects of ABI-H0731, a hepatitis B virus core inhibitor: a randomised, placebo-controlled phase 1 trial*. Lancet Gastroenterol Hepatol, 2020. **5**(2): p. 152-166.
155. van den Berg, F., et al., *Advances with RNAi-Based Therapy for Hepatitis B Virus Infection*. Viruses, 2020. **12**(8).
156. Guo, F., et al., *STING agonists induce an innate antiviral immune response against hepatitis B virus*. Antimicrob Agents Chemother, 2015. **59**(2): p. 1273-81.
157. Lanford, R.E., et al., *GS-9620, an oral agonist of Toll-like receptor-7, induces prolonged suppression of hepatitis B virus in chronically infected chimpanzees*. Gastroenterology, 2013. **144**(7): p. 1508-17, 1517 e1-10.
158. Kah, J., et al., *Lymphocytes transiently expressing virus-specific T cell receptors reduce hepatitis B virus infection*. J Clin Invest, 2017. **127**(8): p. 3177-3188.
159. Wisskirchen, K., et al., *T cell receptor grafting allows virological control of Hepatitis B virus infection*. J Clin Invest, 2019. **129**(7): p. 2932-2945.
160. Michel, M.L., Q. Deng, and M. Mancini-Bourgine, *Therapeutic vaccines and immune-based therapies for the treatment of chronic hepatitis B: perspectives and challenges*. J Hepatol, 2011. **54**(6): p. 1286-96.
161. von Weizsacker, F., et al., *The tupaia model for the study of hepatitis B virus: direct infection and HBV genome transduction of primary tupaia hepatocytes*. Methods Mol Med, 2004. **96**: p. 153-61.
162. Wieland, S.F., *The chimpanzee model for hepatitis B virus infection*. Cold Spring Harb Perspect Med, 2015. **5**(6).
163. Seeger, C., D. Ganem, and H.E. Varmus, *Nucleotide sequence of an infectious*

- molecularly cloned genome of ground squirrel hepatitis virus.* J Virol, 1984. **51**(2): p. 367-75.
164. Menne, S. and P.J. Cote, *The woodchuck as an animal model for pathogenesis and therapy of chronic hepatitis B virus infection.* World J Gastroenterol, 2007. **13**(1): p. 104-24.
  165. Mandart, E., A. Kay, and F. Galibert, *Nucleotide sequence of a cloned duck hepatitis B virus genome: comparison with woodchuck and human hepatitis B virus sequences.* J Virol, 1984. **49**(3): p. 782-92.
  166. Mason, W.S., *Animal models and the molecular biology of hepadnavirus infection.* Cold Spring Harb Perspect Med, 2015. **5**(4).
  167. Verrier, E.R., et al., *Cell Culture Models for the Investigation of Hepatitis B and D Virus Infection.* Viruses, 2016. **8**(9).
  168. Tsurimoto, T., A. Fujiyama, and K. Matsubara, *Stable expression and replication of hepatitis B virus genome in an integrated state in a human hepatoma cell line transfected with the cloned viral DNA.* Proc Natl Acad Sci U S A, 1987. **84**(2): p. 444-8.
  169. Sureau, C., J.L. Romet-Lemonne, J.I. Mullins, and M. Essex, *Production of hepatitis B virus by a differentiated human hepatoma cell line after transfection with cloned circular HBV DNA.* Cell, 1986. **47**(1): p. 37-47.
  170. Gripon, P., et al., *Infection of a human hepatoma cell line by hepatitis B virus.* Proc Natl Acad Sci U S A, 2002. **99**(24): p. 15655-60.
  171. Gerets, H.H., et al., *Characterization of primary human hepatocytes, HepG2 cells, and HepaRG cells at the mRNA level and CYP activity in response to inducers and their predictivity for the detection of human hepatotoxins.* Cell Biol Toxicol, 2012. **28**(2): p. 69-87.
  172. Burwitz, B.J., et al., *Hepatocytic expression of human sodium-taurocholate cotransporting polypeptide enables hepatitis B virus infection of macaques.* Nat Commun, 2017. **8**(1): p. 2146.
  173. Ruan, P., et al., *Histopathological changes in the liver of tree shrew (Tupaia belangeri chinensis) persistently infected with hepatitis B virus.* Virol J, 2013. **10**: p. 333.
  174. Chisari, F.V., et al., *A transgenic mouse model of the chronic hepatitis B surface antigen carrier state.* Science, 1985. **230**(4730): p. 1157-60.
  175. Milich, D.R., et al., *Is a function of the secreted hepatitis B e antigen to induce immunologic tolerance in utero?* Proc Natl Acad Sci U S A, 1990. **87**(17): p. 6599-603.
  176. Kim, C.M., et al., *HBx gene of hepatitis B virus induces liver cancer in transgenic mice.* Nature, 1991. **351**(6324): p. 317-20.
  177. Guidotti, L.G., B. Matzke, H. Schaller, and F.V. Chisari, *High-level hepatitis B virus replication in transgenic mice.* J Virol, 1995. **69**(10): p. 6158-69.
  178. Dandri, M. and J. Petersen, *Animal models of HBV infection.* Best Pract Res Clin Gastroenterol, 2017. **31**(3): p. 273-279.
  179. Yang, P.L., A. Althage, J. Chung, and F.V. Chisari, *Hydrodynamic injection of viral DNA: a mouse model of acute hepatitis B virus infection.* Proc Natl Acad Sci U S A, 2002. **99**(21): p. 13825-30.
  180. Du, Y., et al., *In Vivo Mouse Models for Hepatitis B Virus Infection and Their Application.* Front Immunol, 2021. **12**: p. 766534.
  181. Sprinzl, M.F., H. Oberwinkler, H. Schaller, and U. Protzer, *Transfer of hepatitis B virus genome by adenovirus vectors into cultured cells and mice: crossing the species barrier.* J Virol, 2001. **75**(11): p. 5108-18.

182. Jirtle, R.L., C. Biles, and G. Michalopoulos, *Morphologic and histochemical analysis of hepatocytes transplanted into syngeneic hosts*. Am J Pathol, 1980. **101**(1): p. 115-26.
183. Demetriou, A.A., et al., *Survival, organization, and function of microcarrier-attached hepatocytes transplanted in rats*. Proc Natl Acad Sci U S A, 1986. **83**(19): p. 7475-9.
184. Ricordi, C., et al., *Trophic factors from pancreatic islets in combined hepatocyte-islet allografts enhance hepatocellular survival*. Surgery, 1989. **105**(2 Pt 1): p. 218-23.
185. Kusano, M. and M. Mito, *Observations on the fine structure of long-survived isolated hepatocytes inoculated into rat spleen*. Gastroenterology, 1982. **82**(4): p. 616-28.
186. Azuma, H., et al., *Robust expansion of human hepatocytes in Fah<sup>-/-</sup>/Rag2<sup>-/-</sup>/Il2rg<sup>-/-</sup> mice*. Nat Biotechnol, 2007. **25**(8): p. 903-10.
187. Nakamura, K., Y. Tanaka, H. Mitsubuchi, and F. Endo, *Animal models of tyrosinemia*. J Nutr, 2007. **137**(6 Suppl 1): p. 1556S-1560S; discussion 1573S-1575S.
188. Bissig, K.D., et al., *Human liver chimeric mice provide a model for hepatitis B and C virus infection and treatment*. J Clin Invest, 2010. **120**(3): p. 924-30.
189. Washburn, M.L., et al., *A humanized mouse model to study hepatitis C virus infection, immune response, and liver disease*. Gastroenterology, 2011. **140**(4): p. 1334-44.
190. Bility, M.T., et al., *Hepatitis B virus infection and immunopathogenesis in a humanized mouse model: induction of human-specific liver fibrosis and M2-like macrophages*. PLoS Pathog, 2014. **10**(3): p. e1004032.
191. Gutti, T.L., et al., *Human hepatocytes and hematolymphoid dual reconstitution in treosulfan-conditioned uPA-NOG mice*. Am J Pathol, 2014. **184**(1): p. 101-9.
192. Wilson, E.M., et al., *Extensive double humanization of both liver and hematopoiesis in FRGN mice*. Stem Cell Res, 2014. **13**(3 Pt A): p. 404-12.
193. Strick-Marchand, H., et al., *A novel mouse model for stable engraftment of a human immune system and human hepatocytes*. PLoS One, 2015. **10**(3): p. e0119820.
194. Okazaki, A., et al., *Severe necroinflammatory reaction caused by natural killer cell-mediated Fas/Fas ligand interaction and dendritic cells in human hepatocyte chimeric mouse*. Hepatology, 2012. **56**(2): p. 555-66.
195. Rhim, J.A., E.P. Sandgren, R.D. Palmiter, and R.L. Brinster, *Complete reconstitution of mouse liver with xenogeneic hepatocytes*. Proc Natl Acad Sci U S A, 1995. **92**(11): p. 4942-6.
196. Heckel, J.L., et al., *Neonatal bleeding in transgenic mice expressing urokinase-type plasminogen activator*. Cell, 1990. **62**(3): p. 447-56.
197. Petersen, J., M. Dandri, S. Gupta, and C.E. Rogler, *Liver repopulation with xenogenic hepatocytes in B and T cell-deficient mice leads to chronic hepadnavirus infection and clonal growth of hepatocellular carcinoma*. Proc Natl Acad Sci U S A, 1998. **95**(1): p. 310-5.
198. Tateno, C., et al., *Near completely humanized liver in mice shows human-type metabolic responses to drugs*. Am J Pathol, 2004. **165**(3): p. 901-12.
199. Dandri, M. and J. Petersen, *Chimeric mouse model of hepatitis B virus infection*. J Hepatol, 2012. **56**(2): p. 493-5.
200. Meuleman, P., et al., *Morphological and biochemical characterization of a human liver in a uPA-SCID mouse chimera*. Hepatology, 2005. **41**(4): p. 847-56.
201. Oehler, N., et al., *Binding of hepatitis B virus to its cellular receptor alters the*

- expression profile of genes of bile acid metabolism*. Hepatology, 2014. **60**(5): p. 1483-93.
202. Gao, B., W.I. Jeong, and Z. Tian, *Liver: An organ with predominant innate immunity*. Hepatology, 2008. **47**(2): p. 729-36.
  203. Racanelli, V. and B. Rehermann, *The liver as an immunological organ*. Hepatology, 2006. **43**(2 Suppl 1): p. S54-62.
  204. McConnell, M.J., E. Kostallari, S.H. Ibrahim, and Y. Iwakiri, *The evolving role of liver sinusoidal endothelial cells in liver health and disease*. Hepatology, 2023. **78**(2): p. 649-669.
  205. Wang, B.Y., et al., *Effects of ethanol on liver sinusoidal endothelial cells-fenestrae of rats*. Hepatobiliary Pancreat Dis Int, 2005. **4**(3): p. 422-6.
  206. Braet, F. and E. Wisse, *Structural and functional aspects of liver sinusoidal endothelial cell fenestrae: a review*. Comp Hepatol, 2002. **1**(1): p. 1.
  207. Elvevold, K., B. Smedsrod, and I. Martinez, *The liver sinusoidal endothelial cell: a cell type of controversial and confusing identity*. Am J Physiol Gastrointest Liver Physiol, 2008. **294**(2): p. G391-400.
  208. Li, W., N. Chang, and L. Li, *Heterogeneity and Function of Kupffer Cells in Liver Injury*. Front Immunol, 2022. **13**: p. 940867.
  209. Gale, R.P., R.S. Sparkes, and D.W. Golde, *Bone marrow origin of hepatic macrophages (Kupffer cells) in humans*. Science, 1978. **201**(4359): p. 937-8.
  210. Lalor, P.F., P. Shields, A. Grant, and D.H. Adams, *Recruitment of lymphocytes to the human liver*. Immunol Cell Biol, 2002. **80**(1): p. 52-64.
  211. Friedman, S.L., D.C. Rockey, and D.M. Bissell, *Hepatic fibrosis 2006: report of the Third AASLD Single Topic Conference*. Hepatology, 2007. **45**(1): p. 242-9.
  212. Iredale, J.P., *Models of liver fibrosis: exploring the dynamic nature of inflammation and repair in a solid organ*. J Clin Invest, 2007. **117**(3): p. 539-48.
  213. Seo, W. and W.I. Jeong, *Hepatic non-parenchymal cells: Master regulators of alcoholic liver disease?* World J Gastroenterol, 2016. **22**(4): p. 1348-56.
  214. Lyons, A.B. and C.R. Parish, *Determination of lymphocyte division by flow cytometry*. J Immunol Methods, 1994. **171**(1): p. 131-7.
  215. Parish, C.R., M.H. Glidden, B.J.C. Quah, and H.S. Warren, *Use of the intracellular fluorescent dye CFSE to monitor lymphocyte migration and proliferation*. Curr Protoc Immunol, 2009. **Chapter 4**: p. 4 9 1-4 9 13.
  216. Traum, D., et al., *Highly multiplexed 2-dimensional imaging mass cytometry analysis of HBV-infected liver*. JCI Insight, 2021. **6**(7).
  217. Chang, Q., et al., *Imaging Mass Cytometry*. Cytometry A, 2017. **91**(2): p. 160-169.
  218. Elaldi, R., et al., *High Dimensional Imaging Mass Cytometry Panel to Visualize the Tumor Immune Microenvironment Contexture*. Front Immunol, 2021. **12**: p. 666233.
  219. Herkel, J., et al., *MHC class II-expressing hepatocytes function as antigen-presenting cells and activate specific CD4 T lymphocytes*. Hepatology, 2003. **37**(5): p. 1079-85.
  220. Li, Q., et al., *Interferon and interferon-stimulated genes in HBV treatment*. Front Immunol, 2022. **13**: p. 1034968.
  221. Yuen, M.F., et al., *Hepatitis B virus infection*. Nat Rev Dis Primers, 2018. **4**: p. 18035.
  222. Nishio, A., et al., *Clearance of pegylated interferon by Kupffer cells limits NK cell activation and therapy response of patients with HBV infection*. Sci Transl Med, 2021. **13**(587).
  223. Novotny, L.A., et al., *Review of Lambda Interferons in Hepatitis B Virus Infection:*

- Outcomes and Therapeutic Strategies*. Viruses, 2021. **13**(6).
224. Zhang, Z. and S. Urban, *New insights into HDV persistence: The role of interferon response and implications for upcoming novel therapies*. J Hepatol, 2021. **74**(3): p. 686-699.
  225. Li, S.F., et al., *Type I Interferons: Distinct Biological Activities and Current Applications for Viral Infection*. Cell Physiol Biochem, 2018. **51**(5): p. 2377-2396.
  226. Tao, Y., et al., *Immunologic and MRI markers of the therapeutic effect of IFN-beta-1a in relapsing-remitting MS*. Neurol Neuroimmunol Neuroinflamm, 2015. **2**(6): p. e176.
  227. Ivashkiv, L.B., *IFN-gamma: signalling, epigenetics and roles in immunity, metabolism, disease and cancer immunotherapy*. Nat Rev Immunol, 2018. **18**(9): p. 545-558.
  228. Damm, G., et al., *Human parenchymal and non-parenchymal liver cell isolation, culture and characterization*. Hepatol Int, 2013. **7**(4): p. 951-8.
  229. Crispe, I.N., *The liver as a lymphoid organ*. Annu Rev Immunol, 2009. **27**: p. 147-63.
  230. Rodriguez, T., et al., *Patterns of constitutive and IFN-gamma inducible expression of HLA class II molecules in human melanoma cell lines*. Immunogenetics, 2007. **59**(2): p. 123-33.
  231. Khanam, A., J.V. Chua, and S. Kottilil, *Immunopathology of Chronic Hepatitis B Infection: Role of Innate and Adaptive Immune Response in Disease Progression*. Int J Mol Sci, 2021. **22**(11).
  232. Zhang, X., X. Lv, and Y. Song, *Short-term culture with IL-2 is beneficial for potent memory chimeric antigen receptor T cell production*. Biochem Biophys Res Commun, 2018. **495**(2): p. 1833-1838.
  233. Guo, Y., L. Luan, N.K. Patil, and E.R. Sherwood, *Immunobiology of the IL-15/IL-15Ralpha complex as an antitumor and antiviral agent*. Cytokine Growth Factor Rev, 2017. **38**: p. 10-21.
  234. Cooper, M.A., T.A. Fehniger, and M.A. Caligiuri, *The biology of human natural killer-cell subsets*. Trends Immunol, 2001. **22**(11): p. 633-40.
  235. Poli, A., et al., *CD56bright natural killer (NK) cells: an important NK cell subset*. Immunology, 2009. **126**(4): p. 458-65.
  236. Cho, H.J. and J.Y. Cheong, *Role of Immune Cells in Patients with Hepatitis B Virus-Related Hepatocellular Carcinoma*. Int J Mol Sci, 2021. **22**(15).
  237. Thomas, E. and T.F. Baumert, *Hepatitis B Virus-Hepatocyte Interactions and Innate Immune Responses: Experimental Models and Molecular Mechanisms*. Semin Liver Dis, 2019. **39**(3): p. 301-314.
  238. He, X.S., et al., *Differential transcriptional responses to interferon-alpha and interferon-gamma in primary human hepatocytes*. J Interferon Cytokine Res, 2010. **30**(5): p. 311-20.
  239. Thomas, E., et al., *HCV infection induces a unique hepatic innate immune response associated with robust production of type III interferons*. Gastroenterology, 2012. **142**(4): p. 978-88.
  240. Chisari, F.V., *Cytotoxic T cells and viral hepatitis*. J Clin Invest, 1997. **99**(7): p. 1472-7.
  241. Rehmann, B., et al., *The cytotoxic T lymphocyte response to multiple hepatitis B virus polymerase epitopes during and after acute viral hepatitis*. J Exp Med, 1995. **181**(3): p. 1047-58.
  242. Blumberg, B.S., et al., *Hepatitis and Australia antigen: autosomal recessive inheritance of susceptibility to infection in humans*. Proc Natl Acad Sci U S A, 1969.

- 62(4): p. 1108-15.
243. Bertoletti, A. and C. Ferrari, *Adaptive immunity in HBV infection*. J Hepatol, 2016. **64**(1 Suppl): p. S71-S83.
  244. Kim, C.W. and K.M. Chang, *Hepatitis C virus: virology and life cycle*. Clin Mol Hepatol, 2013. **19**(1): p. 17-25.
  245. Iqbal, H., B.F. Mehmood, A. Sohal, and M. Roytman, *Hepatitis E infection: A review*. World J Virol, 2023. **12**(5): p. 262-271.
  246. Tham, C.Y.L., et al., *Hepatitis Delta Virus Acts as an Immunogenic Adjuvant in Hepatitis B Virus-Infected Hepatocytes*. Cell Rep Med, 2020. **1**(4): p. 100060.
  247. Edwards, J.A., et al., *Differential expression of HLA class II antigens in fetal human spleen: relationship of HLA-DP, DQ, and DR to immunoglobulin expression*. J Immunol, 1986. **137**(2): p. 490-7.
  248. O'Brien, T.R., et al., *Risk alleles for chronic hepatitis B are associated with decreased mRNA expression of HLA-DPA1 and HLA-DPB1 in normal human liver*. Genes Immun, 2011. **12**(6): p. 428-33.
  249. Prokunina, L. and M.E. Alarcon-Riquelme, *Regulatory SNPs in complex diseases: their identification and functional validation*. Expert Rev Mol Med, 2004. **6**(10): p. 1-15.
  250. Ou, G., et al., *Variation and expression of HLA-DPB1 gene in HBV infection*. Immunogenetics, 2021. **73**(3): p. 253-261.
  251. Stevanovic, S., et al., *HLA class II upregulation during viral infection leads to HLA-DP-directed graft-versus-host disease after CD4+ donor lymphocyte infusion*. Blood, 2013. **122**(11): p. 1963-73.
  252. Niehrs, A. and M. Altfeld, *Regulation of NK-Cell Function by HLA Class II*. Front Cell Infect Microbiol, 2020. **10**: p. 55.
  253. Gill, U.S., et al., *Interferon Alpha Induces Sustained Changes in NK Cell Responsiveness to Hepatitis B Viral Load Suppression In Vivo*. PLoS Pathog, 2016. **12**(8): p. e1005788.
  254. Wagner, J.A., et al., *CD56bright NK cells exhibit potent antitumor responses following IL-15 priming*. J Clin Invest, 2017. **127**(11): p. 4042-4058.
  255. Poznanski, S.M. and A.A. Ashkar, *Shining light on the significance of NK cell CD56 brightness*. Cell Mol Immunol, 2018. **15**(12): p. 1071-1073.
  256. Zhang, P., G. Zhang, and X. Wan, *Challenges and new technologies in adoptive cell therapy*. J Hematol Oncol, 2023. **16**(1): p. 97.
  257. Tsounis, E.P., E. Tourkochristou, A. Mouzaki, and C. Triantos, *Toward a new era of hepatitis B virus therapeutics: The pursuit of a functional cure*. World J Gastroenterol, 2021. **27**(21): p. 2727-2757.
  258. Ye, B., et al., *T-cell exhaustion in chronic hepatitis B infection: current knowledge and clinical significance*. Cell Death Dis, 2015. **6**(3): p. e1694.
  259. Lau, G.K., et al., *Clearance of hepatitis B surface antigen after bone marrow transplantation: role of adoptive immunity transfer*. Hepatology, 1997. **25**(6): p. 1497-501.
  260. Bohne, F., et al., *T cells redirected against hepatitis B virus surface proteins eliminate infected hepatocytes*. Gastroenterology, 2008. **134**(1): p. 239-47.
  261. Gehring, A.J., et al., *Engineering virus-specific T cells that target HBV infected hepatocytes and hepatocellular carcinoma cell lines*. J Hepatol, 2011. **55**(1): p. 103-10.
  262. Koh, S., et al., *Nonlytic Lymphocytes Engineered to Express Virus-Specific T-Cell Receptors Limit HBV Infection by Activating APOBEC3*. Gastroenterology, 2018. **155**(1): p. 180-193 e6.

263. Medicine, N.L.o. *Clinical Trials.gov*. [cited 2024 25.04.2024]; Available from: <https://clinicaltrials.gov/search?cond=HBV&intr=TCR%20T%20cells>.
264. Fergusson, J.R., et al., *Immune-Mobilizing Monoclonal T Cell Receptors Mediate Specific and Rapid Elimination of Hepatitis B-Infected Cells*. *Hepatology*, 2020. **72**(5): p. 1528-1540.
265. Bertoletti, A., *ImmTAV, a New Immunotherapy Targeting the Source of HBV Infection*. *Hepatology*, 2020. **72**(5): p. 1514-1517.

## 6 List of publications

1. **“Hepatitis Delta Virus Acts as an Immunogenic Adjuvant in Hepatitis B Virus-Infected Hepatocytes.”**

Tham CYL, Kah J, Tan AT, Volz T, Chia A, Giersch K, **Ladiges Y**, Loglio A, Borghi M, Sureau C, Lampertico P, Lütgehetmann M, Dandri M, Bertoletti A.

Cell Rep Med. (2020) doi: 10.1016/j.xcrm.2020.100060

2. **“Hepatitis B Virus Particles Activate Toll-Like Receptor 2 Signaling Initially Upon Infection of Primary Human Hepatocytes.”**

Zhang Z, Trippler M, Real CI, Werner M, Luo X, Schefczyk S, Kemper T, Anastasiou OE, **Ladiges Y**, Treckmann J, Paul A, Baba HA, Allweiss L, Dandri M, Gerken G, Wedemeyer H, Schlaak JF, Lu M, Broering R.

Hepatology (2020) doi: 10.1002/hep.31112

## 7 Ehrenwörtliche Erklärung

Ich versichere hiermit ehrenwörtlich, dass ich meine vorliegende Abschlussarbeit selbstständig verfasst und keine anderen als die angegebenen Hilfsmittel – insbesondere keine im Quellenverzeichnis nicht benannten Internet-Quellen – benutzt habe.

Die Arbeit wurde vorher nicht in einem anderen Prüfungsverfahren eingereicht und die eingereichte schriftliche Fassung entspricht derjenigen auf dem elektronischen Speichermedium.

Wörtlich oder dem Sinn nach aus anderen Werken entnommene Stellen sind unter Angabe der Quellen kenntlich gemacht.

---

Ort, Datum

---

Unterschrift (Vor- und Nachname)